NUCLEAR SPARING OF ANTHRACYCLINE CHEMOTHERAPEUTICS AND CHEMORESISTANCE IN CANCER

by

Tevriz Dilan Demir

A Dissertation Submitted to the

Graduate School of Health Sciences in Partial
Fulfilment of the Requirements for the Degree of

Doctor of Philosophy

in

Cellular and Molecular Medicine

Jan 17, 2023

Nuclear Sparing of Anthracycline Chemotherapeutics and Chemoresistance in Cancer

Koc University

Graduate School of Health Sciences

This is to certify that I have examined this copy of a doctoral dissertation by

Tevriz Dilan Demir

and have found that it is complete and satisfactory in all respects,

and that any and all revisions required by the final

examining committee have been made.

Committee Members:

_____

Assist. Prof. Gülnihal Özcan (Advisor)

_____

Prof. Hakan Sedat Orer (Co-Advisor)

_____

Prof. Tuğba Bağcı Önder

_____

Assist. Prof. Safacan Kölemen

_____

Prof. Alper Okyar

_____

Prof. Engin Ulukaya

Date: _____

To my beloved family…

ABSTRACT

NUCLEAR SPARING OF ANTHRACYCLINE CHEMOTHERAPEUTICS AND CHEMORESISTANCE IN CANCER

Tevriz Dilan DEMİR

Doctor of Philosophy in Cellular and Molecular Medicine

January 17, 2023

Anthracyclines are one of the most potent and widely used chemotherapeutics in cancer treatment. Their main anti-cancer mechanisms of action are to bind to DNA and topoisomerase II enzyme, causing DNA damage. Hence, the intranuclear concentration of anthracyclines is an important determinant of their anticancer efficacy. However, nuclear accumulation cannot be observed in resistant cells, known as "nuclear sparing". To overcome resistance to anthracyclines, mechanisms of nuclear sparing should be clarified.

P-gps are drug efflux pumps localized in the cellular membrane which decrease the intracytoplasmic concentration of various drug molecules. Recent studies have shown that P-gp can also be localized in the nucleus. In this thesis, we investigated the role of nuclear P-glycoproteins (P-gp) in the nuclear sparing of doxorubicin and chemoresistance in gastric cancer since it is one of the most chemo-resistant cancers. We developed gastric adenocarcinoma cell lines with varying degrees of resistance to doxorubicin. In these cells, we observed that increased doxorubicin resistance was significantly correlated with the increase in the nuclear P-gp.

To validate the role of nuclear P-gp in nuclear sparing and chemoresistance, we overexpressed P-gp in parental cells and suppressed P-gp in our resistant cells. We were able to increase the cell's resistance to doxorubicin in parental cells while reversing resistance by silencing P-gp in resistant cells. Our findings suggest that doxorubicin can induce the nuclear translocation of P-gp by a process where nuclear localization signals are involved.

In conclusion, increased expression of nuclear P-gps may be a pivotal mechanism for nuclear sparing and acquired resistance in gastric cancer.

Keywords: Chemoresistance, Anthracycline, Nuclear Sparing, Nuclear P-gp, Gastric Cancer

ÖZETÇE

ANTRASIKLIN KEMÖTERAPÖTIKLERE KARŞI NÜKLEER KORUNMA VE KANSERDE KEMOTERAPI DIRENCI

Tevriz Dilan DEMİR

Hücresel ve Moleküler Tıp, Doktora

Ocak 17, 2023

Günümüzde antrasiklinler, kanser tedavisinde en güçlü ve yaygın olarak kullanılan kemoterapötiklerden biridir. Başlıca anti-kanser etki mekanizmaları, DNA'ya ve topoizomeraz II enzimine bağlanarak DNA hasarına sebep olmaktır. Bu nedenle, antrasiklinlerin intranükleer konsantrasyonu anti kanser etkinliği için en önemli belirleyicilerden biridir. Ancak dirençli hücrelerde ilacın nükleer birikimi gözlenememektedir. Bu fenomen "nükleer korunma" olarak bilinmektedir. Antrasiklinlere karşı ilaç direncinin üstesinden gelmek için, nükleer koruma mekanizmaları açıklığa kavuşturulmalıdır.

P-glikoproteinler (P-gp), hücre zarında yerleşen ve çeşitli ilaç moleküllerinin intrasitoplazmik konsantrasyonunu azaltan ilaç atım pompalarıdır. Son araştırmalar, P-gp'nin aynı zamanda hücre çekirdeğinde de bulunduğunu göstermiştir. Bu tezde, nükleer P-glikoproteinlerin (P-gp) doksorubisinin nükleer korunmasında ve kanserde kemoterapi direncindeki rolünü klinikteki en agresif ve kemorezistansı en yüksek olan mide kanserinde araştırdık. İlk olarak, en güçlü antrasiklinlerden biri olan doksorubisine değişen derecelerde dirençli gastrik adenokarsinom hücre modelleri geliştirdik. Bu hücrelerde, artan doksorubisin direncinin nükleer P-gp'deki artışla önemli ölçüde ilişkili olduğunu gözlemledik.

Nükleer P-gp'nin nükleer koruma ve kemodirençteki rolünü doğrulamak için, doksorubisine duyarlı ebeveyn mide adenokarsinomu hücrelerinde P-gp'yi aşırı ifade ettirirken bir yandan da dirençli hücrelerimizde P-gp ifadesini baskıladık. Doksorubisine duyarlı hücrelerde P-gp'yi aşırı ifade ettirerek hücrelerin doksorubisine direncini artırabildik, aynı zamanda doksorubisine dirençli hücrelerde P-gp'yi susturarak bu direnci tersine çevirebildik. Daha ileri çalışmalarla, doksorubisinin P-gp'nin çekirdeğe translokasyonunda indükleyebileceğini gözlemledik. Ayrıca nükleer lokalizasyon sinyalinin, P-gp'nin çekirdeğe translokasyonunda rol oynayabileceği anlaşılmıştır.

Tüm bu bulgular, artan nükleer P-gp ifadesinin, mide kanserinde nükleer korunma ve kazanılmış direnç için çok önemli bir mekanizma olabileceğini düşündürmektedir.

Anahtar Kelimeler: Kemoterapi Direnci, Antrasiklin, Nükleer Korunma, Nükleer P-gp, Mide Kanseri

ACKNOWLEDGMENTS

Foremost, I would like to especially thank my advisor Dr. Gülnihal Özcan for her endless support and guidance. She encouraged me to find the strength to get up every time in every circumstance. I would like to also, especially thank my co-advisor Dr. Hakan S. Orer for his great interest and guidance. I have been very lucky to have advisors like them. I am grateful for performing this study under their supervision.

A special thanks to Dr. Tuğba Bağcı Önder, and Dr. Alper Okyar due to their contributions and guidance to my study during the thesis progresses and in my thesis committee. I would also like to thank Dr. Safacan Kölemen and Dr. Engin Ulukaya for their participation and comments in my thesis jury.

I am also very grateful to TBO Lab, especially Alişan Kayabölen and Özlem Yedier for their supports in the designing and generation of P-gp-NLS plasmids and generation of CRISPR/Cas9 vectors, respectively.

I owe the greatest appreciation to members of GO Lab; Ece Özmen, Özen Leylek and Cemre Uçaryılmaz for their great friendships, helps, and great contributions during this study. I would like to thank Özen Leylek for her supports in the cloning studies. I'd like to mention Hande Özkan' helps in the establishment of resistant cells.

To Cemre, you know this was never the end, we will definitely meet again one day. Your chicks love you so much.

I owe the biggest and most special thanks to my mother Zeynep Demir and my father Kazım Demir for their endless support and belief in me. Having such a family is the most precious thing in the world. I dedicate this thesis to my family.

I am especially grateful to Nar for being the most beautiful, good girl in the world.

This study was funded by the Scientific and Technological Research Council of Turkey (TUBITAK) ARDEB 3001 Grant No 217S342. This study was conducted using the service and infrastructure of Koç University Research Center for Translational Medicine (KUTTAM). So, I would like to extend my acknowledgments to TUBITAK and KUTTAM.

TABLE OF CONTENTS

1. INTRODUCTION 1

1.1 Chemoresistance in Cancer 1

1.2 Anthracyclines 5

1.2.1 Doxorubicin 7

1.3 Nuclear Sparing 10

1.4 ATP-binding cassette (ABC) transporter superfamily in Drug Efflux 11

1.4.1 P-Glycoprotein (P-gp) 12

1.4.2 Multidrug Resistance Related Protein 1 (MRP-1) 15

1.4.3 Lung Resistance Related Protein (LRP) 16

1.4.4 Breast Cancer Resistance Protein (BCRP) 16

1.5 Gastric Cancer 17

1.5.1 Anthracyclines in Gastric Cancer Treatment 18

1.5.2 Multidrug Resistance in Gastric Cancer 19

1.6 Challenges In Overcoming Chemoresistance by Targeting P-gp: The Inability of P-gp Inhibitors to Overcome Chemoresistance in cancer 21

2. MATERIAL and METHODs 25

2.1 Cell Lines 25

2.2 Cytotoxic Assay 25

2.3 Establishment of Cell Lines That Show Different Levels of Resistance to Doxorubicin 26

2.3.1 Establishing Resistant AGS Cells by Continuous Exposure to 10 nM Doxorubicin (AGS/Dox_Pro10s) 26

2.3.2 Establishing Resistant AGS Cells by Continuous Exposure to 40 nM Doxorubicin (AGS/Dox_Pro40s) 27

2.3.3 Establishment of P-gp Overexpressing AGS Cell Lines 27

2.4 Establishment of P-gp_NLS Overexpressing AGS Cell Lines 30

2.5 Establishment of P-gp Knock-Out AGS/Dox Cells 31

2.5.1 CRISPR/Cas9 Genome Editing System 31

2.5.2 P-gp Knock-Down by siRNA Technology 32

2.6 Colony Formation Assay- Clonogenic Assay 32
2.7 Establishment of sub-cellular fractions and investigation of P-gp expression33
2.8 Western Blot 35
2.9 qRT-PCR 35
2.10 Investigation of Intracellular distribution of P-gp protein by immunofluorescence method 36
2.11 Investigation of the intracellular distribution of doxorubicin..... 37
2.12 Investigation of the Effect of P-gp Inhibitors on the Kinetics of Nuclear Efflux of Doxorubicin 37
2.13 Statistics Analysis..... 38
3. RESULTS..... 39
3.1 Establishment of Doxorubicin Resistant Gastric Adenocarcinoma Cell Models (AGS/Dox) 39
3.2 Intracellular Distribution of P-gp in AGS and AGS/Dox Cells 41
3.3 Investigation of Nuclear P-gp Expression in Western Blots 42
3.4 Intracellular Distribution of Doxorubicin in AGS and AGS/Dox Cells..... 44
3.5 Assessment of the Role of DMSO..... 46
3.6 Establishment of Doxorubicin Resistant Gastric Adenocarcinoma Cell Models by Using Saline as a Doxorubicin Solvent (AGS/Dox-Saline) 47
3.7 Intracellular Distribution of P-gp in AGS/Dox-Saline cells Compared to the AGS/Dox-DMSO cells 48
3.8 Intracellular Distribution of Doxorubicin in AGS/Dox-Saline cells Compared to the AGS/Dox-DMSO cells 50
3.9 The Establishment of a P-gp Overexpressing Gastric Adenocarcinoma Cell Model (AGS/P-gp_Oexp) 52
3.10 Investigation of P-gp Expression in AGS/P-gp_Oexp Cells..... 53
3.11 Intracellular Distribution of P-gp in AGS/P-gp_Oexp Cells..... 55
3.12 Intracellular Distribution of Doxorubicin in AGS/P-gp_Oexp Cells 56
3.13 Assessment of Intracellular Translocation of P-gp in AGS/P-gp_Oex Cells. 57
3.14 Establishment of AGS/P-gp_NLS Cells..... 62
3.15 Intracellular Distribution of P-gp in AGS/P-gp_NLS Cells..... 63
3.16 Intracellular Distribution of Doxorubicin in AGS/P-gp_NLS Cells 63
3.17 Assessment of Nuclear Translocation of P-gp in AGS/P-gp_NLS Cells..... 65
3.18 Comparison of Intracellular Distribution of Doxorubicin in AGS, AGS/Dox, AGS/P-gp_Oexp, AGS/P-gp_NLS cells..... 67
3.19 Comparison of Intracellular Distribution of P-gp in AGS, AGS/Dox, AGS/P-gp_Oexp, AGS/P-gp_NLS cells 69

3.20 The Effect of P-gp Inhibitors on the Nuclear Efflux Kinetics of Doxorubicin 72

3.21 The Effect of P-gp Inhibitors on the Doxorubicin Resistance 74

3.22 Assessment of Other Efflux Pumps..... 75

3.23 Establishment of P-gp Knock-Out AGS Cells 76

3.24 Intracellular Distribution of P-gp in AGS/Dox_Pro40c8_P-gp_siRNA and AGS/Dox_Pro40c8 cells..... 79

3.25 Intracellular Distribution of Doxorubicin in P-gp Knockdown AGS/Dox cells 80

3.26 Assessment of Doxorubicin-Induced Increase in Nuclear P-gp in P-gp Knockdown Cells..... 82

3.27 The Effect of P-gp knock-down on doxorubicin resistance in AGS/Dox cells 84

4. DISCUSSION 87

5. CONCLUSION 94

BIBLIOGRAPHY 95

LIST OF TABLES

Table 1-1 Adverse reactions caused by doxorubicin 9

Table 1-2 Main anticancer drugs which are the substrates of P-gp 20

Table 1-3 Classification of the P-gp inhibitors 23

Table 2-1 Drug concentrations and culture plate charts used in studies for obtaining doxorubicin concentration-response curves and calculating IC 50 value in AGS cells. 25

Table 2-2 Primer pairs to amplify hMDR1 cDNA sequence in the RDC0891 plasmid by the polymerase chain reaction 28

Table 2-3 Sequence of primers used to generate NLS-tagged P-gp overexpression plasmids. 31

Table 2-4 Primer pairs to the hMDR1 gene 36

LIST OF FIGURES

Figure 1-1 Intrinsic and acquired chemoresistance in cancer cells. 2

Figure 1-2 Drug resistance mechanisms in the cancer cells. 3

Figure 1-3 Illustration of nuclear sparing.. 6

Figure 1-4 Primary mechanism of action of doxorubicin in cancer cells. 7

Figure 1-5 Doxorubicin induced reactive oxygen formation mechanism in cancer cells.. 8

Figure 1-6 Schematic structures of the main ABC transporters. 12

Figure 2-1 Diagnostic restriction testing of the pENTR1A_MDR1 plasmid. 28

Figure 2-2 Plasmid vector maps used to generate P-gp overexpression plasmids 29

Figure 2-3 Guide RNAs that are designed for P-gp knock down by CRISPR/Cas9 genome editing system. 32

Figure 2-4 Testing the subcellular fractionation protocols by western blot.. 34

Figure 3-1 Concentration-response curves of AGS/Dox cell models with varying levels of resistance to doxorubicin..... 41

Figure 3-2 Intracellular distribution of P-gp in parental and doxorubicin resistant cells 42

Figure 3-3 Evaluation of P-gp expression by western blot in intracellular fractions obtained by REAP method. 43

Figure 3-4 AGS/Dox cells and their corresponding resistance indices.. 44

Figure 3-5 Intracellular distribution of Doxorubicin in parental AGS cells, AGS/DMSO and doxorubicin resistant AGS/Dox cells 45

Figure 3-6 The effect of DMSO on nuclear P-gp expression.. 46

Figure 3-7 The pattern of the increase in resistance index through time in doxorubicin resistance cells established with doxorubicin dissolved in Saline (Saline-Dox) or DMSO (DMSO-Dox)..... 48

Figure 3-8 Intracellular distribution of P-gp in AGS/Dox-Saline and AGS/Dox-DMSO cells..... 49

Figure 3-9 Intracellular distribution of doxorubicin in AGS/Dox-Saline and AGS/Dox-DMSO cells 50

Figure 3-10 Concentration-response curve of P-gp overexpressing AGS/P-gp_Oexp cells. 53

Figure 3-11 Validation of P-gp overexpression in AGS/P-gp_Oexp Cells by qPCR and Western Blot studies 54

Figure 3-12 Evaluation of P-gp expression in subcellular fractions by western blot in AGS/P-gp_Oexp and AGS Control cells. 54

Figure 3-13 Immunofluorescence images obtained from parental AGS cells P-gp overexpressed AGS/P-gp_Oexp and AGS/NT control cells 55

Figure 3-14 Zoomed in immunofluorescence images obtained from AGS/Dox cells, P-gp overexpressing AGS/P-gp_Oexp cells, parental AGS cells, and AGS/NT control cells. 56

Figure 3-15 Intracellular distribution of doxorubicin in parental AGS cells, AGS/NT Control cells and P-gp overexpressing AGS/P-gp_Oexp cells 57

Figure 3-16 Intracellular distribution of P-gp in AGS/P-gp_Oexp cells after exposure to doxorubicin for 1, 6, 24, 48 and 72 hours 58

Figure 3-17 Intracellular distribution of P-gp in AGS/P-gp_Oexp cells after exposure to paclitaxel for 1-, 6-, 24-, 48- and 72-hours 59

Figure 3-18 Investigation of P-gp expression in parental AGS cells and AGS/P-gp_NLS cells by western blot. 62

Figure 3-19 Intracellular distribution of P-gp in parental AGS cells and AGS/P-gp_NLS cells 63

Figure 3-20 Intracellular distribution of doxorubicin in wild type AGS cells and AGS/P-gp_NLS cells exposed to 1.6uM doxorubicin for 1-, 6-, or 24-hours 64

Figure 3-21 Intracellular distribution of P-gp in AGS cells after exposure to doxorubicin for 1-, 6-, 24-, 48-, or 72-hours 66

Figure 3-22 Comparison of Intracellular Distribution of Doxorubicin in AGS, AGS/Dox, AGS/P-gp_Oexp, AGS/P-gp_NLS 68

Figure 3-23 Comparison of intracellular distribution of P-gp in AGS, AGS/Dox, AGS/P-gp_Oexp, and AGS/P-gp_NLS cells 70

Figure 3-24 The effect of verapamil and zosuquidar on intracellular doxorubicin accumulation in AGS/Dox cells 73

Figure 3-25 Effect of P-gp inhibitors verapamil or zosuquidar on doxorubicin concentration-response curves in AGS/Dox cells. 74

Figure 3-26 Investigation of three other efflux pumps expression in subcellular fractions by western blot in AGS/Dox, AGS/DMSO and AGS/Cell control cells 75

Figure 3-27 Investigation of P-gp expression in pLentr1a_guideRNA [1-2-3] transfected cells, vehicle control cells, and parental cells..... 76

Figure 3-28 Evaluation of P-gp expression by western blot in AGS/Dox cells transfected with P-gp siRNA, or control siRNA..... 77

Figure 3-29 Evaluation of P-gp expression by western blot in AGS/Dox cells transfected with P-gp siRNA, or control siRNA compared to control cells 78

Figure 3-30 Intracellular distribution of P-gp in P-gp knock down (AGS/Dox_Pro40c8_P-gp_siRNA) and control cell groups: AGS/Dox_Pro40c8_siRNA Control, AGS/Dox_Pro40c8, AGS/DMSO, AGS/Cell 79

Figure 3-31 Intracellular distribution of doxorubicin in P-gp knock down AGS/Dox_Pro40c8_P-gp_siRNA and control cell groups; AGS/Dox_Pro40c8_siRNA Control, AGS/Dox_Pro40c8, AGS/DMSO, AGS/Cell 81

Figure 3-32 Intracellular distribution of P-gp after exposure to doxorubicin for 1-, 6-, or 24-hours in AGS/Dox_Pro40c8_P-gp_siRNA and control cell groups; AGS/Dox_Pro40c8_siRNA Control, AGS/Dox_Pro40c8, AGS/DMSO, AGS/Cell and 84

Figure 3-33 Phase contrast images of AGS/Dox_Pro40c8, AGS/Dox_Pro40c8_P-gp_siRNA and control cells..... 85

Figure 3-34 Effect of P-gp siRNA on doxorubicin concentration-response curves in AGS/Dox_Pro40c8 cells 86

ABBREVIATIONS

5-FU	5-Fluorouracil
ABC	ATP-Binding Cassette
ATP	Adenosine Triphosphate
BCRP	Breast Cancer Resistance Protein
cDNA	Complementary DNA
CRISPR	Clustered Regularly Interspaced Short Palindromic Repeats
DMSO	Dimethyl Sulfoxide
DNA	Deoxyribonucleic Acid
Dox	Doxorubicin
dsDNA	double stranded DNA
FBS	Fetal Bovine Serum
GFP	Green Fluorescent Protein
gRNA	guide RNA
IC50	Half Maximal Inhibitory Concentration
LRP	Lung Resistance Related Protein
MDR	Multidrug Resistance
MRP	Multidrug Resistance Related Protein
MTT	(3-(4,5-Dimethylthiazol-2-yl)-2,5-Diphenyltetrazolium Bromide)
MVP	Major Vault Protein
NBD	Nucleotide Binding Domain
NLS	Nuclear Localization Signal
PBS	Phosphate-Buffered Saline
P-gp	P-Glycoprotein
qRT-PCR	Real-Time Quantitative Reverse Transcription PCR
RNA	Ribonucleic Acid
ROI	Region of Interest
SCLC	Small-Cell Lung Cancer

siRNA	small interfering RNA
TMD	Transmembrane Domain
TOPO	Topoisomerase
WHO	World Health Organization

1. INTRODUCTION

1.1 Chemoresistance in Cancer

Chemoresistance is a major obstacle in cancer treatment. Cancer cells can be intrinsically resistant to chemotherapy (intrinsic or natural resistance) or can acquire resistance after exposure to chemotherapy (acquired resistance) (Baguley, 2010; Chern & Tai, 2020).

In innate resistance, drug resistance exists even before the chemotherapy treatment, therefore, tumor shrinkage cannot be achieved after drug administration (Lim & Ma, 2019; Wang et al., 2019). The primary cause of this phenomenon is high tumor heterogeneity with initially drug-resistant cell populations. This highly heterogeneous tumor population includes several resistant subpopulations with cancer stem cells. Upon drug treatment, these resistant populations are selected and end with tumor relapse (Lim & Ma, 2019). Most of these cells have preexisting mutations, that decrease their sensitivity to the drug (Figure 1-1A). For instance, the initial mutations cause the upregulation of human epidermal growth factor (HER2) receptors. This upregulation of HER-2 expression induces epithelial-mesenchymal transition patterns. These two initial rearrangements serve as a defense barrier against many cytotoxic agents and end with intrinsic resistance. This phenomenon occurs in many pan cancers such as gastric, ovarian, and breast cancer (Emran et al., 2022; Nedeljković & Damjanović, 2019; Pils et al., 2007). Also, initial HER2 and VEGFR2 (vascular endothelial growth factor receptor) upregulation mutation is characterized by poor prognosis and increased resistance to conventional chemotherapy in gastric cancer (Lei et al., 2022; Miettinen et al., 2012).

In acquired resistance, even though there is a shrinkage of the tumor at the beginning of drug administration, the anticancer efficacy of the drug gradually decreases over time (Figure 1-1B). (Wang et al., 2019). This may lead to tumor regrowth with more aggressive character. Activation of the second oncogene, mutations in drug targets, and changes in the tumor microenvironment were observed in the relapsed tumor upon chemotherapy treatment compared to the primary tumor (Wang et al., 2019). For instance, upregulation of Bcl-2 gene expression (B-cell lymphoma 2) after treatment is accepted as an acquired resistance mechanism in gastric and breast cancer (Gryko et al., 2014; Murray et al., 2012).

Also, downregulation of top2a gene expression (topoisomerase II) after treatment is an important acquired resistance mechanism in gastric cancer (Beck et al., 1999; Stahl et al., 1997).

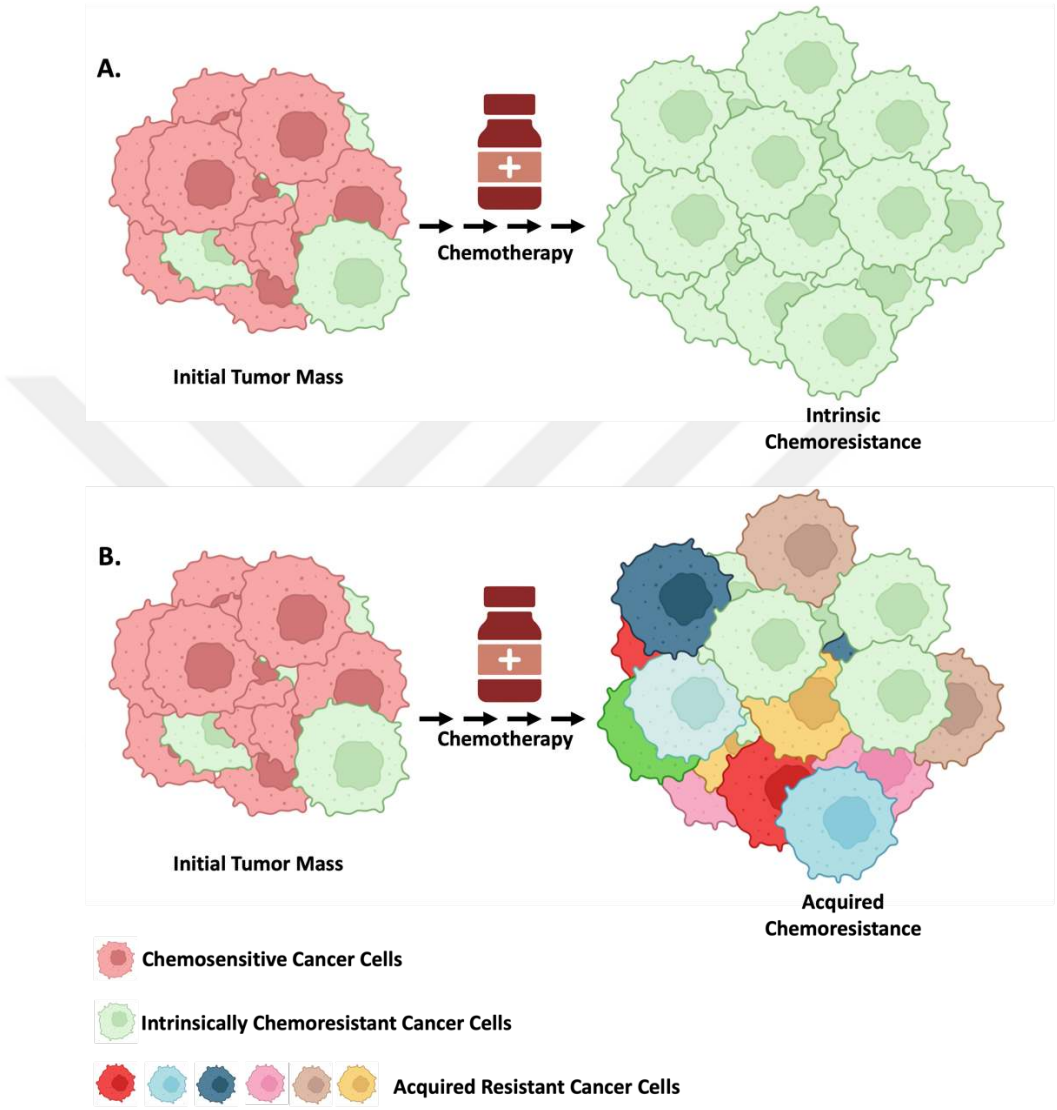

Figure 1-1 Intrinsic and acquired chemoresistance in cancer cells. They are present at the treatment initiation phase and after the treatment phase. **A.** Intrinsically chemo-resistant population selected after chemotherapy administration. **B.** Increased tumor heterogeneity and acquired chemo-resistant cell populations after chemotherapy administration.

Several mechanisms are involved in both natural and acquired resistance including drug inactivation within the cell, reduced drug uptake, upregulated drug export, altered drug targets, metabolic adaptations, dysregulation of DNA damage repair pathways, defective

apoptotic signaling, activation of pro-survival signaling, pro-tumorigenic microenvironments, and cellular adaptive response (Figure 1-2) (Holohan et al., 2013).

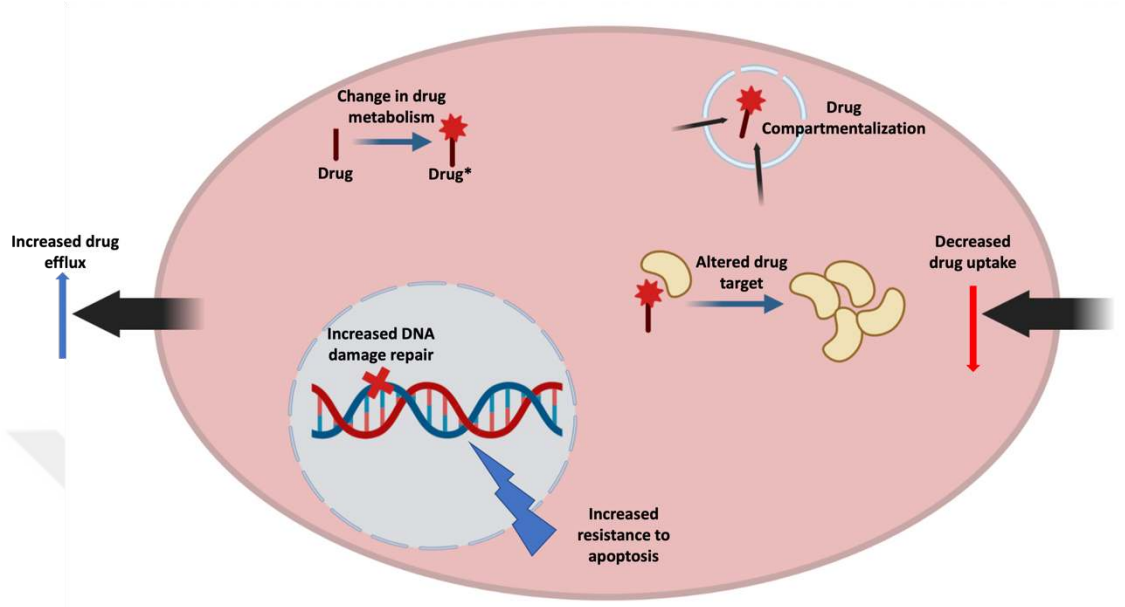

Figure 1-2 Drug resistance mechanisms in the cancer cells. The main resistance mechanisms are; changes in drug import and export mechanisms, drug inactivation, change in drug metabolism, altered drug target and increased DNA damage repair and resistance to apoptosis. Adapted from "The Different Mechanisms of Cancer Drug Resistance: A Brief Review." by Mansoori B, Mohammadi A, Davudian S, Shirjang S, Baradaran B., 2017, Adv Pharm Bull., 3, p. 339-348 (Mansoori et al., 2017).

Drug accumulation into the cell is an important determinant for their anticancer efficacy. In resistant cells this accumulation decreased mainly by two ways, downregulation of drug import or upregulation of drug export. Anti-cancer agents are generally imported into the cell by free diffusion through the membrane or import through solute protein family transporters (SLC) (Muley et al., 2020). To show an efficient mechanism of action in the cell, the drug must be imported properly. Thus, emphasizing the importance of the activity of these transporters in drug resistance. In many cancers, chemotherapy failure is associated with decreased drug uptake. For instance, in epithelial ovarian cancer; downregulation of SLC31A1 is highly associated with platinum-based chemotherapy resistance (Wu et al., 2021). Moreover, by enhancing efflux of drug, cancer cells can avoid the anticancer effect of drugs. Drug efflux mainly driven by ATP-binding cassette (ABC) transporter family proteins (Housman et al., 2014). In normal physiology, these

transporters have role in maintaining cellular homeostasis, protecting duct and intestinal luman from harmful molecules and maintaining blood-brain barrier. In many solid and hematologic cancers, such as gastric, breast, lung cancer and leukaemia ABC transporters are upregulated to protect cancer cells from drug (Housman et al., 2014).

Inactivation of the anticancer drug within the cell is the other important anticancer mechanism. Drug activation within the cell is a piece of complex machinery. Many anticancer drugs undergo metabolic activation which includes the interaction between drugs and numerous proteins. For instance, 5-fluorouracil (5-FU) which is one of the most potent anticancer drug, is metabolized to active and also inactive metabolite forms by enzymes within the cells. The dihydropyridine dehydrogenase enzyme is responsible for the catabolism of the drug to its inactive form; 5,6-dihydro-5-fluorouracil (DHFU) (Miura et al., 2010). Studies demonstrated that the upregulation of dihydropyridine dehydrogenase expression is highly associated with the acquired resistance to 5-FU in many cancer types (Longley & Johnston, 2005).

Alteration of drug targets by mutations and modifications is another important resistance mechanism in cancer cells. Anticancer drugs could target, topoisomerase, epidermal growth factor receptor (EGFR) and its downstream signaling partners, tyrosine kinases, and microtubules (Housman et al., 2014). Changes in the expression and function of these targets highly associate with drug resistance. For example, topoisomerases are the nuclear enzymes that function in unraveling the DNA twists during the replication and transcription. Upregulation of topoisomerase expression ends with resistance to drugs and a decrease in overall survival (Marin et al., 2016).

Cytotoxic drugs directly or indirectly cause DNA damage. Therefore, protection from DNA or reversing the damage by DNA repair pathways are important survival mechanisms for cancer cells (Mansoori et al., 2017). For this, drug-resistant cancer cells could enhance the DNA repair pathway. Thus, targeting the repair pathway to decrease or block the activity in cancer cells can re-sensitize the cancer cells. Unrepaired DNA damage may induce apoptosis in these cells and leads to cell death(Housman et al., 2014). Morever, apoptosis pathway blockage is the other important escape mechanism from death. For instance, Bcl-2 acts as an antiapoptotic protein in the internal apoptosis

pathway (Czabotar et al., 2014). In several cancer its expression is upregulated (Murray et al., 2012).

Since the 1950s, important improvements have been made in the development of effective chemotherapeutics and molecular-targeted agents for overcoming chemoresistance (Chu & DeVita Jr., 2018). Although these agents provide a significant reduction in tumor size in the first-line therapy, the remaining cancer cells can adapt to chemotherapy in most of the patients which results in the formation of chemo-resistant clones and eventually re-growth of the tumor mass. This re-growing tumor mass has much more aggressive progress than the original tumor mass. Therefore, current chemotherapy protocols are still based on the combination of chemotherapeutics with different mechanisms of action (Housman et al., 2014). However, when resistance to a chemotherapeutic develops, resistance to other chemotherapeutics frequently accompanies and treatment fails due to multidrug resistance (Wu, 2014). To overcome chemoresistance and increase survival in cancer, there is an urgent need to delineate underlying mechanisms with further detail and develop new therapeutic strategies.

In this thesis, we aim to investigate a specific chemoresistance mechanism, multidrug resistance to anthracycline chemotherapeutics in cancer cell models.

1.2 Anthracyclines

Anthracyclines are one of the most potent and widely used chemotherapeutics in today's chemotherapy protocols. First anthracycline derivatives, doxorubicin (adriamycin) and daunorubicin were produced from the *Streptomyces peucetius* early in the 60s (Minotti et al., 2004). After World Health Organization (WHO) listed anthracyclines as essential medicines and their effectiveness over other cancer drugs is discovered, new anthracyclines drugs were developed such as epirubicin, idarubicin, and mitoxantrone and valrubicin (McGowan et al., 2017). In clinics, FDA-approved use for the treatment of many cancer types like breast cancer, bladder cancer, childhood solid tumors, soft tissue sarcomas, lymphomas, and other metastatic cancers (Kasi, 2022). Also, in advanced gastric cancer with long-distance metastasis, combination therapy with anthracyclines and antimetabolites increases survival by around 40% (Wadler et al., 1985).

Anthracyclines have several mechanisms of action including intercalation into DNA, generation of free radicals, DNA binding and alkylation, DNA cross-linking, interference with DNA unwinding or DNA strand separation and helicase activity, direct membrane effects, and inhibition of topoisomerase II (Bachur, 2002). However, their primary anti-cancer effect is through binding to DNA and inhibiting the topoisomerase II enzyme which is responsible for the correction of DNA supercoils (Sartiano et al., 1979). As a result, they exhibit cytotoxic effects through DNA damage.

Anthracyclines tend to accumulate in the nucleus due to their binding ability to DNA and protein structures within the nucleus such as proteasomes (Minotti et al., 2004). Since they act by binding to DNA, the intra-nuclear concentration of anthracyclines is the most important determinant for their anti-cancer efficacy. In sensitive cancer cells anthracyclines predominantly accumulate in the nucleus (Burrow et al., 2003). However, in resistant cells, there is a decrease in nuclear accumulation, despite the presence of the drug in the cytoplasm. This phenomenon is known as "nuclear sparing" (Figure 1-3) (Lewin et al., 2007). Although nuclear sparing was shown to be associated with resistance to anthracyclines, the mechanisms that lead to nuclear sparing are still unknown. It is of great importance to investigate these mechanisms in detail, to be able to overcome chemoresistance and achieve success in chemotherapy.

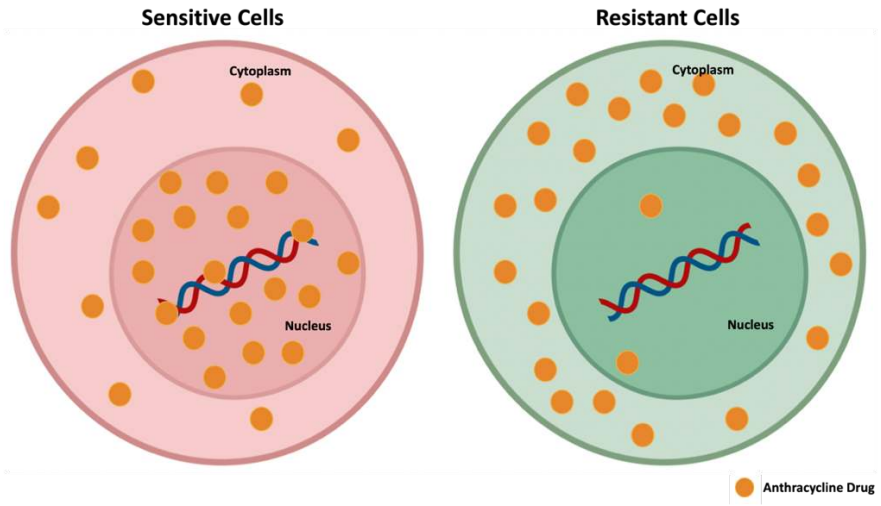

Figure 1-3 Illustration of nuclear sparing. In sensitive cancer cells anthracycline drugs predominantly accumulates at the nucleus leading to cell death. On the other hand, nuclear

accumulation could not be achieved in resistant cells despite the presence of the drug at the cytoplasm.

1.2.1 Doxorubicin

Doxorubicin (DOX) has been one of the most widely used anthracyclines, alone or in combination with other agents, in cancer treatment since the 1960s (Carvalho et al., 2009). In clinics, doxorubicin is approved for the treatment of solid tumors, leukemias, and lymphomas (Rivankar, 2014). The combination therapy regimens with doxorubicin are used for the treatment of many advanced-stage cancers, like metastatic ovarian cancers and childhood hepatoblastoma (Katzenstein et al., 2022) (Rivankar, 2014).

There are two main mechanisms of action proposed for doxorubicin. First mechanism is the inhibition of the progression of topoisomerase II, through binding to DNA. Topoisomerase II is a nuclear enzyme that unwinds supercoiled DNA by cutting and passing double-stranded DNA (Nitiss et al., 2012). After topoisomerase II cuts dsDNA, doxorubicin stabilizes the enzyme. By this way, DNA cannot be resealed, DNA damage is induced and cell cannot complete replication (Figure 1-4) (Rivankar, 2014). This is a direct effect of doxorubicin that takes place in the nucleus.

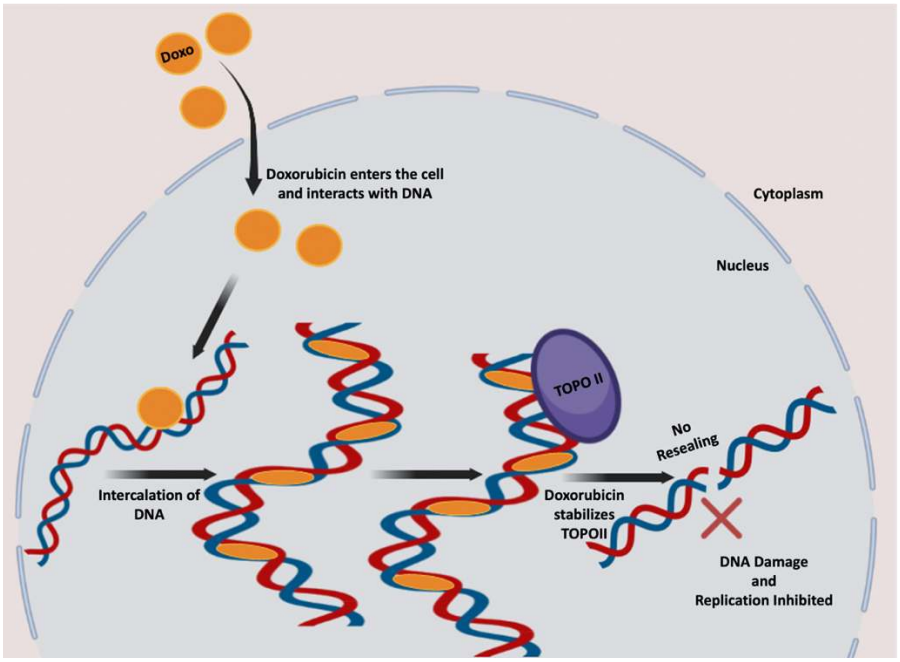

Figure 1-4 Primary mechanism of action of doxorubicin in cancer cells. In the nucleus, doxorubicin intercalates the DNA and inhibits the activity of topo II. This leads to DNA

damage and inhibition of replication. Adapted from "Molecular avenues in targeted doxorubicin cancer therapy" by Sayantani Roychoudhury, Ajay Kumar, Devyani Bhatkar, Nilesh Kumar Sharma, 2020, Future Medicine, 16(11), p. 687-700 (Roychoudhury et al., 2020).

The second mechanism of action of doxorubicin is the generation of free oxygen radicals in subcellular systems (Thorn et al., 2011). In several cell compartments, doxorubicin is metabolized to generate reactive oxygen species and these species mainly cause lipid peroxidation, and protein peroxidation and thereby cell injury (Figure 1-5) (Qu et al., 2016). However, this free radical formation required an extremely high dose of doxorubicin concentration which could not be used in clinics (Keizer et al., 1990). Also, for most tumors, this mechanism does not have a major role (Keizer et al., 1990). Even though this mechanism is thought to be a minor mechanism for doxorubicin's anti-cancer action, many adverse effects of doxorubicin is highly associated with it. (Keizer et al., 1990).

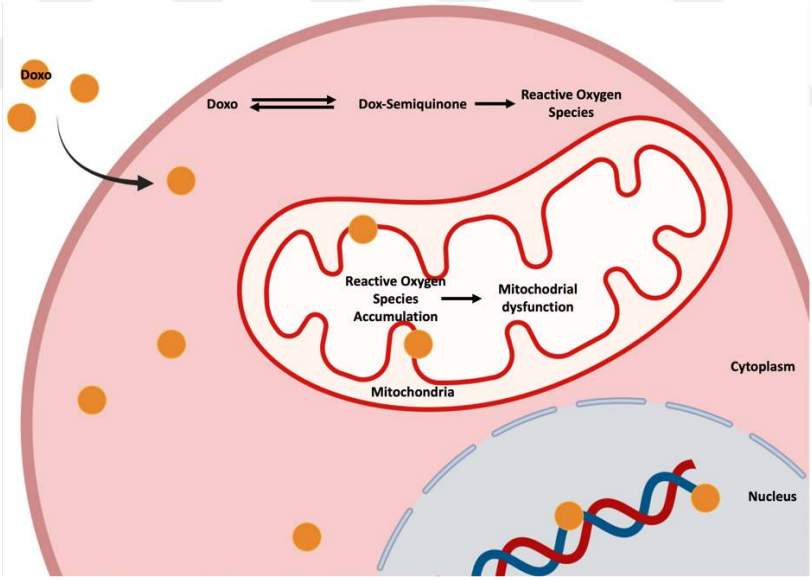

Figure 1-5 Doxorubicin induced reactive oxygen formation mechanism in cancer cells. In cytoplasm and several organelles, doxorubicin can be metabolized to dox-semiquinone. This metabolite has an increased tendency to generate reactive oxygen species. These species cause mitochondrial dysfunction. Adapted from "High Density Lipoprotein and Its Precursor Protein Apolipoprotein A1 as Potential Therapeutics to

Prevent Anthracycline Associated Cardiotoxicity" by Kluck GEG, Durham KK, Yoo JA, Trigatti BL., 2020, Front Cardiovasc Med, 7:65 (Kluck et al., 2020)

Doxorubicin has several limitations in anti-cancer therapy; lack of tumor specificity and severe adverse effects like bone marrow depression, dose-limited cardiotoxicity, and myelosuppression (Table 1-1) (Rivankar, 2014). Especially, dose-dependent cardiotoxicity is the most important factor that limits the clinical effectiveness of doxorubicin. The risk of cardiac dysfunction increases rapidly with increasing doses and occurs during the drug application (Sikora et al., 2022).

Table 1-1 Adverse reactions caused by doxorubicin (Rivankar, 2014).

Adverse Reactions	
Hematological	Bone marrow depression
Symptomatic side effects	Nausea, vomiting, alopecia
Cardiotoxicity	Arrhythmia, cardiac failure, cardiomyopathy
Nephrotoxicity	Glomerular atrophy

To decrease these side effects and increase the efficiency of doxorubicin, many studies have been conducted. The most conventional method in clinics is; doxorubicin administered rapidly (over 15 to 20 minutes) to patients by continuous infusion through central catheters. Administration repeated 21-28 days intervals (Harris et al., 2002). Different application schemes and methodologies are in trials. One study suggested that the prolonged continuous intravenous infusion of doxorubicin reduces cardiotoxicity (Legha et al., 1982). In more recent studies, use of liposomal doxorubicin formulations decreased cardiotoxicity (Volkova & Russell, 2012). These liposomal formulations reduce the plasma clearance of doxorubicin and allow the drug to accumulate in tumor tissue rather than healthy tissue due to the high vascular permeability around the tumor. Thus, they decrease the risk of adverse effects and increase the effectiveness of chemotherapy (Pisano et al., 2013). In addition, liposomal formulations can cause doxorubicin to accumulate in the cytoplasm by surpassing the action of P-gp in the cell membrane. However, due to the accumulation of many liposomes in endo-lysosomal

organelles by the ion trap mechanism, doxorubicin cannot be transferred to the nucleus (Kiyokawa et al., 1999). While liposomes that can overcome the ion trap mechanism can accumulate in the nucleus in sensitive cells, it is noteworthy that the same is not observed in resistant cancer cells (Kiyokawa et al., 1999).

1.3 Nuclear Sparing

It is known that anthracyclines can cross the cellular membranes by simple diffusion depending on the concentration gradient and reach to the nucleus by passing through the pores in the nuclear membrane. Free drug molecules that reach the nucleus can be dispersed back into the cytoplasm (Deepthi et al., 2013). Some authors have commented that drug efflux pumps located in the cell membrane can reduce the drug concentration in the nucleus indirectly by decreasing the drug concentration in the cytoplasm. However, studies suggest that drug transport between the cytoplasm and the nucleus does not only occur by passive mechanisms dependent on the concentration gradient but also some active mechanisms are involved in the process (Gervasoni et al., 1991). In a study in which epirubicin, a chemotherapeutic from the anthracycline group, was applied directly to bladder cancer cells by microinjection, it was observed that epirubicin accumulated in the nucleus of epirubicin-sensitive MGH-U1 cells. However, in epirubicin-resistant MGH-U1R cells, no accumulation was achieved in the nucleus although direct injection was performed into the cytoplasm (Featherstone et al., 2005). This data indicates that increasing the free drug concentration in the cytoplasm alone is not sufficient to increase the drug concentration in the nucleus, and therefore drug transport between the cytoplasm and the nucleus does not occur solely by passive mechanisms dependent on the concentration gradient.

Besides free diffusion, anthracyclines can be actively transported to the nucleus via proteosomes (Kiyomiya et al., 2002). The fact that they bind to DNA and protein structures such as proteosomes in the nucleus facilitates the accumulation of these drugs in the nucleus. A mechanism that prevents these drugs from being transported to the nucleus by proteosomes or actively expels free drug molecules from the nucleus may be responsible for the inability of anthracyclines to accumulate in the nucleus in resistant cells. However, observations that free anthracyclines can pass into the nucleus within minutes and accumulate in the nucleus (Kiyomiya et al., 2002), but drug accumulation in

the nucleus cannot be achieved despite the direct increase of free drug concentration in the cytoplasm by microinjection in resistant cells, (Featherstone et al., 2005); strengthens the hypothesis that "nuclear sparing" in resistant cells may be caused by a carrier that actively expels the free drug out of the nucleus rather than a mechanism that prevents the drug from entering the nucleus. Among the known drug carriers, the strongest candidate to cause this condition is P-gp from the ATP-binding cassette transporter superfamily.

1.4 ATP-binding cassette (ABC) transporter superfamily in Drug Efflux

The ATP-binding cassette (ABC) transporter superfamily is composed of membrane proteins that are found in all living species and transport various substrates across extra- and intracellular membranes (Dean et al., 2022) (Jaramillo et al., 2018). They are conserved through the species due to their important role in cellular homeostasis to import essential nutrients and expel toxins (Jones & George, 2004). Based on these transportation directions, ABC transporters are divided into two subgroups; ABC importers and ABC exporters (Hollenstein et al., 2007). In prokaryotes, both ABC importers and ABC exporters exist. In bacteria, they play a major role in toxin and antimicrobial agent secretion and nutrient uptake (Davidson & Chen, 2004). In eukaryotes, they are functional only as efflux pumps and are mainly involved in the development of multidrug resistance (Jaramillo et al., 2018; Xu et al., 2021).

In recent years high resolution structures of the ABC transporters have been revealed. They consist of transmembrane domains (TMDs) and nucleotide binding domains (NBDs) (Figure 1-1). Transmembrane domains have multiple hydrophobic segments that span the membrane which function as a channel for the passage of the cargo. Whereas, nucleotide binding domains hydrolyze the ATP to supply energy for the transport of the cargo (Jones & George, 2004).

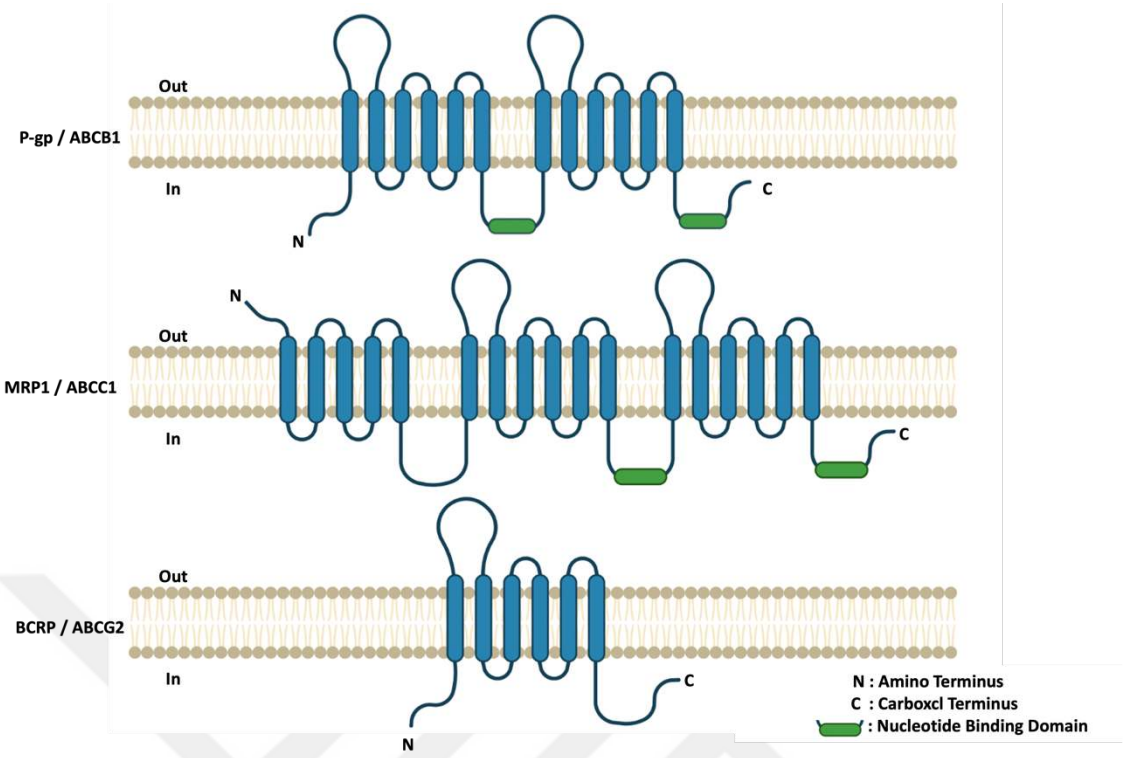

Figure 1-6 Schematic structures of the main ABC transporters. All three ABC transporters shown in the figure share common motifs for transmembrane domains and nucleotide binding domains. Adapted from " How to overcome ATP-binding cassette drug efflux transporter-mediated drug resistance?" by J aramillo AC, Saig FA, Cloos J, Jansen G, Peters GJ. 2018, 1, p. 6-29 (Jaramillo et al., 2018).

This ATP driven efflux of intracellular drugs is highly responsible for the failure of chemotherapy. ABC transporter superfamily has 48 members in humans and 13 of them are directly associated with chemoresistance (Wang et al., 2021). These 13 ABC transporters are ABCA2/3, ABCB1/2/5, ABCC1/2/3/4/5/6/10, and ABCG2. Among these pumps, the first discovered ABCB1 (P-gp), ABCC1 (MRP-1) and ABCG2 (BCRP) are highly associated with drug resistance and progression in cancer (Wang et al., 2021).

1.4.1 P-Glycoprotein (P-gp)

P-gp or "Multi-drug resistance 1" (MDR1) is the first identified member of the ABC transporter superfamily, and is the drug efflux pump most frequently associated with chemoresistance. It was discovered by Victor Ling in 1973 and it is the relationship with multidrug resistance was revealed in 1976 (Gottesman & Ling, 2006). However,

understanding its mechanism of action; ATP hydrolysis and, substrate binding abilities, established in 2000.

The P-gp in the cell membrane pumps the drug molecules with different physical and chemical structures in the cytoplasm out of the cell through active transport. P-gp's located in the intestinal epithelium, hepatocytes and renal tubules change the absorption and elimination kinetics of drugs, reducing the drug concentration in the plasma and causing drug resistance (Lin & Yamazaki, 2003). This mechanism plays an important role in chemoresistance in tumor cells (Thorn, 2011). P-gp is overexpressed in about half of human tumors including chronic myeloid leukemia, non-small cell lung cancer, colon, kidney, adrenal gland, liver, and pancreas cancers which are naturally resistant to chemotherapy, and acute lymphoblastic leukemia, breast cancer, neuroblastoma, pheochromocytoma, and lymphoma (Gottesman, 2002). Its over-expression plays an important role in both acquired resistance and innate resistance to chemotherapy. It has been observed that in cancers with low P-gp expression at the beginning, repeated treatments with chemotherapeutics, which are the substrate of P-gp, can increase P-gp expression (Krishna & Mayer, 2000). When P-gp expression increases in the tumors, these chemotherapeutics are no longer effective, which necessitates the use of chemotherapeutics that are not P-gp substrates (Krishna & Mayer, 2000). However, chemotherapeutics such as anthracyclines and taxanes, which are among the chemotherapeutic groups used as the first choice in chemotherapy and have the strongest anticancer efficacy, are the substrates of P-gp substrates. Therefore, development of resistance to these potent chemotherapeutics via the action of P-gp is a big handicap in cancer therapy.

Nearly 30 years after the first discovery of P-gp, it was understood that P-gp can move from the cell membrane to intracellular compartments and can be located in the mitochondria, endoplasmic reticulum, Golgi, endosome, lysosome and, nucleus membrane (Calcabrini et al., 2000; Molinari et al., 2002) (Munteanu et al., 2006) (Palmeira et al., 2012a; Szaflarski et al., 2013).

Mitochondrial localization of P-gp has been conducted in the study with doxorubicin-resistant hepatocellular carcinoma cell lines (HCC). These doxorubicin resistant HCCs had lower susceptibility to reactive oxygen species formation, and oxidative stress levels

compare to naïve parental control HCCs. When the intracellular localization of P-gp has investigated, they observed the P-gp localization in the mitochondrial membrane. It was suggested that mitochondrial P-gp might be involved in mitochondrial DNA protection and decreased the reactive oxygen species accumulation in mitochondria as an acquired resistant mechanism to doxorubicin (Solazzo et al., 2006). The study with human breast cancer (MCF-7) and its multidrug resistant variant showed that doxorubicin was in the Golgi of sensitive MCF-7 cells. However, this accumulation could not be achieved in the resistant variant of MCF-7 cells.

The confocal studies conducted that P-gp expression increased in the Golgi apparatus of resistant cells to protect organelle from doxorubicin accumulation (Molinari et al., 1994). On the other hand, some studies suggested that the endoplasmic reticulum and Golgi localization of P-gp have directly related to the cytoplasmic membrane translocation of P-gp. After the synthesis of P-gp; chaperone proteins guided it to the ER for reaching its fully folded state (Braakman & Hebert, 2013; Fu, 2013). After that, P-gp is directed to the Golgi for glycosylation. Glycoprotein glucosyl transferase enzyme (UGGT) is localized on the Golgi and responsible for the glycosylation of glycoproteins. Also, this enzyme can sense the folding state of P-gp. If P-gp is not properly folded ER, UGGT directed it back to ER for correct folding. When P-gp is successfully folded in ER and glycosylated in Golgi, 170 kDa mature P-gp is directed to the plasma membrane (Fu & Roufogalis, 2007). Although the intracellular trafficking mechanism of P-gp is unknown yet, the most powerful applicant mechanism is endosomal trafficking (Fu, 2013).

In addition to all these intracellular localization patterns of P-gp, especially the nuclear membrane localization of it may have a crucial role in chemoresistance. It has been suggested that P-gp, located in the nucleus membrane in some types of cancer, may play a role in doxorubicin efflux from the nucleus (Alfarouk et al., 2015). It has been observed that P-gp is predominantly located in the nucleus of doxorubicin-resistant osteosarcoma cells (U-2 OS / DX580), compared to doxorubicin-sensitive osteosarcoma cells, and the accumulation of doxorubicin in the nucleus is reduced in resistant cells (Baldini et al., 1995). The presence of P-gp was observed in the nuclear membrane of doxorubicin-resistant MCF-7-DX breast cancer cells. With increasing pH, the localization of P-gp in the nuclear membrane also increased in these cells. While the doxorubicin efflux from the nucleus isolated from MCF-7-DX cells slowed down in the presence of P-gp inhibitor

cyclosporin A, the same effect was not observed in wild-type MCF-7 cells (Calcabrini et al., 2000). Furthermore, P-gp expression was not observed in the nucleus of doxorubicin-sensitive LoVo colon cancer cells. However, nuclear P-gp expression in doxorubicin-resistant derivatives of these cells was demonstrated by both immunofluorescence and western blot methods. In addition, it has been found that P-gp can move from the cell membrane to the nucleus with doxorubicin administration in LoVo cells (Szaflarski et al., 2013). These observations suggested that P-gps located in the nucleus membrane can reduce the effective drug concentration in the nucleus by the efflux of the anthracyclines from the nucleus. Thus, nuclear P-gps may play a much more critical role in the development of chemoresistance in cancer than the P-gps located in the cell membrane.

1.4.2 Multidrug Resistance Related Protein 1 (MRP-1)

Although the drug carrier that is most associated with chemoresistance is P-gp, it is known that other drug carriers, especially MRP1, LRP and BCRP, also play a role in drug efflux and chemoresistance (Nobili et al., 2012). It can be thought that these transporters may also play a role in drug efflux from the nucleus. Multidrug resistance related protein 1, MRP-1, also belongs to the ATP-binding cassette superfamily of membrane-bound transporters (Cai et al., 2013). Hydrophobic drugs and glutathione are the main substrates of MRP-1. Its association with multidrug resistance was discovered in a multidrug-resistant small cell lung cancer (SCLC) cell line by Cole et al. (Cole et al., 1992). They developed a multidrug resistant variant of SCLC cell line; H69AR, by stepwise selection in doxorubicin containing medium and they found that this resistant cell line does not over-express P-gp protein or its cognate mRNA. Southern (DNA) blot analysis of H69 and H69AR DNA indicated that MRP gene is overexpressed in resistant lines due to gene amplification (Cole et al., 1992). Till 2011, the MRP-1 protein was thought to be localized only in the cytoplasm membrane of cells. However, Cai et. al. observed that, MRP-1 could translocate into the nucleus in resistant tumor cells similar to P-gp (Cai et al., 2011). They established a 5- fluorouracil resistant metastatic human mucoepidermoid carcinoma cell line MC3/5FU. They realized that although MRP1 was localized on the plasma membranes of parental MC3 cells, it was mainly localized in the nuclei of MC3/5FU cells.

1.4.3 Lung Resistance Related Protein (LRP)

Lung resistance-related protein (LRP) is a human major vault protein (MVP), first discovered in the lung cancer cell line and used as a prognostic marker in cancer therapy (Mossink et al., 2003). Over-expression of LRP has also been found in primary NSCLC cells, especially in well-differentiated squamous cell carcinomas and it has been suggested that LRP plays a major role in multidrug resistance of NSCLC (Nooter et al., 1996). LRPs are composed of vaults which are ribonucleoprotein particles that could be localized at the cytoplasm and nuclear membrane, nuclear pore complex (NPC), or nucleoplasm of the nucleus (Chen et al., 2016). Although nuclear localization of LRPs was proved with previous studies, whether they are involved in drug efflux from the nucleus to the cytoplasm is still contradictory.

1.4.4 Breast Cancer Resistance Protein (BCRP)

Breast cancer resistance protein, BCRP, is another member of the ABC transporter superfamily that is responsible for chemoresistance. This protein was firstly investigated in MCF-7 human breast carcinoma cells. First, adriamycin resistant breast cancer cell line, named MCF-7Adr was produced by stepwise selection in doxorubicin (Ke et al., 2010). This cell type became highly resistant to doxorubicin and showed cross resistance to daunorubicin and mitoxantrone. Multidrug resistance in this cell was based on the overexpression of P-gp and MRP-1 proteins. After that, in 1990, it was realized that MCF-7Adr cells are still resistant to doxorubicin even in the presence of the P-gp inhibitor verapamil, but depletion of ATP resulted in complete abrogation of the enhanced efflux of drugs (Doyle & Ross, 2003). These findings led to the discovery of a new type of ATP-dependent efflux pump, which was named BCRP. Unlike the other ABC transporters, BCRP has been mainly identified in subcellular membranes rather than cellular membranes (Bhatia et al., 2012). Bhatia et. al. detected that BCRP was expressed in the nuclear extracts of 6/7 different cell lines by immunoblotting and confocal laser microscopy (Bhatia et al., 2012). BCRP expression was especially observed in glioblastoma multiforme cell lines.

1.5 Gastric Cancer

Gastric cancer is the fifth most common cancer and is responsible for 7.7% of all cancer deaths (Ilic & Ilic, 2022). The 5th-year survival rate in gastric cancer patients with early diagnosis (stage 1) is around 85%, however, the overall 5-year survival rate is around 5-20%. Gastric cancer is diagnosed generally in advanced stages due to the subclinical progression of the disease (Ilic & Ilic, 2022; Piazuelo & Correa, 2013).

Approximately ninety-five percent of the gastric cancers are gastric adenocarcinomas. According to Lauren's classification, gastric adenocarcinomas are histologically divided into two main groups; the intestinal type adenocarcinoma and the diffuse type adenocarcinoma (Piazuelo & Correa, 2013). The intestinal type adenocarcinoma is highly associated with *Helicobacter pylori* infections and is more common in the males and the elderly (Yao et al., 2020). It originates from precancerous legions. When normal gastric epithelium was infected with *Helicobacter pylor*i, chronic gastritis develops. If the patients are not treated, a cascade of atrophic gastritis, intestinal metaplasia, and dysplasia occur, finally leading to cancer. Resulting intestinal type adenocarcinoma is characterized by glandular differentiation, infiltration of the stroma, and lymphatic - vascular invasion (Ma et al., 2016). On the other hand, diffuse-type adenocarcinoma is more frequent in young females. Signet-ring cells, which are characterized by the accumulation of intracellular mucus pushing the nucleus to the periphery, are prominent in the diffuse type gastric adenocarcinoma (Ma et al., 2016). Diffuse-type gastric cancer has the worst prognosis among gastric cancer subtypes.

Today’s gastric cancer treatment protocols are based on surgery; total or partial resection of the stomach accompanied with perioperative and/or adjuvant chemotherapy (Orditura et al., 2014). In the first-line treatment of gastric cancer, mainly platinum derivatives ± anthracyclines or taxanes are combined (Ajani et al., 2022). In primary tumor, topoisomerase II expression significantly increased. This makes anthracyclines a very suitable treatment method. On the other hand, doxorubicin, mitomycin, and hydroxycamptothecin-resistant gastric cancer cells have significantly reduced the expression of topo II (Marin et al., 2020).

Advanced-stage, metastatic gastric cancer patients' overall survival improves significantly with a triple cytotoxic drug combination. These triple-drug regimens include

platinum derivatives + anthracycline + taxanes. However, this protocol increases toxicities such as myelosuppression and infectious complications (Ajani et al., 2022). To overcome these problems, several new strategies have been developed, for instance, targeted therapies. National Cancer Institute (NCI) defined targeted therapy as "a treatment that uses drugs to attack specific cancer cells" (Peters, 2019). Therefore, targeted therapy that attacks the acquired resistance mechanism may increase the overall survival in advanced, tumor-relapsed patients. Genome profile studies that conduct mutations between primary and relapsed tumors can shed light on new therapeutic strategies. In one study, 394 differentially expressed gene (DEGs) defined after chemotherapy administration to gastric cancer patients (Sun et al., 2021). Within these DEGs, 72 of them identified as highly associated with acquired resistance mechanism and clinical predictor for overall survival of treated patients (Sun et al., 2021). Based on these identifications, in selected patients with advanced stage disease and target positivity, targeted therapy with VEGFR inhibitors, Her2 inhibitors or PD-1 inhibitors follow first-line conventional chemotherapy (Lordick et al., 2022).

Especially the development of multidrug resistance both to conventional chemotherapeutics and molecular targeted agents is the main challenge in gastric cancer therapy.

1.5.1 Anthracyclines in Gastric Cancer Treatment

The conventional chemotherapy for gastric cancer is based on single-agent usage in the 1960s. These single agents were mitomycin C; antineoplastic antibiotic, and 5-Fluorouracil; antimetabolite (Wadler et al., 1985). Even though they are very potent cytotoxic drugs, they could not be successful in increasing overall survival in advanced gastric cancer patients (Wadler et al., 1985). They only had modest responses and the overall responses were limited to 17%. In the 1970s, the usage of fluorouracil and mitomycin C dual combination began. However, this combination could not have a significant effect on overall survival (Cullinan et al., 1985). Patients' overall response remained at the same level. In 1978, anthracycline drug doxorubicin was added to this regimen and named as FAM (doxorubicin, mitomycin C and fluorouracil) (Cullinan et al., 1985; MacDonald et al., 1980). With this triple combination therapy, the overall response increased to 40% (Wohrer et al., 2004). After that, authorities accepted

anthracycline-based chemotherapy regimens as gold therapy for advanced gastric cancer patients (Xu et al., 2017). However, this time drug toxicity became the major problem. To overcome this, mitomycin C usage replaced with the antimetabolite drug methotrexate (Cullinan et al., 1985). This combination of drugs (FAMTX) increased overall success to 40-50% and was accepted as superior to the rest. (Wohrer et al., 2004). On the other hand, scientists also reported that doxorubicin-based treatment regimens had many adverse effects and a bad prolonged survival ratio. Studies revealed that there was a rapid acquisition of resistance to doxorubicin. To solve this problem, studies have focused on two mechanisms. First one was discovering new strategies to re-sensitization cells to doxorubicin. Second, the replacement of doxorubicin with another anthracycline epirubicin (FEMTX). Clinical results showed that the equimolar concentration of epirubicin had less toxicity. Epirubicin yields less cardiotoxicity, which is the main limitation of doxorubicin (Khasraw et al., 2012). Then, epirubicin, fluorouracil, and cisplatin combination protocol started to be tested. By this, the overall response increases the 71% with moderate toxicity (Aitini et al., 2001). Nowadays, to treat unresectable and long-distance metastatic gastric, docetaxel, cisplatin, and fluorouracil combination could be used. By this 4.9% of advanced gastric cancer patients showed complete response (Rosenberg et al., 2019).

After all these developments, today anthracyclines are the essential cytotoxic agents in gastric cancer treatment. Even though their efficiency over other agents has been revealed, the intrinsic and acquired resistance to anthracyclines is still an essential handicap over chemotherapy success. To overcome chemoresistance and increase the overall survival rates, we must clarify the underlying mechanisms.

1.5.2 Multidrug Resistance in Gastric Cancer

The rate of P-gp positivity in gastric cancer varies between 41.7% and 87% (Arbabi Bidgoli, 2006; Gürel et al., 1999; Hu et al., 2014; Xu et al., 2021). It has been observed that P-gp positivity is more common in gastric cancers resistant to doxorubicin, etoposide, and campotecin than in sensitive gastric cancers (Xu et al., 2010).In a study conducted in our country, Gurel et al. found that 87% of gastric cancer patients had P-gp positivity and survival was significantly lower in patients with high levels of P-gp (Gürel et al., 1999). In addition, P-gp positivity has been associated with unresponsiveness to treatment and

multi-drug resistance in gastric cancer (Orita et al., 1994; Xu et al., 2010). Data on whether P-gp expression increases in correlation with tumor progression in gastric cancer is unclear (Wallner et al., 1993; Choi et al., 2002). However, it was observed that P-gp positivity in patients increased after doxorubicin chemotherapy. P-gp positivity after chemotherapy was found to be correlated with high systemic recurrence in gastric cancer (Chung et al., 1996). These data suggested that P-gp expression increases with exposure to doxorubicin in gastric cancer. Additionally, several studies in many solid cancer cells suggested that P-gp can move into the intracellular compartments with exposure to doxorubicin (Abbaszadegan et al. 1996a, 1996b; Szaflarski et al., 2013). However, P-gp translocation in gastric cancer is not revealed yet.

Anthracyclines, taxanes, and many molecular targeted agents are known to be substrates of P-gp (Kim, 2002). Therefore, a detailed understanding of the mechanisms of chemotherapy resistance with P-gp; is of great importance in terms of increasing the success of combination chemotherapy protocols used in both the first and second-line treatment of gastric cancer. Moreover, potent chemotherapeutics which could be alternatives to anthracyclines and taxanes, such as vinca alkaloids (e.g. vinblastine) and podophyllotoxins (e.g. etoposide), are also the substrates of P-gp (Table 1-2). Therefore, these chemotherapeutics could not gain a sufficient weight in the treatment of gastric cancer (Kim, 2002).

Table 1-2 Main anticancer drugs which are the substrates of P-gp (Sikic et al., 1997)

Vinca Alkaloids	Anthracyclines	Taxanes	Epipodophyllotoxins	Others
Vinblastine Vincristine Vinorelbine	Doxorubicin Daunorubicin Epirubicin Idarubicin	Paclitaxel Docetaxel	Etoposide Teniposide	Mitoxantrone Dactinomycin Amsacrine Trimetrexate Topotecan Mithramycin Mitomycin C

1.6 Challenges In Overcoming Chemoresistance by Targeting P-gp: The Inability of P-gp Inhibitors to Overcome Chemoresistance in cancer

The role of P-gp in tumor multidrug resistance and chemotherapy failure gives rise to studies on the discovery and delivery of drugs that inhibit drug release by P-gp. P-gp can be inhibited by following three mechanisms; first, competitive or non-competitive blockage of binding site; second, inhibition of ATP hydrolysis; and third structural alterations (Lehne & Rugstad, 1998). Usage and the efficacy of many P-gp inhibitors in overcoming chemotherapy resistance have been studied in preclinical and clinical studies (Palmeira et al., 2012b).

P-gp inhibitors are classified into three subgroups; first-generation inhibitors, second-generation, and third-generation, based on their specificity, affinity, and toxicity (Table 1-3) (Amin, 2013). The first-generation inhibitors are already clinically used drugs for specific diseases. They competitively inhibit the efflux of other drugs by P-gp, since they are also the substrates of P-gp. Among these first-generation inhibitors, verapamil was the one whose inhibitory effect on P-gp was discovered first, at 1981 (Tsuruo et al., 1981). Verapamil is a calcium channel blocker and slows the efflux of other P-gp substrates from the cell by competitive inhibition. However, for the inhibition of P-gp verapamil is required to be administered at doses up to 106 times the therapeutic dose required for calcium channel blockade (MacGowan et al., 1992). Therefore, it is not used clinically as a P-gp inhibitor since it causes serious cardiac toxicity at these doses. Cyclosporin A is another first-generation P-gp inhibitor. Similarly, the use of cyclosporine A as a P-gp inhibitor is limited due to its immunosuppressive effect (Lehne & Rugstad, 1998). Other first-generation agents could not be translated into the clinical application because of their low potency and the need for the use of toxic level doses for P-gp inhibition (Srivalli and Lakshmi, 2012).

Second generation inhibitors of P-gp are not pharmacologically active molecules and are more potent compared to first-generation inhibitors. They are derivatives of verapamil and cyclosporin A; namely dexverapamil and valspodar, that have higher affinity to P-gp (Amin, 2013). However, although they are 5-10 times more potent than the first generation in terms of the inhibition of P-gp, their P-gp-inhibiting doses remained well above the maximum tolerable dose since they are also substrates of P-gp. In addition,

interactions at the cytochrome p450 level have made their use with chemotherapeutics impossible (Srivalli and Lakshmi, 2012).

Using the structure-activity relationship, third generation P-gp inhibitors have been developed. They are much more potent than the second-generation P-gp inhibitors and directly inhibit P-gp non-competitively. Zosuquidar, tariquidar, and elacridar are examples of third generation inhibitors. Although tariquidar is a very potent inhibitor of P-gp, the Phase III study was suspended due to toxicity caused by interactions at the cytochrome p450 level. Thereupon, tariquidar derivatives that did not cause an interaction at the cytochrome p450 level were developed (Callaghan et al., 2014). Elacridar and zosuquidar have been moved to clinical trials based on strong evidence from preclinical studies. However, the significant clinical efficacy of these in combination with chemotherapeutics has not been demonstrated yet (Palmeira et al., 2012; Callaghan et al., 2014; Dash et al., 2017).

Table 1-3 Classification of the P-gp inhibitors (Amin, 2013)

Inhibitor Generation	Inhibitor Name	Mechanism of action and specificty	Limitations
First-Generation Inhibitors	1. Verapamil 2. Cyclosporin- A 3. Tamoxifen 4. Toremifera	Competitive inhibitors Non-selective Low binding affinities	Substrate to other transporters. Pharmacologically active molecules P-gp substrates
Second-Generation Inhibitors	1. Dexverapamil 2. Valspodar 3. Dexniguldipine	Higher specificity compared to the first generation Interaction with other systems	Substrate of cyp3A4 Substrate of other transporters
Third-Generation Inhibitors	1. Zosuquidar 2. Tariquidar 3. Mitotane 4. Laniquidar	Highest specificity Specific inhibition More potent	No clinically significant effect observed

In this thesis, primarily; AGS cells with different levels of resistance to doxorubicin (AGS/Dox) were established. The intracellular distribution of P-gp in parental and resistant cells was evaluated to understand whether nuclear P-gp expression increases with increasing resistance to doxorubicin and the correlation between the doxorubicin resistance index and P-gp expression in the nuclear membrane. Using the autofluorescence property of doxorubicin, the intracellular distribution of doxorubicin was investigated by confocal microscope to compare the nuclear sparing ability difference between doxorubicin-resistant cells and parental cells. To validate the role of nuclear P-gp in nuclear sparing and chemoresistance in further, ectopically P-gp overexpressing naïve AGS cells were established. By this, the changes in the nuclear/cytoplasmic doxorubicin concentration ratio, nuclear efflux kinetics, and IC50 values in AGS cells by overexpressing the P-gp were investigated. Further validations of these observations were investigated by inhibiting and suppressing P-gp expression in our resistant cells. Moreover, the mechanisms that underly localization of P-gp in the nucleus, especially after doxorubicin exposure were studied. The nuclear localization signal role in this mechanism was researched.

2. MATERIAL and METHODs

2.1 Cell Lines

In the study, AGS cell lines were used as a primary gastric adenocarcinoma cell model. AGS cell line purchased from the American Tissue Culture Collection, was derived from the primary tumor of a gastric cancer patient prior to chemotherapy and grows attached to the culture flasks. AGS cells were stored in F-12K medium containing 10% FBS, in an incubator with 5% CO2 at 37 ° C. The reported IC50 value of doxorubicin in AGS cells is 0.0161 µM (Genomics of drug sensitivity in cancer).

2.2 Cytotoxic Assay

To obtain doxorubicin concentration-response curves in AGS cells and calculate IC50 values MTT assay was used. AGS cells were seeded in 96-well plates at a cell count of 1000 cells/well. After waiting 24 hours for the cells to adhere to the plates, 9 different concentrations of doxorubicin were added to the treatment groups. The examination was performed in six wells (6 technical replicates, replicas 1-6) in a single experiment for each drug group and control group. The plate chart of the experiments and the final doxorubicin concentrations are given in Table 2-1.

Table 2-1 Drug concentrations and culture plate charts used in studies for obtaining doxorubicin concentration-response curves and calculating IC 50 value in AGS cells

Doxorubicin (nM)	**0**	**0.78**	**1.56**	**3.12**	**6.25**	**12.5**	**25**	**50**	**100**	**200**
Replicate 1	Control	Dox1	Dox2	Dox3	Dox4	Dox5	Dox6	Dox7	Dox8	Dox9
Replicate 2	Control	Dox1	Dox2	Dox3	Dox4	Dox5	Dox6	Dox7	Dox8	Dox9
Replicate 3	Control	Dox1	Dox2	Dox3	Dox4	Dox5	Dox6	Dox7	Dox8	Dox9
Replicate 4	Control	Dox1	Dox2	Dox3	Dox4	Dox5	Dox6	Dox7	Dox8	Dox9
Replicate 5	Control	Dox1	Dox2	Dox3	Dox4	Dox5	Dox6	Dox7	Dox8	Dox9
Replicate 6	Control	Dox1	Dox2	Dox3	Dox4	Dox5	Dox6	Dox7	Dox8	Dox9

After the cells were kept in doxorubicin at the indicated concentrations or in a drug-free medium in the control group for 5 days, 3 mg/ml 32 µl of MTT solution was added to the

cells and the MTT molecule was expected to transform into formazan crystals via mitochondrial enzymes during the 4-hour incubation period. Absorbance values at 570 nm measured from the cell-free wells were subtracted from the absorbance values measured in the control and doxorubicin-treated wells as a background signal. The absorbance values measured from 6 technical replicas in each group were averaged. The percent (%) survival in the drug-treated groups compared to the control group was calculated by dividing the mean absorbance value in each of the doxorubicin-administered groups by the mean absorbance value into the unmedicated control group and multiplying by 100. The % survival responses obtained were plotted against doxorubicin concentrations on a logarithmic scale. Sigmoidal concentration response curves that best describe the data points were obtained using 4-parameter non-linear regression analysis in GraphPad Prism9 software. The resistance indexes (RI) of resistant AGS/Dox cells were calculated by dividing the half maximal inhibitory concentration (IC50) values of resistant cells into parental cells IC50.

2.3 Establishment of Cell Lines That Show Different Levels of Resistance to Doxorubicin

2.3.1 Establishing Resistant AGS Cells by Continuous Exposure to 10 nM Doxorubicin (AGS/Dox_Pro10s)

In our study, we developed resistant cells through continuous exposure to doxorubicin. Cells were first seeded in 6-well plates at 50% confluency (500.000 cells/well). The next day, 10 nM doxorubicin was applied and kept in this medium for 3 days. Passaging was not required as the cells did not reach confluence during this time. Only the medium with doxorubicin on the top of the cells was removed, and the newly prepared medium with 10 nM doxorubicin was added and the cells were incubated for 3 more days without passage. On the seventh day, the cells reached full confluency and were passage into new plates in numbers to be 50% confluent (500.000 cells/well). The next day, 10 nM doxorubicin administration was continued. With this protocol which we call Pro10, cells were passaged only once a week and incubated in 10 nM doxorubicin medium 6 days a week, except for 24 hours after passage.

Parallel to the AGS/Dox group developed with this protocol, AGS cells in the DMSO control group were exposed to an equimolar concentration of DMSO (0.1%), a

doxorubicin solvent. In the AGS cell control group, the cells were only incubated in the medium. MTT survival test was performed every 4 weeks and concentration-response curves and IC50 values were calculated accordingly.

2.3.2 Establishing Resistant AGS Cells by Continuous Exposure to 40 nM Doxorubicin (AGS/Dox_Pro40s)

At the second month of the Pro10 protocol mentioned above, AGS cells reached to a Doxorubicin IC50 value of 40 nM and start to tolerate this concentration in the continuous exposure. To understand the impact of doxorubicin concentration on the rate of acquired resistance, we splitted the cells into 2 at this point. In one arm we continued with Pro10. In the second arm, we started to expose AGS cells to 40 nM doxorubicin (Pro40) in parallel with the Pro10 protocol. MTT survival test was performed in every 4 weeks and concentration-response curves and IC50 values were calculated accordingly.

2.3.3 Establishment of P-gp Overexpressing AGS Cell Lines

Using a plasmid vector with catalog number RDC0891 containing the hMDR1 cDNA sequence in the VersaClone cDNA library from R&D Systems, we established P-gp overexpressing AGS cells. RDC0891 plasmid can be transferred to cells by transfection method and provides transient overexpression in cells. For this reason, we transferred the hMDR1 cDNA (~ 4000 bp) sequence in RDC0891 plasmid to a lentiviral plasmid capable of continuous expression. The gateway cloning method, which is known to have a high success rate in cloning long genetic structures, was chosen as the cloning method. In accordance with the Gateway cloning method, the sequence must first be transferred to a Gateway entry plasmid. In the next step, the sequence in the entry plasmid must be transferred by in vitro recombination via the enzyme clonase in the target viral (destination) plasmid. (This plasmid was generated with the help of Özen Leylek)

In the first step of gateway cloning method, we transferred hMDR1 cDNA (~ 4000 bp) sequence into pENTR1A no ccDB plasmid which is the Gateway entry vector. For this purpose, the hMDR1 cDNA sequence in the RDC0891 plasmid was amplified by polymerase chain reaction using the appropriate primer pair given in table 2-2 and cut by SalI and BamHI cleavage enzymes.

Table 2-2 Primer pairs to amplify hMDR1 cDNA sequence in the RDC0891 plasmid by the polymerase chain reaction

	5'→3'
Forward Primer	TCAGTCGACGCCACCATGGATCTTGA
Reverse Primer	ACCGGATCCCTGTCTCTTTGTTCCAG

A newly generated plasmid that was obtained after successfully transferring hMDR1 cDNA into pENTR1A no ccDB (Addgene Cat # 17398, this plasmid kindly provided by TBO Lab) was named pENTR1A_MDR1. pENTR1A_MDR1 plasmid was transformed into *E.coli* Stbl3 competent bacteria then individual colonies were picked and grown in liquid bacteria culture. To prove the ligation process was successful, pENTR1A_MDR1 plasmid isolated from bacteria was digested with SalI and BamHI enzymes to perform a diagnostic restriction test and the restriction products were run on the agarose gel (Figure 2-1). The cleavage of the pENTR1A_MDR1 plasmid with the restriction enzymes resulted in two-bands at the appropriate size range, indicating that the ligation was successful.

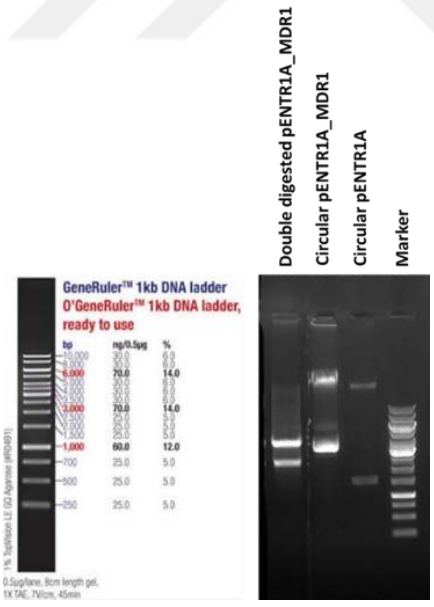

Figure 2-1 Diagnostic restriction testing of the pENTR1A_MDR1 plasmid. pENTR1A_MDR1 was cut with SalI and BamHI. The double band observed in the first column indicates the successful completion of the ligation process.

In the second step of the gateway cloning method, we transferred the hMDR1 cDNA sequence contained in the pENTR1A_MDR plasmid to the selected pLEX_307 (pLex306

plasmid kindly provided by TBO Lab) lentiviral expression plasmid. For this, we used the Gateway LR clonase II enzyme kit (Thermo Fischer Scientific, Cat # 11791020 (USA)). Following the protocol recommended by the company, appropriate amounts of pENTR1A_MDR plasmid, pLEX_307 plasmid, and LR clonase enzyme mixture were incubated at 25°C overnight. Afterwards, the reaction was terminated with proteinase K solution, and the reaction product was transformed into plasmid *E.coli* Stbl3 bacteria. After transformation, individual colonies were picked and grown in liquid bacteria culture and pLEX_307_MDR1 plasmid was isolated. Maps of plasmid vectors used for overexpressing P-gp were given in figure 2-2.

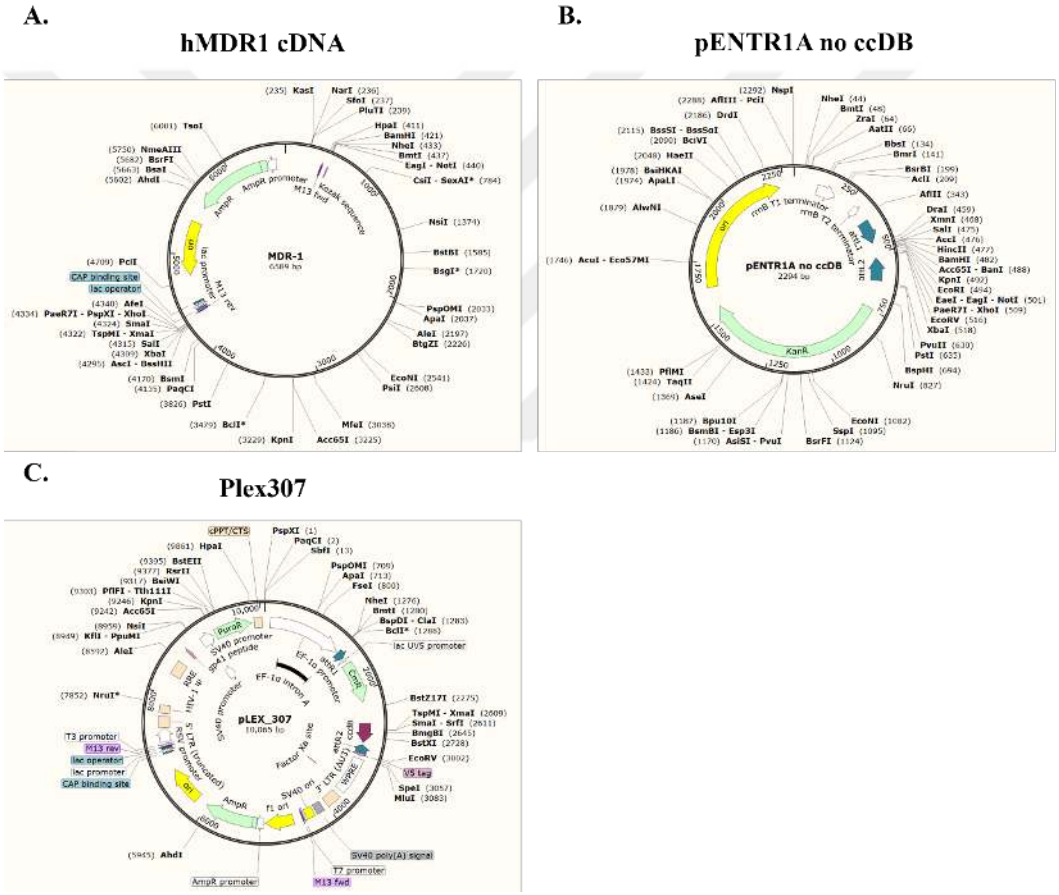

Figure 2-2 Plasmid vector maps used to generate P-gp overexpression plasmids **A.** RDC0891 hMDR-1 cDNA plasmid vector map **B.** pENTR1A no ccDB plasmid vector map **C.** Plex307 plasmid vector map

At the final step, we packed the plasmid pLEX_307_MDR1 by lentiviruses. For this purpose, pLEX_307_MDR1, viral packaging (psPAX2), and outer shell (pCMV-VSV-G) plasmids were transferred to HEK293T cells via transfection agent (Promega, FuGENE6). Viruses were collected and filtered from the supernatant of HEK293T cells

at 48 and 72 hours after transfection. The AGS cells were seeded one day before from infection process and infected with viruses with the protamine sulphate. Successfully infected AGS cells were selected with puromycin (mammalian selection marker, 8µg / ml). Cells that survived after puromycin selection was named "AGS/P-gp_Oexp".

2.4 Establishment of P-gp_NLS Overexpressing AGS Cell Lines

From the plasmid vector catalog number RDC0891, which contains the hMDR1 cDNA sequence in the VersaClone cDNA library from R&D Systems, we replicated the P-gp sequence with primers that allow us to add a nuclear localization signal to the P-gp sequence. Sequence of primers were given in table 2-3. Then we transferred P-gp_NLS sequence to a lentiviral plasmid plex307 which allows stable expression of the gene. Plasmid vectors were used to generate P-gp_NLS plasmids were given in figure 2-2. After that we transferred pLEX_307_MDR_P-gp_NLS, viral packaging (psPAX2), and outer shell (pCMV-VSV-G) plasmids to HEK293T cells via transfection agent (Promega, FuGENE6). Viruses were collected and filtered from the supernatant of HEK293T cells at 48 and 72 hours after transfection. The AGS cells were seeded one day before the infection process and infected with viruses with the protamine sulphate. Successfully infected AGS cells were selected with puromycin (mammalian selection marker, 8µg / ml). Cells that survived after puromycin selection was named "AGS/P-gp_NLS". The gateway cloning method, which is known to have a high success rate in cloning long genetic structures, was chosen as the cloning method. (This plasmid was designed and generated with the help of Alişan Kayabölen)

Table 2-3 Sequence of primers used to generate NLS-tagged P-gp overexpression plasmids.

P-gp-SalI_Kozak_ ATG_F1	GGTTCCAAGTCGACGCCACCATGGATCTTGAAGGGG ACG
P-gp-BamHI-NLS-R2	GTCGATGGATCCCACCTTTCTCTTTTTCTTGGGGCTC TGGCGCTTTGTTCCAGCC

2.5 Establishment of P-gp Knock-Out AGS/Dox Cells

2.5.1 CRISPR/Cas9 Genome Editing System

We planned to use the CRISPR/Cas9 genome editing system to obtain a resistant AGS/DOX cell model in which P-gp expression is knocked down. This system is based on the transfer of gRNA (guide RNA) sequences designed specifically for a specific gene and Cas9 enzyme, which create breaks in the DNA sequence of the target gene.

At this stage, guide RNA sequences specific to the hMDR1 gene were designed using the CHOP CHOP program, and three different guide RNAs were ordered to provide effective knockdown. Guide RNA sequences designed using the CHOP CHOP program are presented in figure 2-3. Cloning processes, in summary, include bringing the lower and upper chains of the guide RNA sequences into a double-stranded form suitable for cloning by annealing. Three different guide RNA sequences brought into this double-stranded form were then transferred to the pLentiCRISPRV2 plasmid vector treated with BsmBI restriction enzyme. This plasmid vector was chosen for its suitability for the lentiviral delivery system and for containing the Cas9 enzyme, which is readily available for genetic editing in human cells. After the guide RNA_1/2/3 sequences have been transferred into the pLentiCRISPRV2 plasmid vector (pLentiCRISPRV2-gRNA1/2/3), the packaging and outer shell plasmid vectors psPAX2 and pCMV-VSV-G with the "transfection reagent" (Promega, FuGENE6) into HEK293T cells using manufacturer's instructions transduced using the lentiviral transducing protocol. Resistant AGS/DOX cells were transduced into AGS/Dox cells using the “transfection reagent” (Promega, FuGENE6) with viruses collected from the supernatant of HEK293T cells at the end of the 2nd and 3rd days and the cells were selected with puromycin. Viral transmission method was chosen for achieving stable silencing of the P-gp. (This plasmid was designed with the help of Özlem Yedier and generated with the support of Özen Leylek)

ABCB1_gRNA1_Top: 5' CACCGTGACAAGTTGTATATGGTGG 3'

ABCB1_gRNA1_Bottom: 5' AAACCCACCATATACAACTTGTCAC 3'

ABCB1_gRNA2_Top: 5' CACCGCCAAACACCAGCATCATGAG 3'

ABCB1_gRNA2_Bottom: 5' AAACCTCATGATGCTGGTGTTTGGC 3'

ABCB1_gRNA3_Top: 5' CACCGTGGACTTCCTCTCATGATGC 3'

ABCB1_gRNA3_Bottom: 5' AAACGCATCATGAGAGGAAGTCCAC 3'

Figure 2-3 Guide RNAs that are designed for P-gp knock down by CRISPR/Cas9 genome editing system.

2.5.2 P-gp Knock-Down by siRNA Technology

Since CRISPR/Cas9 genome editing system was not successful to knock-down P-gp, possibly due to the polyploidy in AGS/Dox cells, we knocked down P-gp by siRNAs targeting the human *ABCB1* gene. For this, we used MISSION® esiRNA with EHU046651 catalog number. We used Universal siRNA negative control as siRNA control that does not have any known gene target.

At day 0, we seeded 200.000 AGS/Dox_Pro40c8 cells/well to 6 well plates. On day 1, we made P-gp siRNA transfection with Lipofectamine 3000 Reagent. We mixed and incubated Lipofectamine, optimem medium, and siRNA for 30 minutes at room temperature and added them into the cell medium drop by drop. Concomitantly, we transfected AGS/Dox cells in the control wells with control siRNA which does not have a known gene target. Only lipofectamine was given to reagent control groups. Then we incubated cells 3 days in a 37°C incubator.

2.6 Colony Formation Assay- Clonogenic Assay

Cells were seeded in 12-well plates at a cell count of 1000 cells/well. After waiting 24 hours for the cells to adhere completely to the plates, 8 different concentrations of doxorubicin were added to the treatment groups.

After the cells were kept in doxorubicin at the indicated concentrations or in a drug-free medium in the control group for 3 days, the medium was removed, cells were washed with PBS, and a fresh medium was added. After one week, cells were fixed with ice-cold

methanol by incubating for 10 minutes at 4°C. Then cells were washed with PBS and stained with crystal violet dye. The colonies were photographed with HP Scanjet G4050.

Colonies were counted by using the Adobe Photoshop Version: 24.0.0 Program. The % survival in the drug-treated groups compared to the control group was calculated by dividing the mean colony intensity value in each of the doxorubicin-administered groups by the mean colony intensity value in the untreated control group and multiplying by 100. The % survival responses obtained were plotted against doxorubicin concentrations on a logarithmic scale. Sigmoidal concentration response curves that best describe the data points were obtained using 4-parameter non-linear regression analysis in GraphPad Prism7 software.

2.7 Establishment of sub-cellular fractions and investigation of P-gp expression

In order to examine intracellular P-gp expression profiles, we aimed to obtain cell sub-fragments. For this purpose, we tried various methods suggested in the literature. Six of these methods made it possible to obtain various fractions. The protein concentration in these fractions obtained by these methods was measured by Bradford Assay. By this we aimed to load constant amount of protein loading onto SDS-polyacrylamide electrophoresis. Then protein expressions were evaluated by western blot. GAPDH was used as cytoplasmic fraction and whole cell lysate marker, Lamin for the nuclear fraction marker, and EGFR for the membrane fraction marker.

First, with the Kufer method, we could obtain cytoplasmic and nuclear fractions (Figure 2-4A) (Kufer et al., 2008). However, we observed cytoplasmic fraction contamination in the nuclear fraction. While we could obtain whole-cell lysate with the Schürrman method, we observed that we lost most of the proteins during the subcellular fractionation process and did not obtain enough protein. This method is inefficient because it requires too much increase in the number of cells for the fractionation process (Figure 2-4B) (Joost & Schürmann, 2001). With Baghirova Method, we aimed to obtain cytoplasmic and nuclear fractions. However, we observed Lamin expression in the cytoplasmic fraction (Figure 2-4C) (Baghirova et al., 2015). This protocol could not provide cytoplasmic fraction with high purity. Although the Ashida method enabled us to obtain nuclear fraction and whole cell lysate, it failed in isolation of cytoplasmic fraction (Figure 2-4D) (Ashida et al., 1996). Finally, using the Reap method, we could efficiently obtain subcellular fractions

(Figure 2-4E) (Suzuki et al., 2010). With this method, it is possible to get a high-purity nuclear fraction, cytoplasmic fraction, and whole-cell lysate.

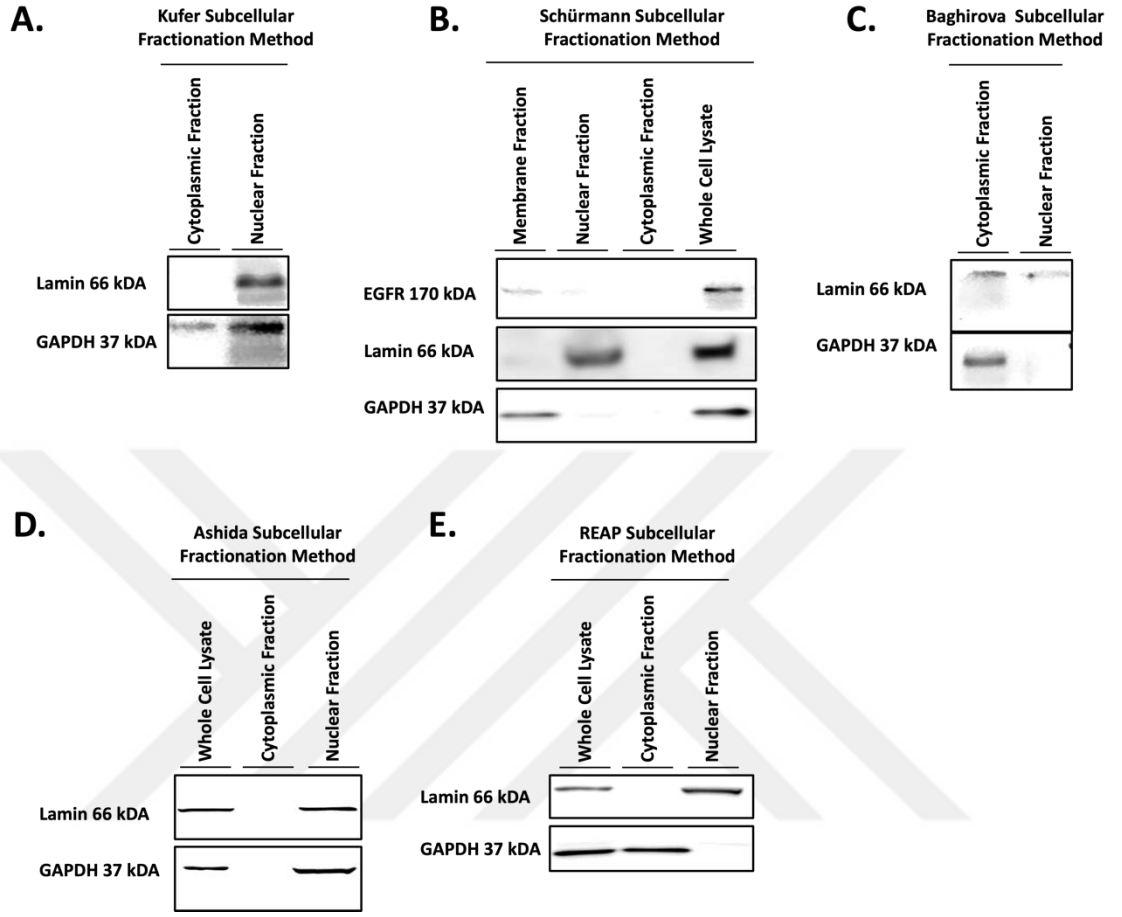

Figure 2-4 Testing the subcellular fractionation protocols by western blot. These subcellular fractionation methods were provided by **A.** Kufer etc. **B.** Schürmann etc. **C.** Baghirova etc. **D.** Ashida etc. **E.** Suzuki etc.

We decided to use the REAP method proposed by Suzuki et al. for subcellular fractionation (Suzuki et al., 2010). For this purpose, 500.000 cells were seeded to 10 cm plates and incubated for 24h for complete adherence to the plate surface. The next day, the medium was discarded, and cells are washed with dPBS. 1 mL dPBS was used to scrap cells. This dPBS and cells mixture was centrifugated 10 seconds at top speed of a benchtop microcentrifuge for 10 seconds. The supernatant was discarded, and pellets were dissolved in 900 µl 0.1% NP40 buffer. 300 µl of this solution was kept as whole cell lysate. The rest of the 600 µl of the solution was centrifugated again for 10 seconds at top speed. 300 µl of supernatant was kept as a cytoplasmic fraction. Then the supernatant was completely removed, and the pellet dissolved at 1 mL 0.1% NP40 buffer and centrifugated

for 10 seconds at top speed. The supernatant was removed, and the pellet was kept as the nuclear fraction.

Western blot method was used to investigate the expression of P-gp protein and other efflux pumps in these sub-cellular fractions.

2.8 Western Blot

Each sample was loaded onto the SDS-polyacrylamide electrophoresis gel at constant volumes. Western blotting was performed after electrophoresis, then the membranes were blocked with 5% Milk Powder and P-gp primary antibody. Membranes were treated with horseradish peroxidase-conjugated anti-rabbit secondary antibodies and chemiluminescent reagents (Pierce ECL substrates) were used for imaging. Imaging was done with LICOR Odyssey Fc (Blot imaging system) and signal size was calculated by densitometric technique. Rabbit anti-GAPDH (primary) and anti-rabbit (secondary) antibodies were used to evaluate GAPDH expression for loading control. Membranes were treated with rabbit polyclonal anti-human Lamin B1 primary antibody specific for nuclear Lamin B1 protein and goat-anti rabbit secondary antibody to control nuclear fractions.

2.9 qRT-PCR

A nucleospin RNA isolation kit (Macharey-Nagel, Germany) was used for RNA isolation by following the manufacturer's instructions. RNA sample concentrations were measured with Nanodrop.

For cDNA synthesis, 1000ng of total RNA was mixed with 2.5 µl of 2mM dNTPs and 1 µl of random hexamer enzyme. Total volume completed up to 16.5 µl with nuclease free water (NF-H2O). This mixture was incubated at 65°C for 5 minutes. After this incubation, RT mix (5 µl 5X First Strand (FS) buffer, 2 µl of DTT (0.1M) and 0.5 µl of RNasin) were added into each tube and incubated 10 minutes at room temperature. 1 µl MMLV-RT enzyme were added and incubated 37°C for 1 hour and 70°C for 15 minutes. Then 75 µl of nuclease free water was added.

qRT-PCR was performed by using SYBR green master mix (Roche, Switzerland), and LightCycler 480 instrument (Roche, Switzerland). 2 µl cDNA, 10 µl of SYBER Green, 1 µl primer mix (10 µM), and 7 µl nuclease free water mixed in LightCycler 480 Multiwell

Plate 96. All quantitative Real Time PCR experiments were carried out in triplicate with a total reaction volume of 20 µl. Plate covered with seal and centrifugated at 1300 rpm for 2 minutes.

qPCR reaction was performed in LightCycler 480 instrument with the following conditions: 95°C for 5 minutes, 45 cycles of (95ºC for 10 seconds, 60ºC for 30 seconds and 72ºC for 30 seconds) and 4ºC ∞. Relative gene expressions were calculated by using ΔΔCt method, and housekeeping gene GAPDH was used as the reference gene. Primers used in qRT-PCR experiments were given in Table 2-4.

Table 2-4 Primer pairs to the hMDR1 gene

	5'→3'
Forward Primer	ACAGAGGGGATGGTCAGTGT
Reverse Primer	TCACGGCCATAGCGAATGTT

2.10 Investigation of Intracellular distribution of P-gp protein by immunofluorescence method

Cells were seeded on glass slides into 12 wells of plates at 200.000 cells per plate. After reaching a 70% confluence level in each plate, the medium was removed from the wells and washed with PBS to get rid of metabolic wastes and dead cells. Then cells were fixed with 4% paraformaldehyde. The pores were opened in the cells by using 1% TritonX100/PBS solution. 10% goat serum/PBS mixture was used for blocking, and it was aimed to get rid of non-specific antibody bindings. It was then incubated with the P-gp antibody overnight at 4°C.After primary antibody incubation, cells washed 3 times with PBS. Then, cells were incubated with Alexa Fluor 594 (red) secondary antibody for 1 hour at 37°C. After rewashing, the nuclei were stained blue with a vectashield solution containing DAPI. We imaged at least three different regions of each condition. Images were taken using Leica DMI8 SP8 CS/DLS microscope at 40x magnification. At least 20 cells were analyzed for each condition. In all images, a "region of interest" (ROI) was determined in the cytoplasm and nucleus, and the intensity of the P-gp signal in the cytoplasm and nucleus was measured separately by using Image J software. To calculate

P-gp densities, intensities of related ROI were divided into an area of related ROI. To draw density graphs, we used GraphPad Prism9 software.

2.11 Investigation of the intracellular distribution of doxorubicin

To examine the intracellular distribution of doxorubicin, 300.000 cells were seeded in 0.16-0.19 mm thick glass-bottom culture dishes suitable for viewing under a confocal microscope, 24 hours after they were transferred to media containing doxorubicin and observed under a confocal microscope over time. Although doxorubicin has autofluorescence, it was not possible to visualize it at low concentrations. 1.6 µM of doxorubicin was determined as the optimum concentration at which its own fluorescence could be seen. Cells were incubated in 37ºC incubators. The cells were excited with a laser at 488 nm, the excitation maximum of doxorubicin, and monitored under emission at 590 nm. We imaged at least three different regions of each condition. Images were taken using Leica DMI8 SP8 CS/DLS microscope at 40x magnification. At least 20 cells were analyzed for each condition. In all images, a "region of interest" (ROI) was determined in the cytoplasm and nucleus, and the intensity of the doxorubicin signal in the cytoplasm and nucleus was measured separately by using Image J software. To calculate doxorubicin densities, intensities of related ROI were divided into an area of related ROI. To draw density graphs, we used GraphPad Prism9 software.

2.12 Investigation of the Effect of P-gp Inhibitors on the Kinetics of Nuclear Efflux of Doxorubicin

To view the nuclear efflux kinetics of doxorubicin with confocal microscopy, cells were seeded in 0.16-0.19 mm thick glass-bottom culture dishes at 300.000 cells per dish. After an overnight incubation period for the cells to fully adhere, the cells were exposed to 40 µM verapamil and 1 µM zosuquidar for two hours. The cells were then exposed to 1.6 µM doxorubicin for one hour, six hours, and twenty-four hours. The cells were excited with a laser at 488 nm, the excitation maximum of doxorubicin, and monitored under emission at 590 nm. In all images, a "region of interest" (ROI) was determined in the cytoplasm and nucleus, and the intensity of the doxorubicin signal in the cytoplasm and nucleus was measured separately. Images were taken using Leica DMI8 SP8 CS/DLS microscope at 40x magnification. At least 20 cells were analyzed for each condition. To

calculate doxorubicin densities, intensities of related ROI were divided into an area of related ROI. To draw density graphs, we used GraphPad Prism9 software.

2.13 Statistics Analysis

Measurement of P-gp level by Western blot, examination of intracellular P-gp distribution by immunofluorescence method, and cytotoxicity studies to generate doxorubicin concentration-response curves were repeated at least 3 different times as triplicates per experiment. Each confocal examination was repeated for at least 20 cells in each of the experiment and control groups. To examine the correlation between P-gp expression, doxorubicin IC50 values, and the nucleus/cytoplasm doxorubicin concentration ratio, the Pearson correlation constant (r) was calculated. $0.5 < r < 1$ was considered a measure of a positive correlation. Student's t-test was used to test whether silencing or overexpressing P-gp in cells causes a statistically significant difference in doxorubicin IC50 values compared to parental cells. A one-way ANOVA test was used to evaluate whether doxorubicin efflux kinetics are different from parental AGS cells in AGS/Dox cells and P-gp overexpressing AGS cells. Similarly, a one-way ANOVA test was used to evaluate the difference between the potency of P-gp inhibitors to inhibit the drug efflux from the cytoplasm and nucleus separately. The p-value of <0.05 will be used as the measure of statistical significance.

3. RESULTS

CHAPTER I

3.1 Establishment of Doxorubicin Resistant Gastric Adenocarcinoma Cell Models (AGS/Dox)

To understand the relation between acquired resistance, nuclear P-gp expression, and nuclear sparing, we established gastric adenocarcinoma cell lines that show different levels of resistance to doxorubicin. For this purpose, we exposed AGS gastric adenocarcinoma cells to 10 nM doxorubicin continuously. In parallel with that in control groups, we have grown cells in a doxorubicin-free medium. Since DMSO was used as the solvent of doxorubicin, in DMSO control groups we exposed AGS cells to an equimolar concentration of DMSO. After that, we investigated the concentration-response curves for doxorubicin and calculated IC50 values at regular intervals. At the end of 2 months, we observed that the cells could tolerate 40 nM of doxorubicin. After that, we continued with two different protocols where we incubated cells either with 10 nM or 40 nM of doxorubicin which we call Protocol10 (Pro10) and Protocol40 (Pro40), respectively. Thus, we aimed to determine the dependence of the resistance index, nuclear sparing, and P-gp expression on the doxorubicin concentration. Using these protocols, we obtained 12 different AGS/Dox cell lines with different resistance indexes. The concentration-response curves and resistance indexes for these AGS/Dox models with varying sensitivities to doxorubicin are given in figure 3-1.

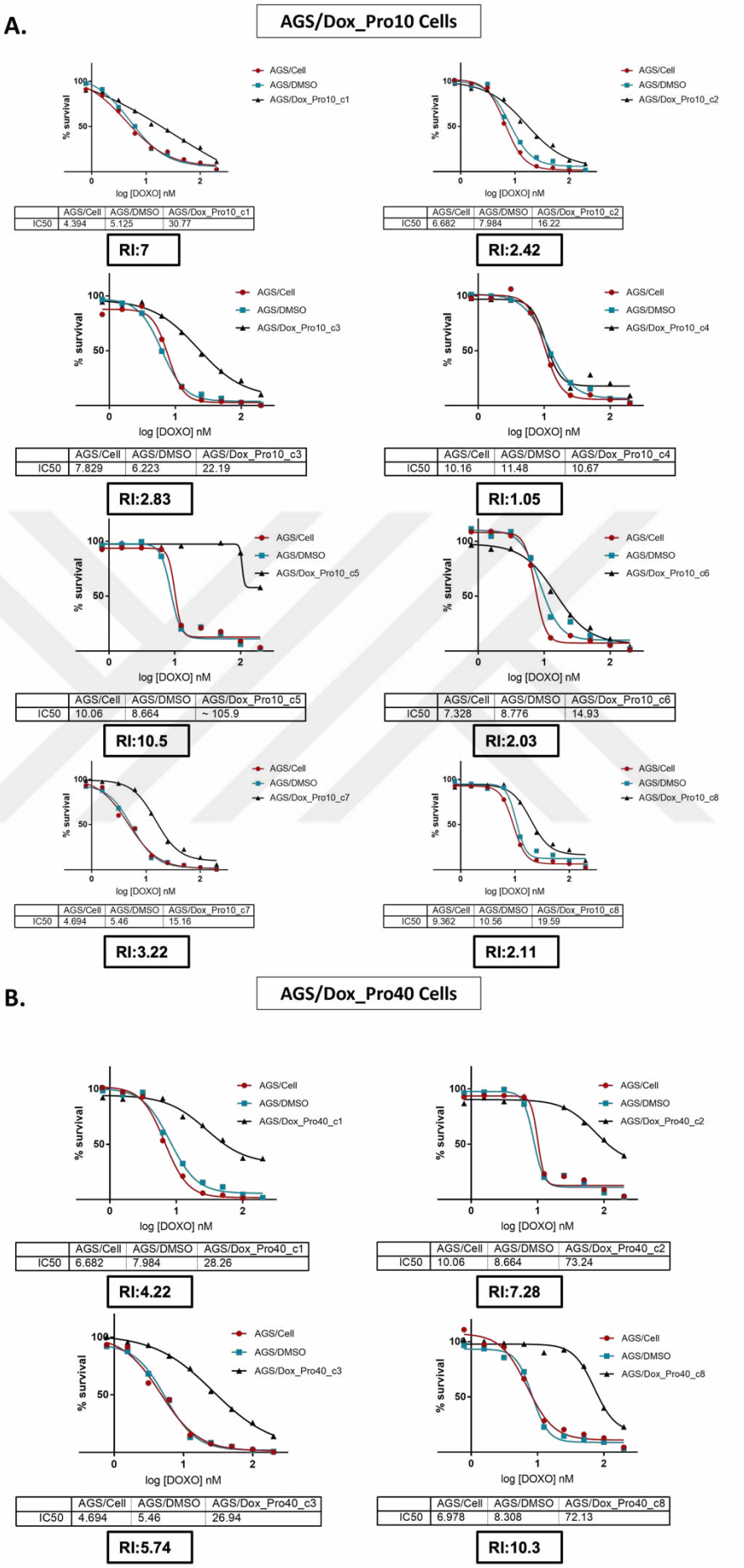
A.
AGS/Dox_Pro10 Cells
AGS/Cell
AGS/DMSO
AGS/Dox_Pro10_c1
% survival
log [DOXO] nM
AGS/Cell | AGS/DMSO | AGS/Dox_Pro10_c1
IC50 | 4.394 | 5.125 | 30.77
RI:7
AGS/Dox_Pro10_c2
AGS/Cell | AGS/DMSO | AGS/Dox_Pro10_c2
IC50 | 6.682 | 7.984 | 16.22
RI:2.42
AGS/Dox_Pro10_c3
AGS/Cell | AGS/DMSO | AGS/Dox_Pro10_c3
IC50 | 7.829 | 6.223 | 22.19
RI:2.83
AGS/Dox_Pro10_c4
AGS/Cell | AGS/DMSO | AGS/Dox_Pro10_c4
IC50 | 10.16 | 11.48 | 10.67
RI:1.05
AGS/Dox_Pro10_c5
AGS/Cell | AGS/DMSO | AGS/Dox_Pro10_c5
IC50 | 10.06 | 8.664 | ~ 105.9
RI:10.5
AGS/Dox_Pro10_c6
AGS/Cell | AGS/DMSO | AGS/Dox_Pro10_c6
IC50 | 7.328 | 8.776 | 14.93
RI:2.03
AGS/Dox_Pro10_c7
AGS/Cell | AGS/DMSO | AGS/Dox_Pro10_c7
IC50 | 4.694 | 5.46 | 15.16
RI:3.22
AGS/Dox_Pro10_c8
AGS/Cell | AGS/DMSO | AGS/Dox_Pro10_c8
IC50 | 9.362 | 10.56 | 19.59
RI:2.11
B.
AGS/Dox_Pro40 Cells
AGS/Dox_Pro40_c1
AGS/Cell | AGS/DMSO | AGS/Dox_Pro40_c1
IC50 | 6.682 | 7.984 | 28.26
RI:4.22
AGS/Dox_Pro40_c2
AGS/Cell | AGS/DMSO | AGS/Dox_Pro40_c2
IC50 | 10.06 | 8.664 | 73.24
RI:7.28
AGS/Dox_Pro40_c3
AGS/Cell | AGS/DMSO | AGS/Dox_Pro40_c3
IC50 | 4.694 | 5.46 | 26.94
RI:5.74
AGS/Dox_Pro40_c8
AGS/Cell | AGS/DMSO | AGS/Dox_Pro40_c8
IC50 | 6.978 | 8.308 | 72.13
RI:10.3

Figure 3-1 Concentration-response curves of AGS/Dox cell models with varying levels of resistance to doxorubicin **A.** Concentration-response curves of AGS cells continuously exposed to 10 nM doxorubicin (AGS/Dox Pro10-cells) **B.** AGS cell lines exposed to 40 nM doxorubicin (AGS/Dox Pro40-cells)

By continuous exposure to doxorubicin, we expected to see gradually increasing resistance index pattern. Contrary to our expectations, these AGS/Dox cells did not show a gradually increasing resistance to doxorubicin but rather exhibited a fluctuation in resistance indexes. We thought that AGS/Dox cells might develop adaptive changes during prolonged exposure to doxorubicin, and these adaptive changes may cause variable resistance index. In Pro10 cells, RI values were between 1.05 to 10.5. In Pro40 cells, RI values were between 4.22 to 10.3. When we compare both protocols, in the Pro40 protocol, the resistance index increased in a more stable pattern throughout the exposure to doxorubicin.

3.2 Intracellular Distribution of P-gp in AGS and AGS/Dox Cells

To understand whether nuclear P-gp has a role in doxorubicin resistance, we investigated the intracellular distribution of P-gp in all AGS models with immunofluorescence methods. Immunofluorescence images were obtained from parental AGS cells, doxorubicin-resistant AGS/Dox cells and DMSO control cells, using P-gp monoclonal antibody. Densitometric analysis was performed on the images to assess the level of P-gp expression in the nucleus. These investigations were performed for all 12 AGS/Dox concomitantly with their corresponding AGS control and DMSO control models. In all of these 12 AGS/Dox cells following similar patterns, we observed nuclear P-gp expression highest in the resistant cell lines compared to control cells. Since we achieved a stable resistance in AGS/Dox-Pro40 cycle 8 cells, we present the immunofluorescent images for this model in Figure 3-2.

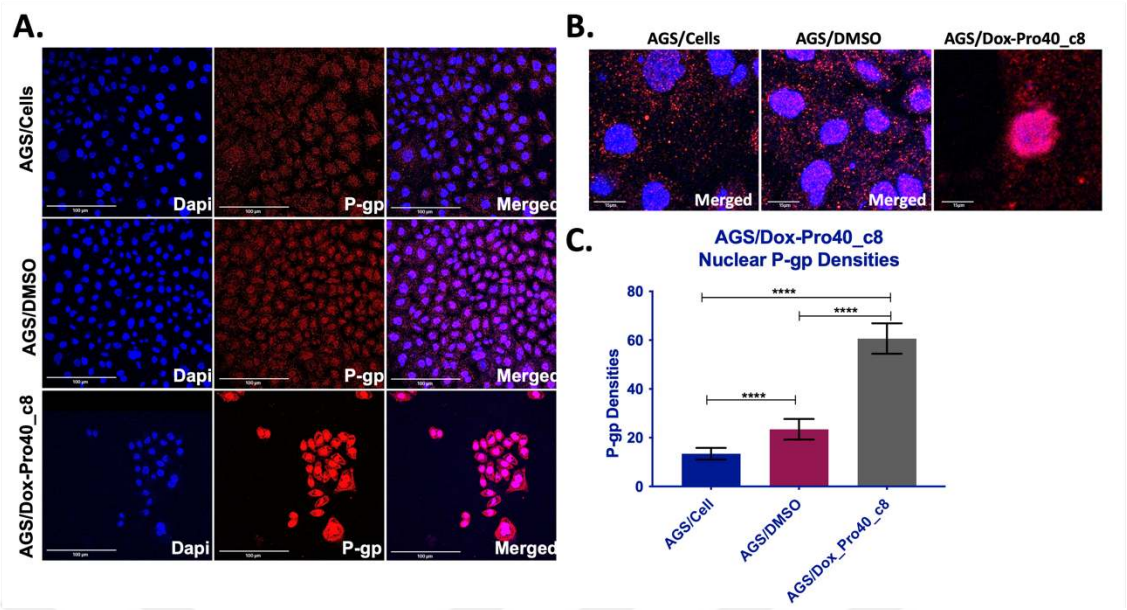

Figure 3-2 Intracellular distribution of P-gp in parental and doxorubicin resistant cells **A**. Immunofluorescence images obtained from parental AGS cells, doxorubicin-resistant AGS/Dox-Pro40_c8 cells. Scale bar, 100 µm. **B.** Zoomed in images obtained from parental AGS cells, doxorubicin-resistant AGS/Dox-Pro40_c8 cells and AGS DMSO control cells. Scale bar, 15 µm. **C.** their densitometric analysis. The nucleus is stained with DAPI (blue), and P-glycoprotein is immunolabelled with AlexaFLuor 594 tagged antibody (red). (20 cells/experiment, ordinary one-way ANOVA, * $p<0.05$, ** $p<0.01$, *** $p<0.001$, **** $p<0.0001$)

In figure 3-2, nuclear staining with DAPI is seen blue, and the staining for P-gp is seen red. Merged images of AGS, DMSO control and AGS/Dox cells are also given in those figures (pink). We observed a significant increase in the expression of P-gp throughout the cell in AGS/Dox compared to AGS control. However, this increase was more prominent in the nucleus as can be seen better in figure 3-2B which shows the high-resolution images. We observed a slight increase in the nuclear expression of P-gp in DMSO control cells. However, this increase was not as prominent as that was observed in AGS/Dox-Pro40_c8 cells.

3.3 Investigation of Nuclear P-gp Expression in Western Blots

To examine the differences in nuclear P-gp expression and confirm the results obtained by the immunofluorescence method, we performed subcellular fractionation of AGS cell

models. Then we investigated the P-gp expression in those subcellular fractions by the western blot technique.

P-gp expression in the nuclear fraction, cytoplasmic fraction, and general cell lysates was prepared by REAP method, which yielded the highest efficiency in obtaining nuclear fraction. In the western blot images, P-gp signals in the nuclear fraction were divided into the Lamin protein signal, which is a nuclear membrane housekeeping protein. GAPDH protein was visualized as the cytoplasmic fraction housekeeping control and the overall cell lysate loading control.

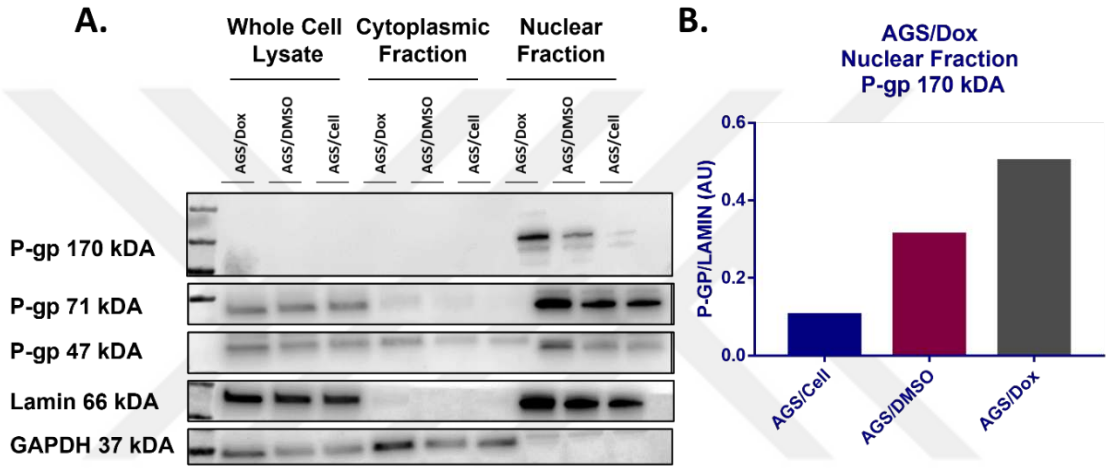

Figure 3-3 A. Evaluation of P-gp expression by western blot in intracellular fractions obtained by REAP method. **B.** Densitometric analysis of P-gp expression in the nuclear fraction.

Western Blot results confirmed that nuclear expression of P-gp increased in the resistant AGS/Dox cells compared to parental control and DMSO control cells (Figure 3-3).

Then, we analyzed the correlation between nuclear P-gp expressions and the resistance index of all 12 resistant cell lines (Figure 3-4).

A.

	Resistance Index
AGS/Dox-Pro10_c4	1.05
AGS/Dox-Pro10_c6	2.03
AGS/Dox-Pro10_c8	2.11
AGS/Dox-Pro10_c2	2.42
AGS/Dox-Pro10_c3	2.83
AGS/Dox-Pro10_c7	3.22
AGS/Dox-Pro40_c1	4.22
AGS/Dox-Pro40_c3	5.74
AGS/Dox-Pro10_c1	7
AGS/Dox-Pro40_c2	7.28
AGS/Dox-Pro40_c5	10.3
AGS/Dox-Pro10_c5	10.5

B.

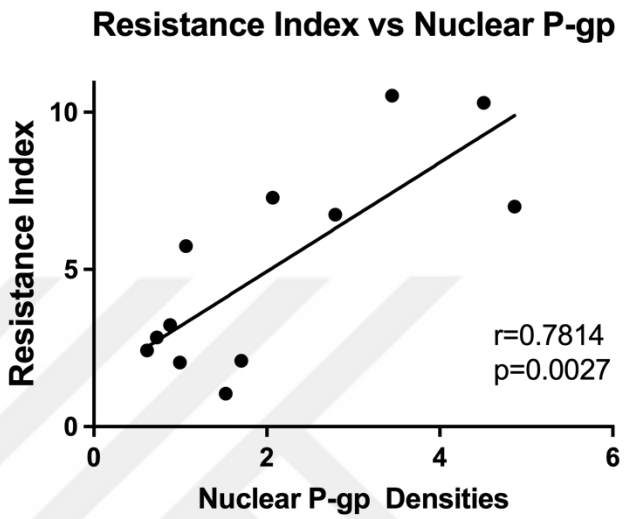

Figure 3-4 A. AGS/Dox cells and their corresponding resistance indices. B. Resistance index vs nuclear P-gp expression correlation graphics.

We observed that nuclear P-gp expression increased in correlation with increasing resistance index. This data with a Pearson correlation constant (r) of 0.7, was statistically significant (p=0.0027).

3.4 Intracellular Distribution of Doxorubicin in AGS and AGS/Dox Cells

Concomitantly with the immunofluorescence and western blot studies, we investigated the intracellular distribution of doxorubicin with a confocal microscope using the autofluorescence property of the doxorubicin. We exposed AGS and AGS/Dox cells to 1.6 µM doxorubicin for 24 hours. Then we removed the media, washed the cells with PBS, and imaged them under a fresh medium. Doxorubicin distribution in AGS, AGS/DMSO, and AGS/Dox cells are shown in figure 3-5.

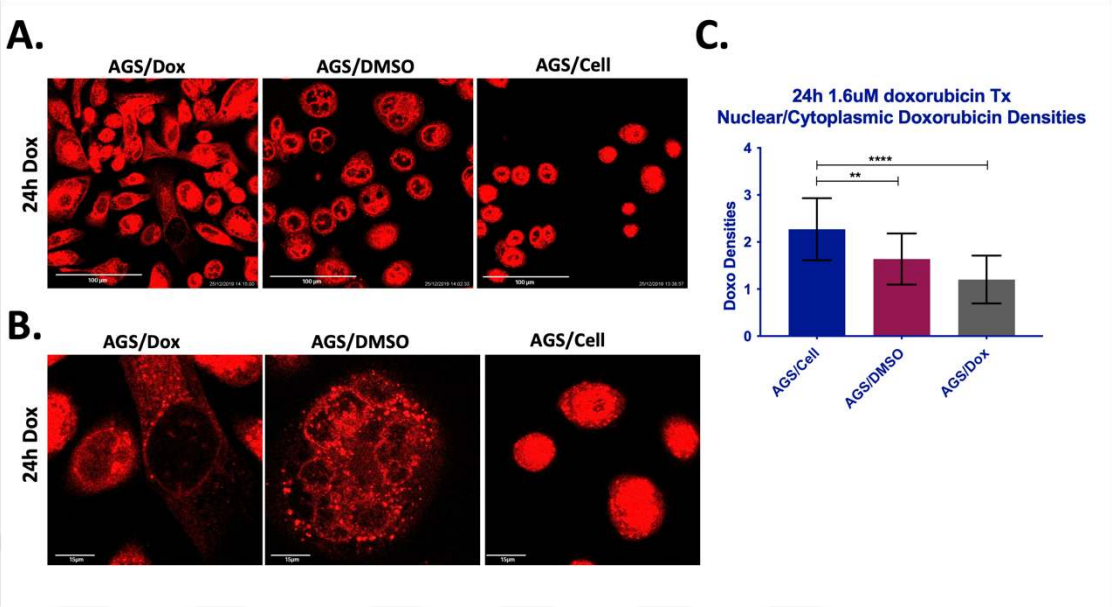

Figure 3-5 A. Intracellular distribution of Doxorubicin in parental AGS cells, AGS/DMSO and doxorubicin resistant AGS/Dox cells after 24h treatment with doxorubicin. (Scale bar, 100 µm) **B.** Zoomed in images to nucleus of cells (Scale bar, 15 µm) and **C**. their densitometric analysis. (20 cells/experiment, ordinary one-way ANOVA, * $p<0.05$, ** $p<0.01$, *** $p<0.001$, **** $p<0.0001$)

In densitometric analysis, we observed that doxorubicin predominantly accumulated in the nucleus of sensitive cells (AGS cells). In our AGS/DMSO cells, doxorubicin predominantly accumulates at the nucleus however, there was a slight decrease compared to naive AGS cells. But the most prominent difference was in AGS/Dox resistant cells. In AGS/Dox resistant cells nuclear density of doxorubicin was significantly low compared control cells, despite the presence of drug at cytoplasm.

A slight decrease in the DMSO control groups might suggest the involvement of DMSO in the process. In DMSO control cells cytoplasmic doxorubicin concentration was also low, different than AGS/Dox cells. Since studies in the literature suggest that DMSO can increase the membrane permeability and our studies showed that replacement of doxorubicin-containing medium with doxorubicin-free medium lead to a rapid decline in doxorubicin signal in these cells, we thought that passive diffusion of doxorubicin is involved in the changes we observed in DMSO control cells (de Ménorval et al., 2012). On the other hand, in AGS/Dox cells, the nuclear density of doxorubicin was low, despite

a cytoplasmic density slightly greater than that of AGS cells. And nucleus/cytoplasmic ratio of doxorubicin was lowest in AGS/Dox cells suggesting an active displacement of the nuclear doxorubicin pool to the cytosolic pool.

3.5 Assessment of the Role of DMSO

Our studies on the intracellular distribution of doxorubicin suggested that DMSO used as a drug solvent itself may interfere with the influx and efflux kinetics of doxorubicin. Additionally, we observed that a prolonged exposure to DMSO even at very low concentrations (0.1%) may lead to the upregulation of nuclear P-gp expression and a slight increase in resistance to doxorubicin.

To assess the role of DMSO on P-gp expression, we exposed AGS cells to either 0.1% DMSO or 1% DMSO for one week. Then, we performed subcellular fractionation by REAP method and we investigated the P-gp expression in nuclear, cytoplasmic fractions, and whole cell lysates by western blot. P-gp signals in the nuclear fraction were divided into the nuclear Lamin protein signal, for normalization. GAPDH protein was visualized as the cytoplasmic fraction housekeeping control and the overall cell lysate loading control (Figure 3-6).

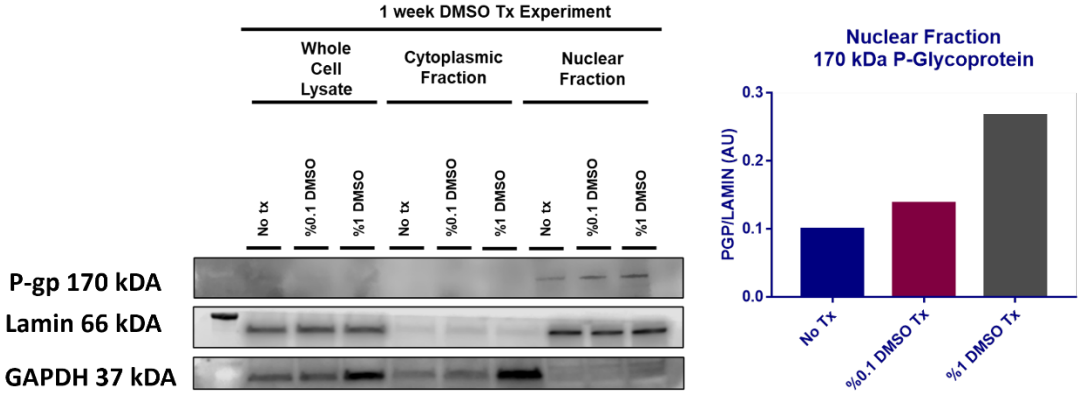

Figure 3-6 The effect of DMSO on nuclear P-gp expression. P-gp expression in AGS cells after 1-week DMSO treatment was investigated by western blot in intracellular fractions obtained by REAP method. Densitometric analysis was performed on western blot images to assess P-gp expression.

Our western blot results shown in figure 3-6 demonstrated that the nuclear expression of P-gp has been affected by DMSO. Nuclear P-gp expression gradually increased by increasing the concentration of DMSO. Nuclear P-gp expression in 1% DMSO-treated

group was almost 3 times higher than the control group. These findings together with our previous observations suggested that long-term exposure to low-dose DMSO and short-term exposure to high-dose DMSO may increase nuclear expression of the P-gp.

3.6 Establishment of Doxorubicin Resistant Gastric Adenocarcinoma Cell Models by Using Saline as a Doxorubicin Solvent (AGS/Dox-Saline)

Our most prominent results were in AGS/Dox resistant cells. However, we observed that DMSO may interfere with P-gp expression and influx/efflux kinetics of doxorubicin, the requirement to exclude the interference of the DMSO in doxorubicin-induced changes arises. For this purpose, we re-followed the protocol that we used to establish doxorubicin-resistant gastric adenocarcinoma cell models (AGS/Dox) previously but used doxorubicin dissolved in saline.

We exposed AGS gastric adenocarcinoma cells to 10nM doxorubicin, dissolved in saline, continuously. In parallel with that in control groups, we have grown cells in a doxorubicin-free medium, and in saline control, cells are exposed to an equimolar concentration of saline. After that, we investigated the concentration-response curves for doxorubicin and calculated IC50 values at regular intervals. At the end of 2 months, we continued with two different protocols where we incubated cells either with 10 nM or 40 nM of doxorubicin which we call Saline-10 and Saline-40, respectively. Thus, we aimed to investigate the evolution of resistance index, nuclear sparing, and P-gp expression under the influence of doxorubicin but without the interference of DMSO.

Using these protocols, we got 10 different AGS/Dox cell lines with different resistance indexes. As like in AGS/Dox-DMSO cells, newly generated AGS/Dox-Saline cells also did not show a gradually increasing resistance to doxorubicin but rather exhibited a fluctuation in resistance indexes. Also, in the Saline-40 protocol, the resistance index was higher than in the Saline-10 protocol. The resistance index comparison graphics of AGS/Dox-Saline and AGS/Dox-DMSO cells by time in the two protocols are given in figure 3-7.

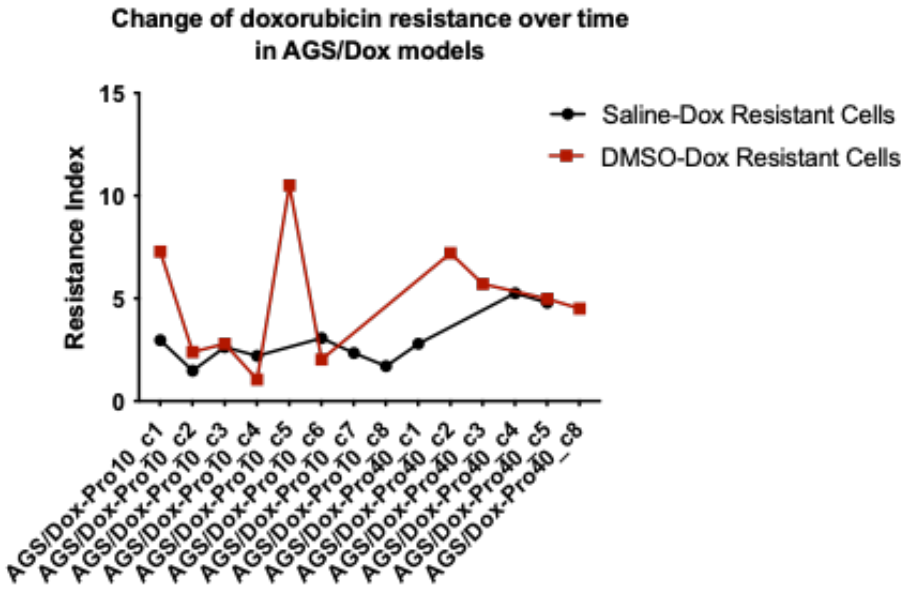

Figure 3-7 The pattern of the increase in resistance index through time in doxorubicin resistance cells established with doxorubicin dissolved in Saline (Saline-Dox) or DMSO (DMSO-Dox).

AGS/Dox cells that were established with doxorubicin in DMSO exhibited more fluctuation in the resistance index. However, the increase in the resistance index of AGS/Dox cells with doxorubicin in Saline was more stable and gradual.

All these data suggested that the changes in the nuclear P-gp expression, resistance index and intracellular distribution of doxorubicin we observed in AGS/Dox cells established with exposure to doxorubicin in DMSO, may not only reflect the effect of doxorubicin but also DMSO. Therefore, we started to repeat all the investigations in AGS/Dox-Saline cells.

3.7 Intracellular Distribution of P-gp in AGS/Dox-Saline cells Compared to the AGS/Dox-DMSO cells

To investigate the intracellular distribution of P-gp in AGS/Dox-Saline cells and compare it with AGS/Dox-DMSO cells, we observed P-gp localization by using the immunofluorescence technique. Immunofluorescence images were obtained from AGS/Dox-Saline-40 cells and AGS/Dox-DMSO cells are given in figure 3-8.

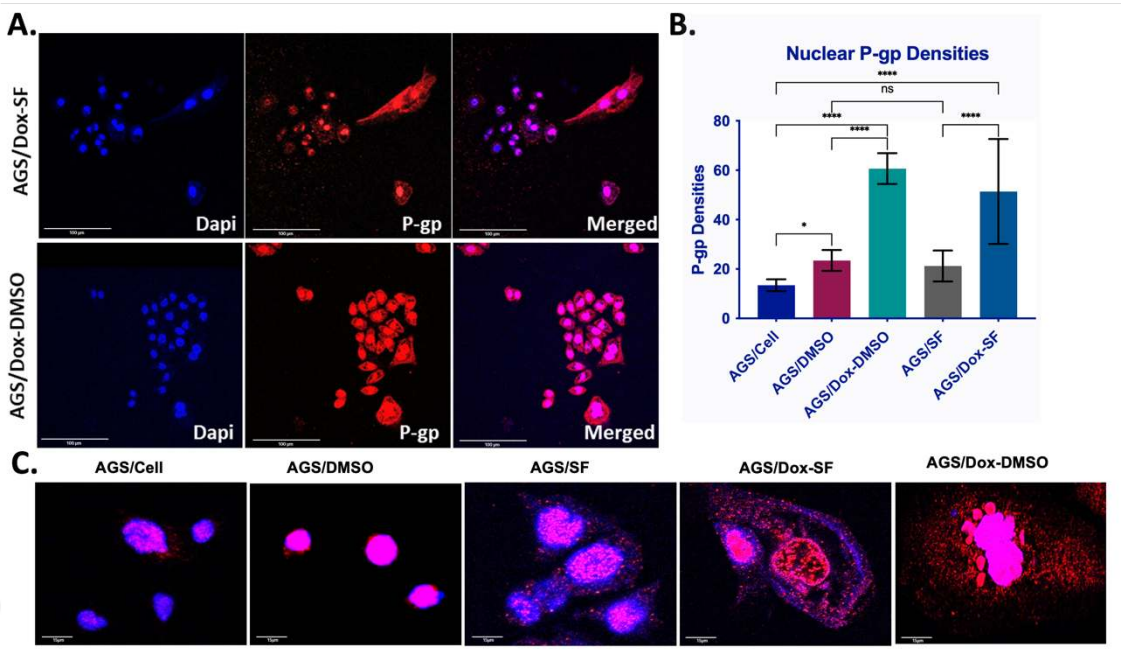

Figure 3-8 Intracellular distribution of P-gp in AGS/Dox-Saline and AGS/Dox-DMSO cells **A.** P-gp immunofluorescence images obtained from parental AGS/Dox-Saline and AGS/Dox-DMSO cells. Scale bar, 100 µm. **B.** and their densitometric analysis. **C.** Zoomed in nuclear images of AGS/Dox-SF and AGS/Dox-DMSO cells and their parental control cells. Scale bar, 15 µm. The nucleus was stained with DAPI (blue), and P-glycoprotein was immunolabelled with AlexaFluor 594 tagged antibody (red). Scale bar, 10 µm. (20 cells/experiment, ordinary one-way ANOVA, * $p<0.05$, ** $p<0.01$, *** $p<0.001$, **** $p<0.0001$)

We observed a significant increase in the expression of P-gp throughout the cell in both AGS/Saline and AGS/Dox-Saline cells compared to AGS control. This increase is more prominent in the nucleus of those cells like the AGS/Dox-DMSO cells. Although AGS/Dox-DMSO and AGS/DMSO cells had slightly higher P-gp expression compared to AGS/Dox-Saline and AGS/Saline cells, this difference is not statistically significant. These observations suggested that even saline can increase the nuclear expression of P-gp.

3.8 Intracellular Distribution of Doxorubicin in AGS/Dox-Saline cells Compared to the AGS/Dox-DMSO cells

We investigated the intracellular distribution of doxorubicin in AGS/Dox-Saline cells under the confocal microscope and compared it with AGS/Dox-DMSO cells. We exposed those cells and their control groups to 1.6 µM doxorubicin for 24 hours (Figure 3-9).

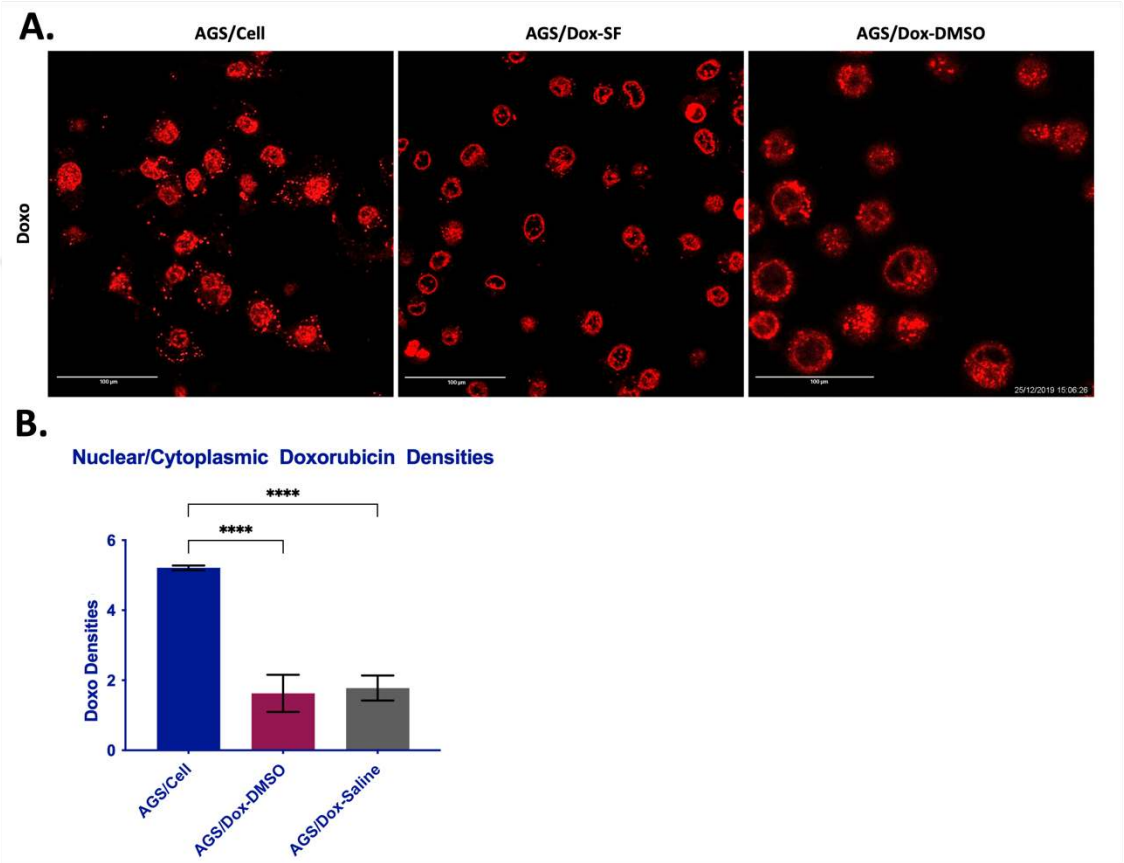

Figure 3-9 A. Intracellular distribution of doxorubicin in AGS/Dox-Saline and AGS/Dox-DMSO cells and **B.** their densitometric analysis. Scale bar, 100 µm. (20 cells/experiment, ordinary one-way ANOVA, * $p<0.05$, ** $p<0.01$, *** $p<0.001$, **** $p<0.0001$)

Nuclear accumulation of doxorubicin in both AGS/Dox-Saline and AGS/Dox-DMSO was lower compared with control cells. And they have a highly similar pattern of nuclear/cytoplasmic doxorubicin ratio.

All those findings suggest that even though DMSO slightly increased the nuclear P-gp expression, this increase does not statistically significantly affect the nuclear sparing and resistance patterns of resistance cells to doxorubicin. Since the resistance index of

AGS/Dox-DMSO-Pro40-c8 cells were more stable than the resistance index of AGS/Dox-Saline-Pro40-c8 cells, we continued our experiments with AGS/Dox-DMSO-Pro40-c8 AGS/Dox cells.

CHAPTER II

Our studies with doxorubicin-resistant AGS gastric adenocarcinoma cells mentioned above suggested that increased expression of nuclear P-gps may be an important mechanism for nuclear sparing and acquired resistance to doxorubicin in gastric cancer. Based on these findings, we investigated whether overexpressing the P-gp in naive AGS cells, changes the nuclear/cytoplasmic doxorubicin concentration ratio, nuclear efflux kinetics, and IC50 values here.

3.9 The Establishment of a P-gp Overexpressing Gastric Adenocarcinoma Cell Model (AGS/P-gp_Oexp)

To test whether overexpression of the P-gp in naive AGS cells can induce nuclear sparing and resistance to doxorubicin, we established P-gp overexpressing AGS cells. We used a commercially available plasmid vector to obtain P-gp cDNA sequence. This plasmid provides transient overexpression in cells, but we want a stable expression of P-gp in our cells. For this we transferred the P-gp cDNA (~ 4000 bp) sequence to a lentiviral plasmid capable of stable expression of P-gp. The gateway cloning method was used for cloning. Plasmid packaging was performed in HEK293T cells. Viruses were collected from HEK293T cells to infect AGS cells. AGS cells overexpressing P-gp (AGS/P-gp_Oexp) were selected with puromycin.

After that, we investigated the concentration-response curves for doxorubicin and calculated IC50 values. We observed that the AGS/P-gp_Oexp cells have a doxorubicin IC50 value of 1.24 μM and a resistance index of 416 compared with parental AGS cells. The concentration-response curves and resistance indexes for these cells are given in figure 3-10.

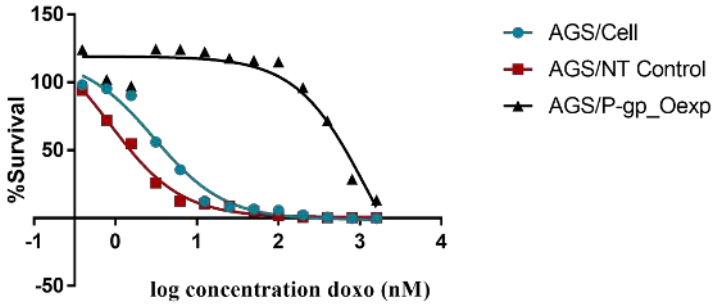

	AGS/Cell	AGS/NT Control	AGS/P-gp_Oexp
IC50	2.986	0.8588	1243

Figure 3-10 Concentration-response curve of P-gp overexpressing AGS/P-gp_Oexp cells.

3.10 Investigation of P-gp Expression in AGS/P-gp_Oexp Cells

To validate the increase in P-gp expression in AGS/P-gp_Oexp cells, we use qPCR and Western blot methods.

In qPCR experiments, we investigated the increase in P-gp at mRNA level. For this purpose, we prepared cDNA from AGS/P-gp_Oexp and naïve AGS control cells. GAPDH which is whole cell housekeeping control was used as standardization for qPCR studies (Figure 3-11A). We observed that expression of P-gp at mRNA level increased significantly in AGS/P-gp_Oexp Cells compared to control cells. Then, to examine P-gp expression at the protein level, we performed the protein lysate extraction from AGS/P-gp_Oexp cells. Then we investigated the P-gp expression in whole cell lysates by using the western blot technique (Figure 3-11B).

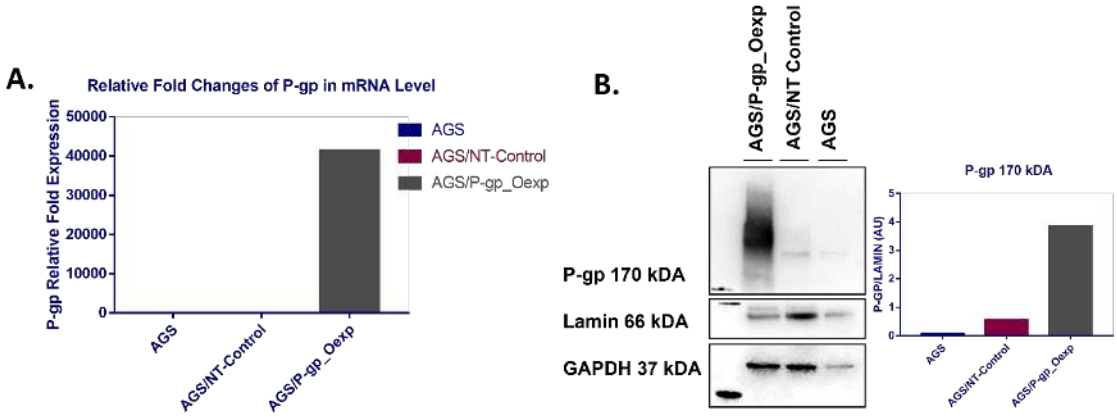

Figure 3-11 Validation of P-gp overexpression in AGS/P-gp_Oexp Cells by qPCR and Western Blot studies **A.** Relative fold changes of P-gp at mRNA level in AGS/P-gp_Oexp and AGS control cells by qPCR method **B.** Evaluation of P-gp expression in whole cell protein lysate by western blot in AGS/P-gp_Oexp and AGS Control cells

Then, we investigated the subcellular expression pattern of P-gp in AGS/P-gp_Oexp cells. We prepared subcellular fractions for AGS/P-gp_Oexp cells (Figure 3-12).

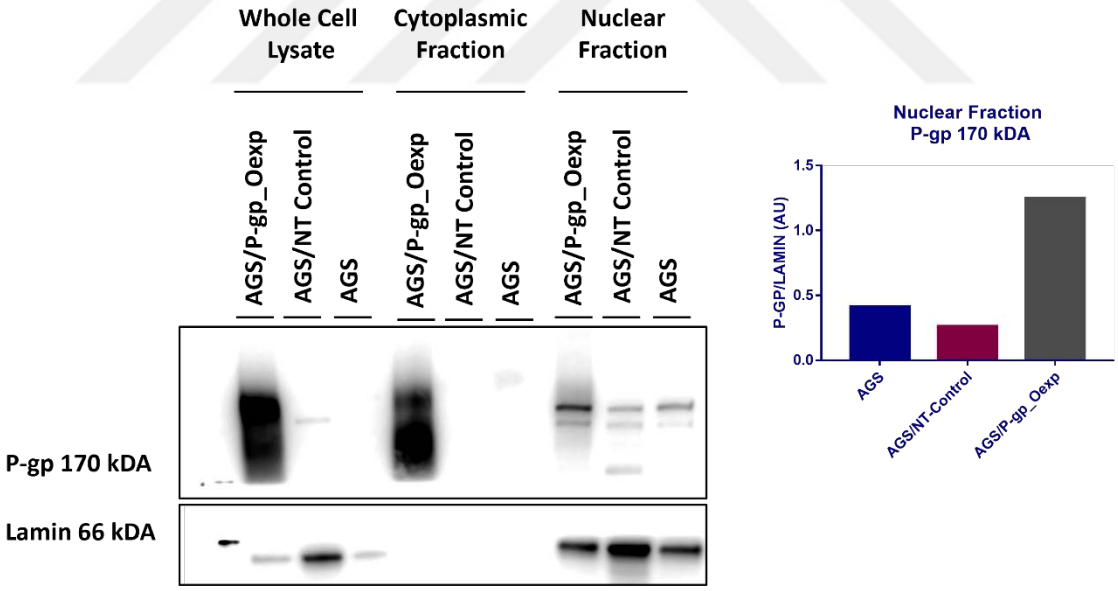

Figure 3-12 Evaluation of P-gp expression in subcellular fractions by western blot in AGS/P-gp_Oexp and AGS Control cells and their densitometric analysis.

We observed that P-gp expression increased in the nuclear fraction of AGS/P-gp_Oexp cells compared to AGS/NT control cells infected with non-targeting vector and naïve

AGS cells. However, P-gp expression was much more predominant in the cytoplasm of AGS/P-gp_Oexp cells compared to the nucleus.

3.11 Intracellular Distribution of P-gp in AGS/P-gp_Oexp Cells

To observe the intracellular distribution of P-gp in overexpressing cells better, we performed immunofluorescence imaging. Immunofluorescence images obtained from parental AGS cells, AGS/P-gp_Oexp and AGS/NT control cells are given in figure 3-13 with the densitometric analysis.

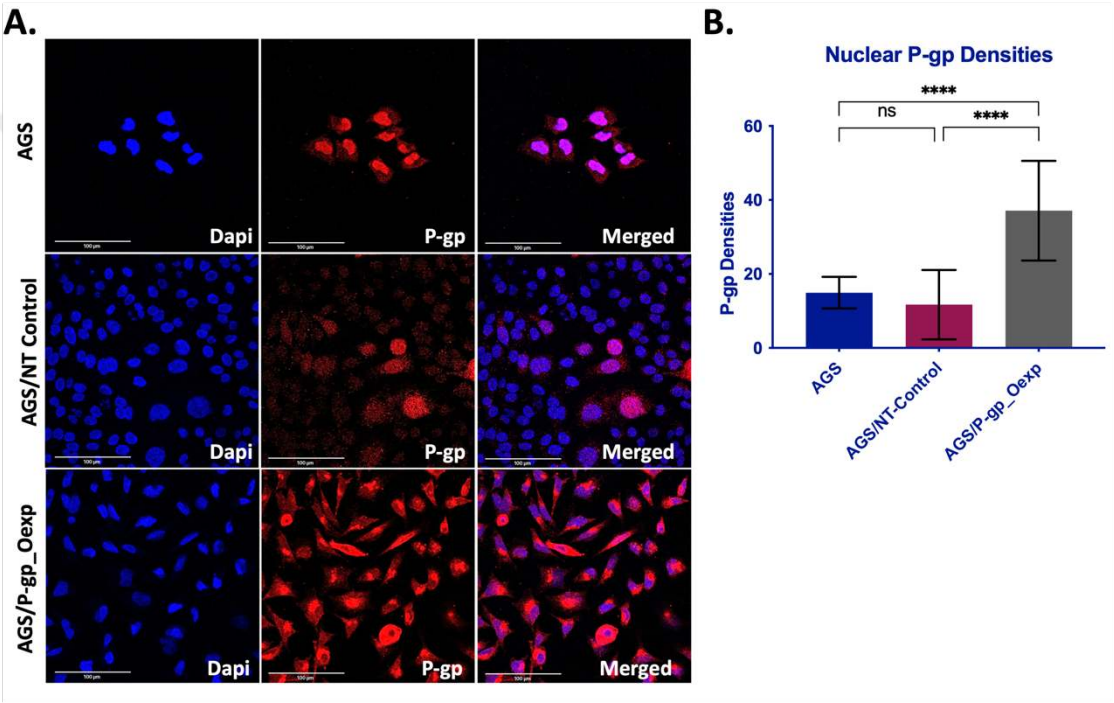

Figure 3-13 A. Immunofluorescence images obtained from parental AGS cells P-gp overexpressed AGS/P-gp_Oexp and AGS/NT control cells and **B.** their nuclear P-gp densitometric analysis. The nucleus was stained with DAPI (blue), and P-glycoprotein was immunolabelled with AlexaFluor 594 tagged antibody (red). Scale bar, 100 µm. (20 cells/experiment, ordinary one-way ANOVA, * $p<0.05$, ** $p<0.01$, *** $p<0.001$, **** $p<0.0001$)

We observed a significant increase in the expression of P-gp throughout the cell in AGS/P-gp_Oexp cells compared to AGS controls. There is approximately a 2-fold increase in nuclear P-gp expression in AGS/P-gp_Oexp cells compared to control cells. However, this increase in P-gp expression is more prominent in the cytoplasm of AGS/P-

gp_Oexp cells compared to AGS/Dox resistant cells that P-gp much more predominant in nucleus (Figure 3-14).

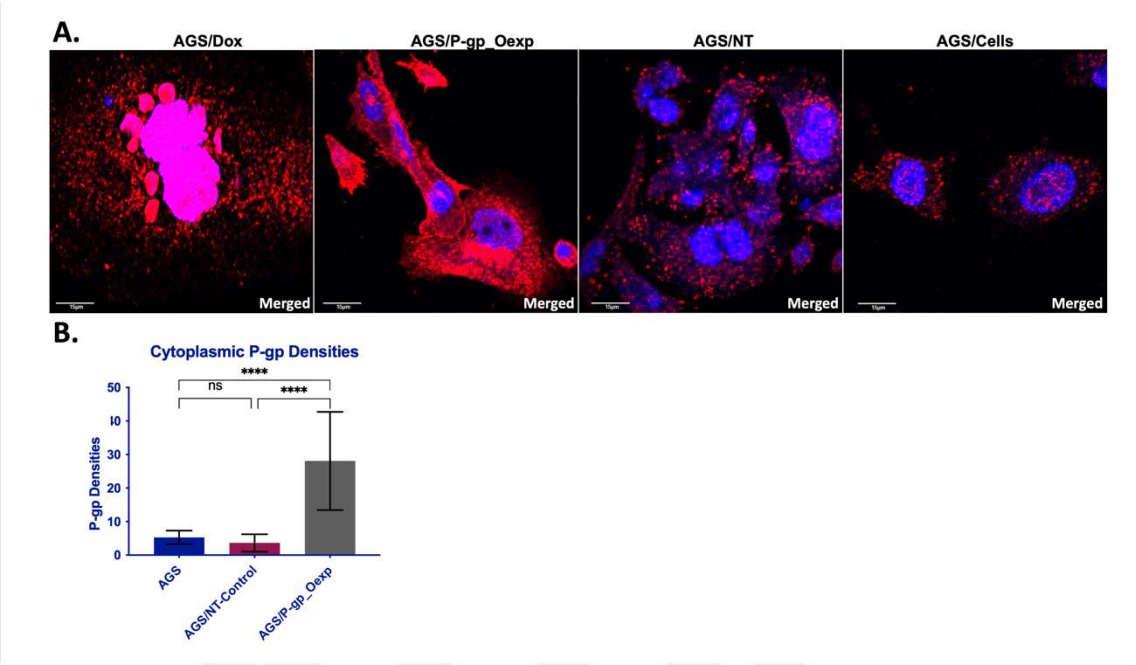

Figure 3-14 A. Zoomed in immunofluorescence images obtained from AGS/Dox cells, P-gp overexpressing AGS/P-gp_Oexp cells, parental AGS cells, and AGS/NT control cells. **B.** Densitometric analysis of the cytoplasmic P-gp expression in the images at figure 3.13A. The nucleus was stained with DAPI (blue), and P-glycoprotein was immunolabelled with AlexaFluor 594 tagged antibody (red). Scale bar, 15 µm. (20 cells/experiment, ordinary one-way ANOVA, * $p<0.05$, ** $p<0.01$, *** $p<0.001$, **** $p<0.0001$)

3.12 Intracellular Distribution of Doxorubicin in AGS/P-gp_Oexp Cells

To understand whether exogenous expression of P-gp can cause nuclear sparing of doxorubicin, we investigated the intracellular distribution of doxorubicin in AGS/P-gp_Oexp cells by using the autofluorescence property of the doxorubicin. We exposed AGS/P-gp_Oexp cells and control groups to 1.6 µM doxorubicin for 1, 6, and 24 hours (Figure 3-15).

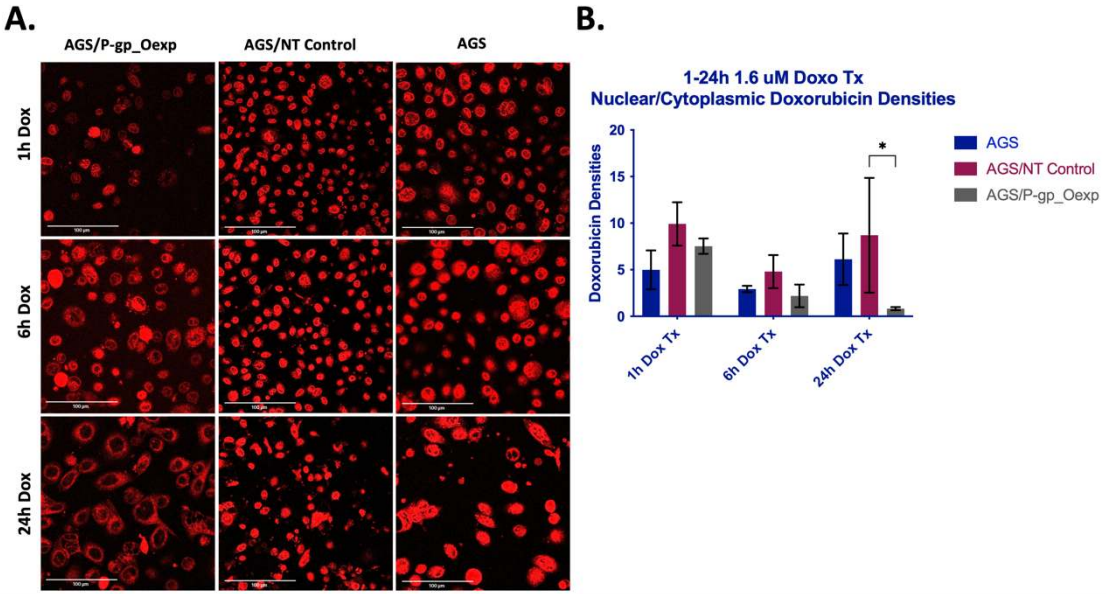

Figure 3-15 A. Intracellular distribution of doxorubicin in parental AGS cells, AGS/NT Control cells and P-gp overexpressing AGS/P-gp_Oexp cells after 24h treatment with doxorubicin and **B.** their densitometric analysis Scale bar, 100 µm. (20 cells/experiment, ordinary one-way ANOVA, * $p<0.05$, ** $p<0.01$, *** $p<0.001$, **** $p<0.0001$)

We observed the densities for doxorubicin, cellular accumulation of doxorubicin, was lower in AGS/P-gp_Oexp cells compared to control cells at each time point. When we investigated the subcellular distribution of doxorubicin in these cells, we observed a significantly decreased nuclear accumulation in AGS/P-gp_Oexp cells compared to control cells. However, this decrease in nuclear accumulation was more prominent at 24 hours. At 24 hours, AGS/P-gp_Oexp cells have doxorubicin in their cytoplasm, but their nucleus is empty. Hence, there was a prominent nuclear sparing at 24 hours in AGS/P-gp_Oexp cells.

3.13 Assessment of Intracellular Translocation of P-gp in AGS/P-gp_Oex Cells

Our findings in AGS/Dox models suggested that continuous exposure to doxorubicin increases nuclear expression of P-gp. As a result, increased nuclear P-gp expression can lead to nuclear-sparing of doxorubicin in resistant cells. However, how doxorubicin increases the nuclear expression of P-gp is not clear. One possibility is that doxorubicin itself may act as a signal for the translocation of P-gp from other cellular compartments to the nucleus in resistant cells, hence protecting the nucleus from the action of

doxorubicin. Since our AGS/P-gp_Oexp cells have P-gp predominantly in the cytoplasm, we tested whether doxorubicin may induce translocation of P-gp from the cytoplasmic pool to the nucleus. We exposed AGS/P-gp_Oexp cell to 1.6 uM doxorubicin for 1, 6, 24, 48 and 72 hours and investigated subcellular distribution of P-gp by immunofluorescence method (figure 3-16).

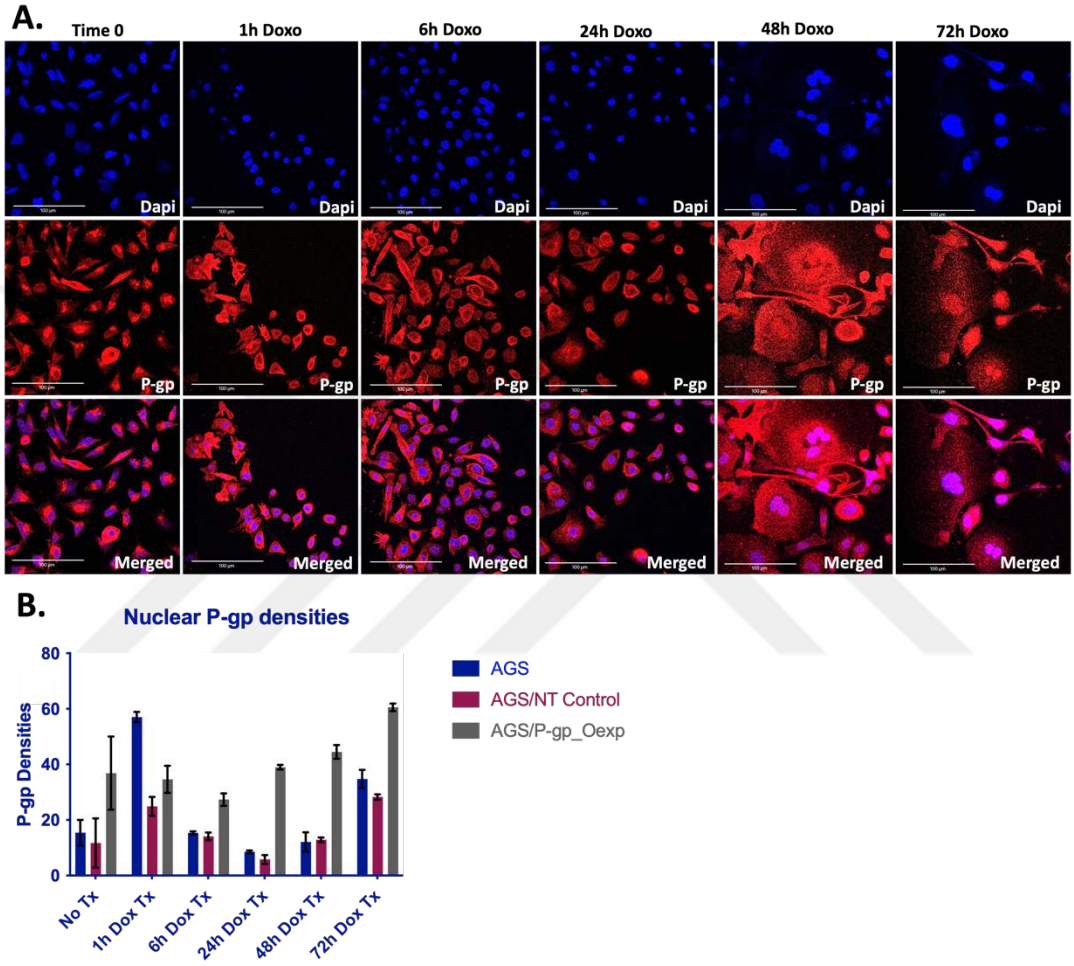

Figure 3-16 Intracellular distribution of P-gp in AGS/P-gp_Oexp cells after exposure to doxorubicin for 1, 6, 24, 48 and 72 hours and **B.** Densitometric analysis of the intracellular distribution of P-gp in parental AGS cells, AGS_NT Control cells and AGS/P-gp_Oexp cells after exposure to doxorubicin for 1, 6, 24, 48 and 72 hours. Scale bar, 100 µm. (20 cells/experiment)

We observed that, after exposure to doxorubicin, P-gp localization in the nucleus increased over time in AGS/P-gp_Oexp cells compared to control cells. This increase in P-gp expression is around 4-fold more in P-gp overexpressing cells compared to cell controls at 24 hours. Moreover, we observed a decrease in the cytoplasmic expression of

P-gp in AGS/P-gp_Oexp cells, especially at the 72nd hour. These findings suggest that doxorubicin may induce translocation of the P-gp from the cytoplasmic pool to nuclear pool in AGS/P-gp_Oexp cells.

To examine whether we could see a translocation of P-gp in the use of another chemotherapeutic, which is a substrate of P-gp but does not directly act in the nucleus, we exposed P-gp overexpressing AGS cells to paclitaxel for 1, 6, 24, 48 and 72 hours. Paclitaxel is a chemotherapeutic that is classified as a plant alkaloid, and it is an antimicrotubular agent. Hence its molecular targets are in the cytoplasm rather than the nucleus. We have chosen a paclitaxel dose of 625 nM drug concentration, 250 times the IC50 of paclitaxel in AGS cells, since 1.6 µM doxorubicin we used in the previous experiments, is 250 times the IC50 of doxorubicin in AGS cells. Immunofluorescence images and densitometric analysis for this experiment are given in figure 3-17.

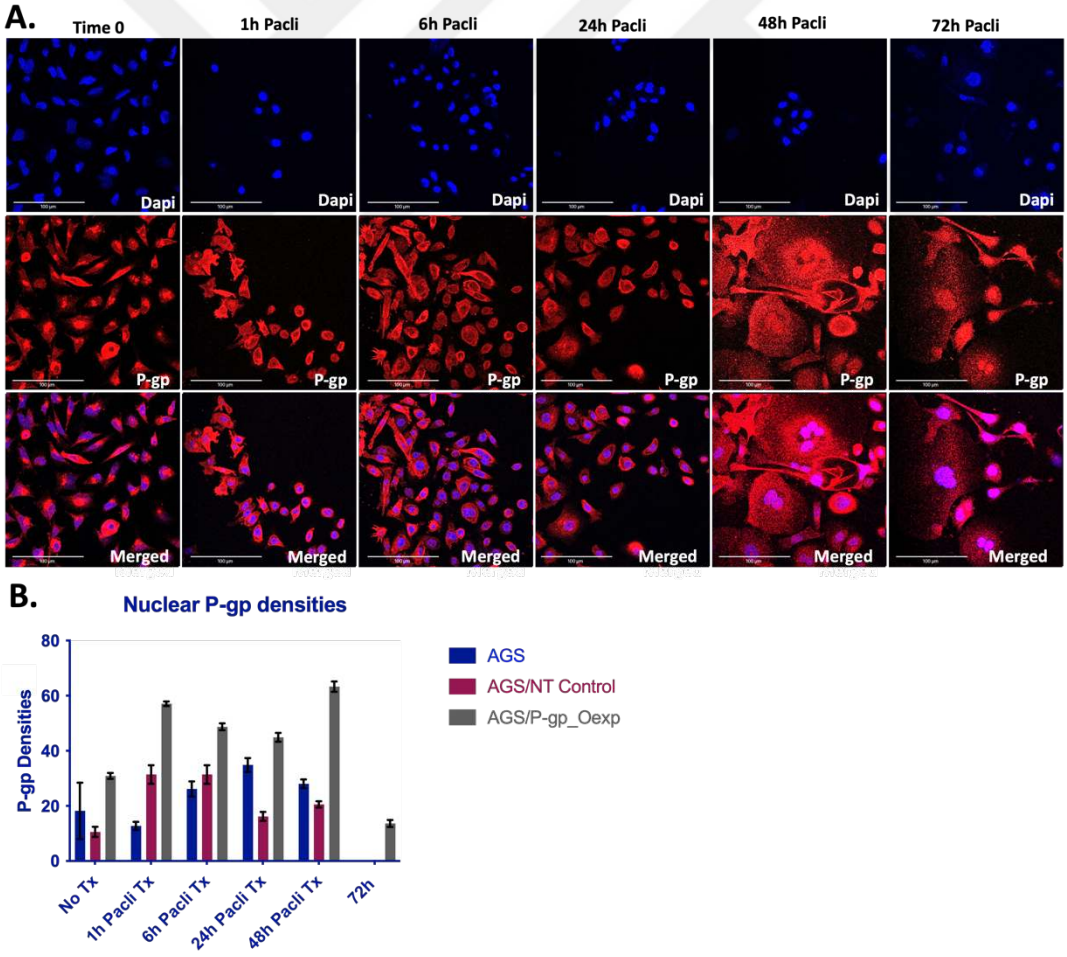

Figure 3-17 Intracellular distribution of P-gp in AGS/P-gp_Oexp cells after exposure to paclitaxel for 1-, 6-, 24-, 48- and 72-hours **B**. Densitometric analysis of the intracellular

distribution of P-gp in parental AGS cells, AGS_NT Control cells and AGS/P-gp_Oexp cells after exposure to paclitaxel for 1-, 6-, 24-, 48- and 72- hours. Scale bar, 100 μm. (20 cells/experiment)

We observed that with increased duration of exposure to paclitaxel, P-gp in the nuclear pool increased over time, like doxorubicin. However, this translocation was not as predominant as in the case of doxorubicin. Additionally, we observed a significant decrease in P-gp expression throughout the cell at the 72th hour of paclitaxel treatment. These findings suggested that doxorubicin may be a stronger signal for the translocation of P-gp to the nucleus in AGS/Dox cells, since protecting nucleus and DNA would be more important for the survival of these cells under exposure to doxorubicin.

CHAPTER III

Our studies in gastric cancer cells indicate that the cytoplasm-to-nucleus translocation of P-gp and the increase in nuclear P-gp expression induced by doxorubicin may cause nuclear sparing and resistance. However, the mechanisms of doxorubicin-induced translocation and nuclear localization of P-gp are unknown. We have two hypotheses; first, doxorubicin can cause the translocation of P-gp to the nucleus through regulation of the nuclear localization signal. Second, doxorubicin can change the glycosylation profile of P-gp and cause its translocation to the nucleus.

In this thesis, we focused on the first hypothesis; the nuclear localization signals (NLS). NLS are short peptide sequences, usually around 20 bp, that direct the proteins synthesized inside the cell to the nucleus. These highly conserved sequences are rich in lysine and arginine, which are generally positive-basic amino acids (Lanford et al., 1986). This intracellular cargo pathway generally begins with the binding of NLS in cargo proteins to the importin protein in the cytoplasm. The importin protein interacts with the nuclear pore complexes, also known as the entrance gate to the nucleus (Lange et al., 2007). After reaching the nucleus the importin-cargo protein complex is cleaved by Ran-GTP. The binding of RanGTP to importin β causes a conformational change that results in the release of the importin α-cargo complex (Lee et al., 2005). Importin is then released back into the cytoplasm and the cargo protein reaches the nucleus. Since the translocation of a protein to the nucleus requires NLS signaling, NLS is one of the candidate mechanisms that may be responsible for the translocation of P-gp to the nucleus in our resistant AGS/DOX cells. Therefore, we searched whether the mature P-gp sequence contains the highly conserved NLS sequence. In the literature, we could not find any information about the presence of the NLS sequence in P-gp. Then we searched the NLS sequence within the P-gp gene sequence by using online informatics tools designed for NLS sequence capture. Two separate scanners from KEIO University and MosesLab were used, but both scanners showed that the P-gp sequence naturally did not contain NLS signals. However, it is known in the literature that the NLS signal can be added or removed by alternative splicing to many proteins. It is a common observation that proteins normally located in the cytoplasm begin to be expressed in the nucleus when NLS is added by alternative splicing. When the NLS sequence is removed from the proteins located in the nucleus by alternative splicing, these proteins begin to be expressed in the

cytoplasm (Srinivasan and Schulman 1994; Wang et al. 2003; Samejima and Earnshaw, 2000; Thakur et al. 1997; Nilsen et al., 1997; Ficca et al. 2004, Gonzales). et al. 2000). In accordance with this evidence in the literature, addition of NLS to the P-gp sequence in Doxorubicin-treated cells may explain P-gp expression in the nucleus.

3.14 Establishment of AGS/P-gp_NLS Cells

In our experiments with P-gp overexpressing AGS/P-gp_Oexp cells, we observed that the P-gp is prominently located at the cytoplasm. On the other hand, we observed that P-gp is located at the nucleus of AGS/Dox resistant cells. To understand whether NLS is required for the direction of ectopically expressed P-gp to the nucleus, we designed a P-gp expression vector with NLS (P-gp_NLS plasmid), and established AGS/P-gp_NLS cells which express P-gp_NLS. Thus, we obtained a chance to compare AGS/Dox cells, AGS/P-gp_Oexp cells (which express P-gp predominantly in the cytoplasm), and AGS/P-gp_NLS cells (which express P-gp directed to the nucleus with NLS). Before the analysis of AGS/P-gp_NLS cells in terms of nuclear P-gp expression, nuclear translocation of P-gp and nuclear sparing, we confirmed that the expression of P-gp increased significantly in AGS/P-gp_NLS cells compared to control cells (Figure 3-18).

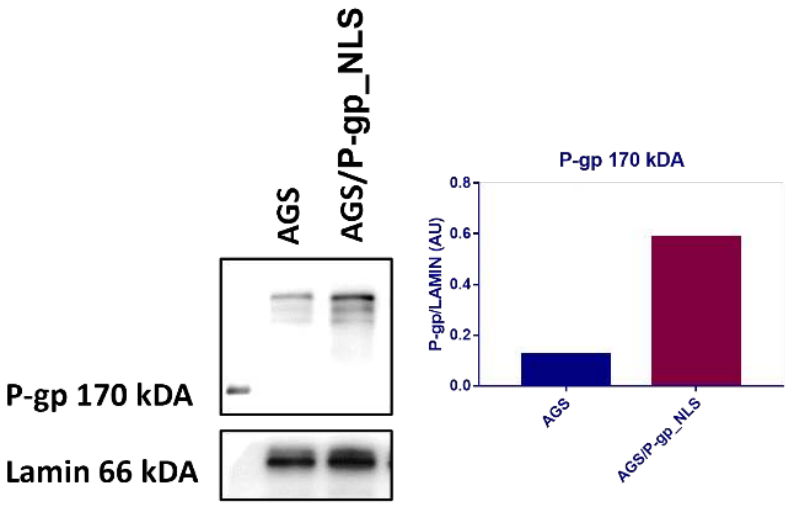

Figure 3-18 Investigation of P-gp expression in parental AGS cells and AGS/P-gp_NLS cells by western blot and densitometric analysis of western blot bands.

3.15 Intracellular Distribution of P-gp in AGS/P-gp_NLS Cells

To see whether NLS directs P-gp to the nucleus in AGS/P-gp_NLS cells, we obtained immunofluorescence images from AGS/P-gp_NLS cells and their parental AGS cells. Immunofluorescence images and densitometric analysis are given in Figure 3-19.

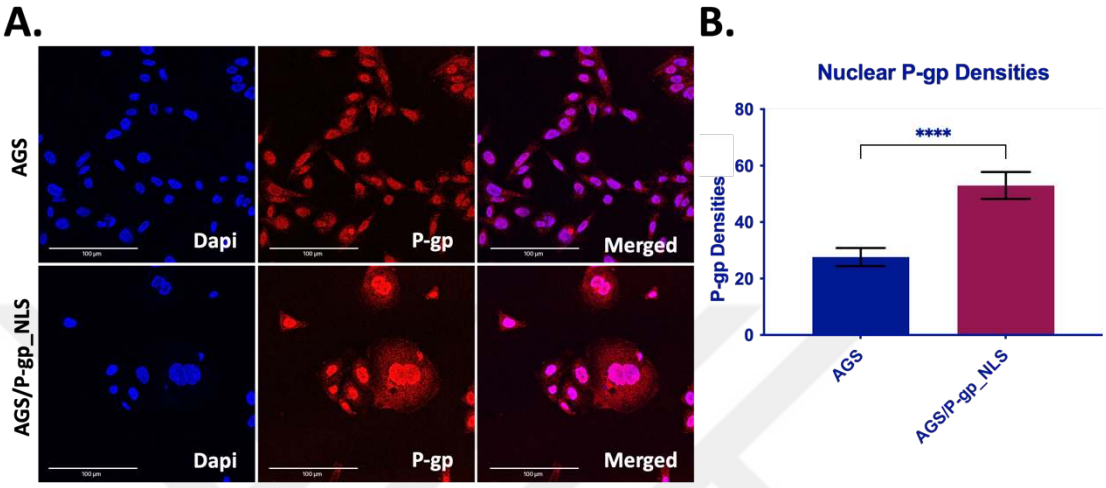

Figure 3-19 A. Intracellular distribution of P-gp in parental AGS cells and AGS/P-gp_NLS cells **B.** Densitometric analysis of the nuclear P-gp expression in the images at A. The nucleus was stained with DAPI (blue), and P-glycoprotein was immunolabelled with AlexaFluor 594 tagged antibody (red). Scale bar, 100 µm. (20 cells/experiment, ordinary one-way ANOVA, * $p<0.05$, ** $p<0.01$, *** $p<0.001$, **** $p<0.0001$)

We observed that nuclear P-gp expression was significantly higher in AGS/P-gp_NLS cells compared to parental cells. Moreover, P-gp was predominantly located in the nucleus of AGS/P-gp_NLS cells, compared to the cytoplasmic dominance of P-gp in AGS/P-gp_Oexp cells which were transduced with plasmids coding P-gp sequence without NLS (compare Fig. 3-19 with Fig. 3-13).

3.16 Intracellular Distribution of Doxorubicin in AGS/P-gp_NLS Cells

To compare the difference between the intracellular doxorubicin distribution in AGS/P-gp_NLS cells and their parental control AGS cells, we exposed those cells to 1.6 µM doxorubicin for 1, 6, and 24 hours (Figure 3-20).

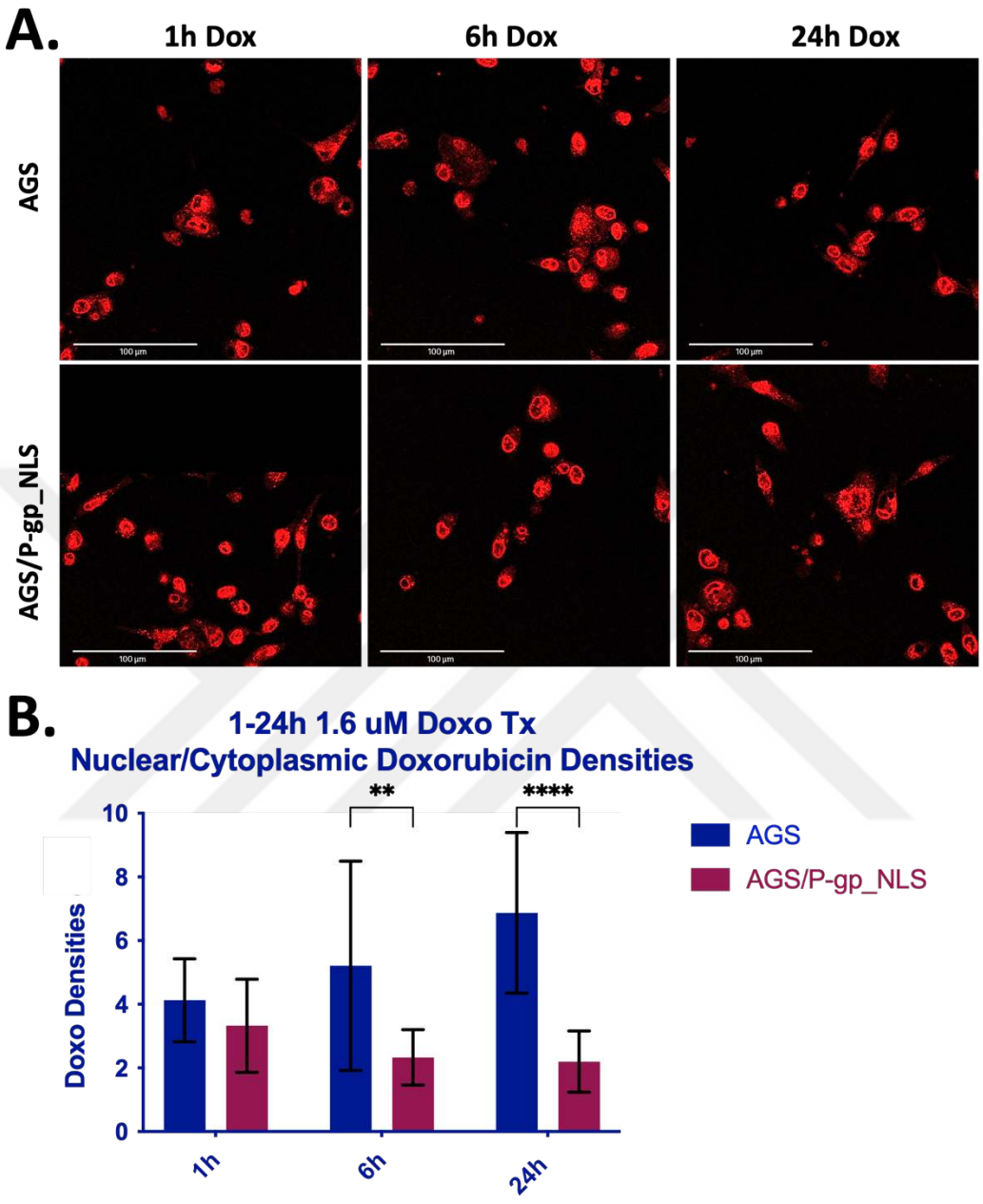

Figure 3-20 A. Intracellular distribution of doxorubicin in wild type AGS cells and AGS/P-gp_NLS cells exposed to 1.6uM doxorubicin for 1-, 6-, or 24-hours **B.** Densitometric analysis of the N/C doxorubicin ratio in the images at A. Scale bar, 10 0µm. (20 cells/experiment, two-way ANOVA, * $p<0.05$, ** $p<0.01$, *** $p<0.001$, **** $p<0.0001$)

In AGS/P-gp_NLS cells we observed that the nuclear accumulation and N/C ratio of doxorubicin were lower than in wild-type AGS cells. As expected, this ratio continuously decreased through the doxorubicin treatment period in resistant cells and nuclear sparing was much more prominent at 24 hours of treatment. This was in parallel to our previous observations with AGS/Dox cells. This data suggested that P-gp in the nucleus can be an important mechanism for nuclear sparing and expressing P-gp in the nucleus of wild-type AGS cells can increase the nuclear protection of those cells against doxorubicin.

3.17 Assessment of Nuclear Translocation of P-gp in AGS/P-gp_NLS Cells

Our previous studies suggested that P-gp could translocate to the nucleus after exposure to doxorubicin. To observe the kinetics of P-gp translocation to the nucleus in AGS/P-gp_NLS cells and compare the difference between parental wild-type AGS cells, we exposed these cells to 1.6 μM doxorubicin for 1, 6, 24, 48, and 72 hours. Immunofluorescence images and densitometric analysis are given in figure 3-21.

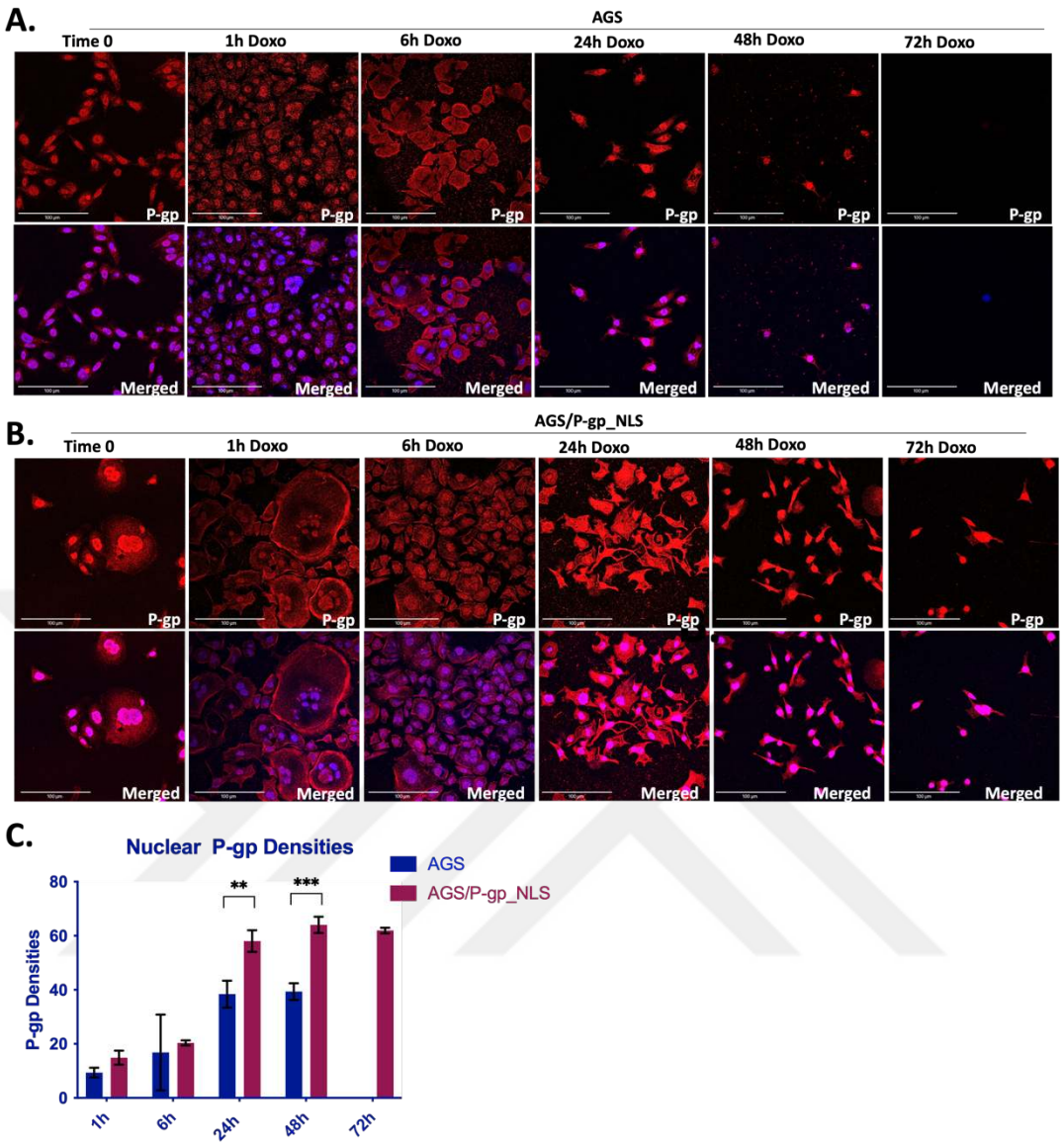

Figure 3-21 A. Intracellular distribution of P-gp in AGS cells after exposure to doxorubicin for 1-, 6-, 24-, 48-, or 72-hours **B.** Intracellular distribution of P-gp in AGS/P-gp_NLS cells after exposure to doxorubicin for 1-, 6-, 24-, 48-, or 72-hours **C.** Results from densitometric analysis of the immunofluorescence images in A and B. Scale bar, 100 µm. (20 cells/experiment, two-way ANOVA, * $p<0.05$, ** $p<0.01$, *** $p<0.001$, *** * $p<0.0001$)

We observed that nuclear P-gp expression starts to increase from the first hour of doxorubicin exposure in AGS/P-gp_NLS cells. Interestingly, at the first hour of the doxorubicin treatment, P-gp was mostly localized on the cytoplasmic membrane of the AGS/P-gp_NLS cells, although P-gp expression was prominent in the nucleus of the untreated AGS/P-gp_NLS cells. After the 1st hour of doxorubicin treatment, the

expression of P-gp on the cytoplasmic membrane decreased gradually and expression of the P-gp in the nucleus increased significantly. It may be speculated that the inner machinery of the resistant cells may direct P-gp to the cell membrane as a primary line of defense upon exposure to doxorubicin. Then breaching of the cell membrane by doxorubicin may induce translocation of P-gp to the nucleus as a secondary line of defense to protect the DNA. However, that this hypothesis should be tested with further studies.

In wild-type parental AGS cells, while P-gp expression was always lower than in AGS/P-gp_NLS cells, they also showed an increasing pattern of nuclear P-gp expression after doxorubicin treatment. However, those cells could not resist longer doxorubicin exposure. They all died at 72 hours of treatment. Those observations supported our previous observations that exposure to doxorubicin causes an increase in nuclear P-gp expression. Although our previous observations in AGS/P-gp_Oexp cells, and observations in AGS/P-gp_NLS cells suggests that cytoplasmic pool of P-gp may translocate to the nucleus after exposure to doxorubicin, it is still not clear whether the nuclear translocation of P-gp or direction of the newly synthesized P-gp to the nucleus is the main mechanism for increased nuclear P-gp expression.

3.18 Comparison of Intracellular Distribution of Doxorubicin in AGS, AGS/Dox, AGS/P-gp_Oexp, AGS/P-gp_NLS cells

We next compared the intracellular distribution and nuclear sparing of doxorubicin in AGS, AGS/Dox, AGS/P-gp_Oexp, AGS/P-gp_NLS cells (Figure 3-22).

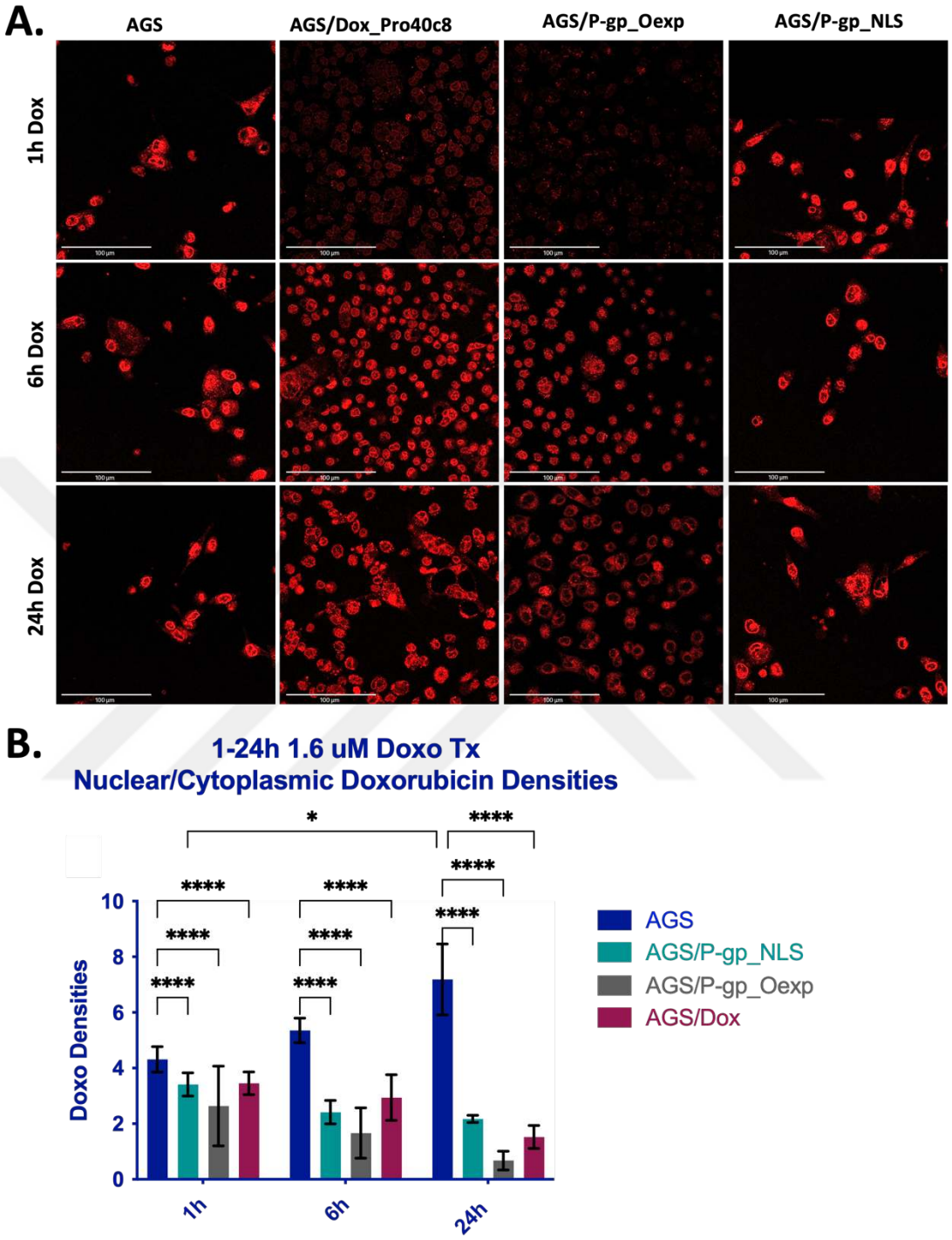

Figure 3-22 A. Comparison of Intracellular Distribution of Doxorubicin in AGS, AGS/Dox, AGS/P-gp_Oexp, AGS/P-gp_NLS and **B.** densitometric analysis of the

confocal images in A. Scale bar, 10 μm. (20 cells/experiment) Scale bar, 100 μm. (20 cells/experiment, two-way ANOVA, * $p<0.05$, ** $p<0.01$, *** $p<0.001$, **** $p<0.0001$)

We observed that doxorubicin-resistant AGS/Dox cells that were established with prolonged exposure to doxorubicin and AGS ectopically overexpressed P-gp by AGS cells whether with nuclear localization signal or not showed a similar nuclear sparing pattern. With increased doxorubicin exposure time, nuclear sparing increased. On the other hand, parental AGS cells had a higher NF/CF doxorubicin ratio at all time points, which increased over time. These results strongly support that P-gp expression is an important determinant for nuclear sparing.

3.19 Comparison of Intracellular Distribution of P-gp in AGS, AGS/Dox, AGS/P-gp_Oexp, AGS/P-gp_NLS cells

We observed that nuclear sparing was maximum at 24h after doxorubicin treatment in resistant and P-gp overexpressing cells. To understand whether nuclear P-gp expression reaches the maximum levels with similar time kinetics, we investigated the distribution of P-gp in AGS, AGS/Dox, AGS/P-gp_Oexp, and AGS/P-gp_NLS cells, comparing their immunofluorescence P-gp images and densitometric analysis results (figure 3-23).

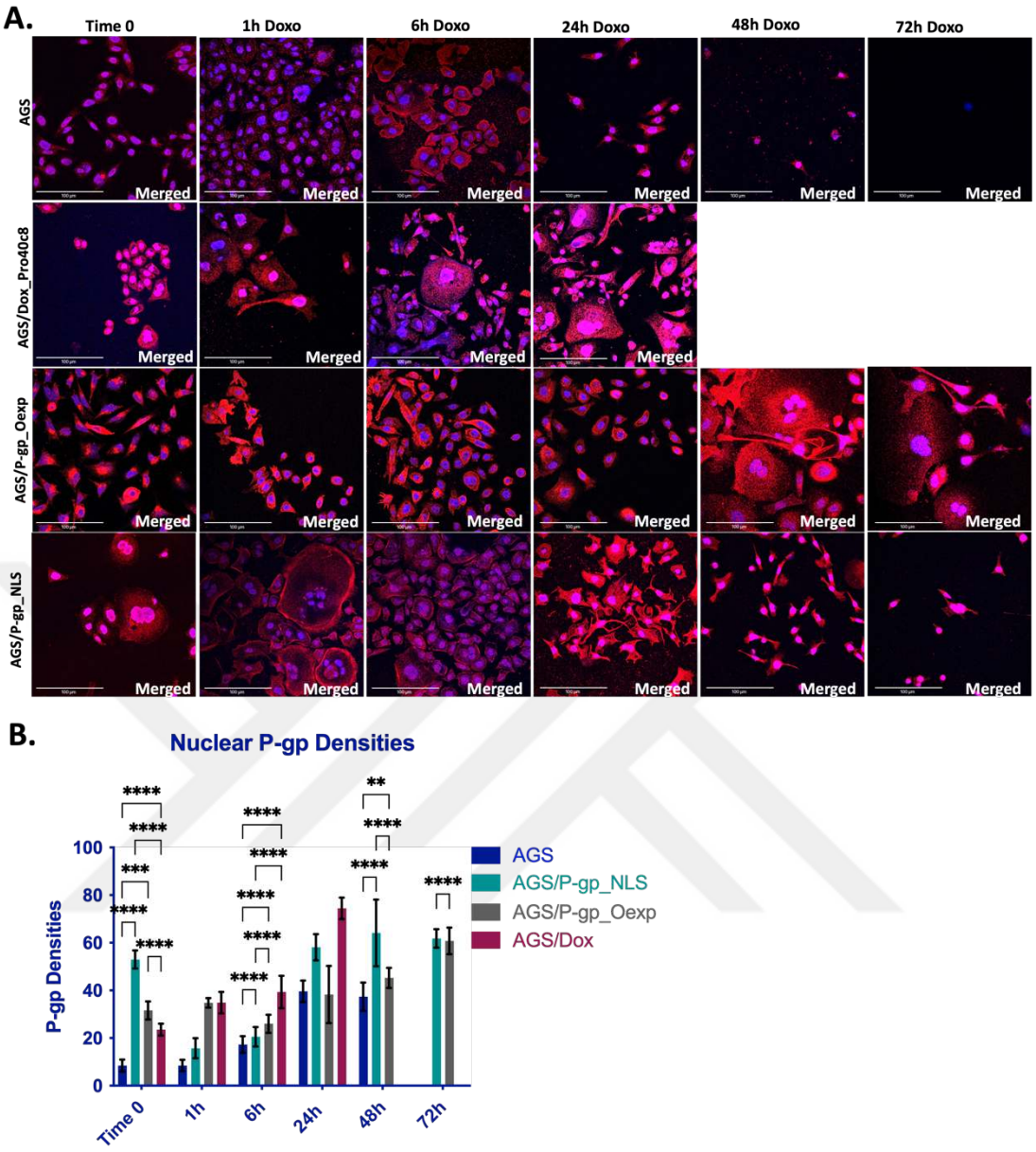

Figure 3-23 A. Comparison of intracellular distribution of P-gp in AGS, AGS/Dox, AGS/P-gp_Oexp, and AGS/P-gp_NLS cells and **B.** Results from densitometric analysis of the immunofluorescence images in A. (20 cells/experiment) Scale bar, 100 µm. (20 cells/experiment, two-way ANOVA, * $p<0.05$, ** $p<0.01$, *** $p<0.001$, **** $p<0.0001$)

We observed nuclear P-gp expression increased over time after doxorubicin treatment and reached to a maximum at the 24th and 48th hours after treatment in AGS/Dox and AGS/P-gp_NLS cells respectively, similar to the kinetics of nuclear doxorubicin sparing in these cells. However, in AGS/P-gp_Oexp cells, the nuclear P-gp expression reached to a peak at the 72nd hour after doxorubicin treatment. These findings suggested that continuous exposure to doxorubicin as in AGS/Dox cells and presence of the NLS in P-

gp sequence as in AGS/P-gp_NLS facilitate nuclear expression of P-gp. Moreover, the similarity in the kinetics of nuclear-P-gp expression and nuclear sparing of doxorubicin, strengthened the role of nuclear P-gp's in nuclear sparing and resistance in gastric adenocarcinoma cells.

CHAPTER IV

To confirm the role of nuclear P-gp's in nuclear sparing and resistance to doxorubicin in gastric adenocarcinoma cells, we investigated whether suppressing P-gp expression in resistant cell lines and P-gp inhibitors could reverse the resistance, in this chapter.

3.20 The Effect of P-gp Inhibitors on the Nuclear Efflux Kinetics of Doxorubicin

To confirm the role of nuclear P-gp in nuclear sparing observed in AGS/Dox cells we investigated the effect of P-gp inhibitors on the nuclear efflux kinetics of doxorubicin. We examined nuclear doxorubicin accumulation in AGS/Dox cells in the presence of the first-generation P-gp inhibitor verapamil, which is a substrate of P-gp, and the third-generation P-gp inhibitor zosuquidar, which is a direct inhibitor of P-gp, under the confocal microscope. We incubated one group of AGS/Dox cells for 2 hours with 40 μM verapamil, the second group of AGS/Dox cells with 1uM zosuquidar, and a control group with fresh medium. Then, those cells were incubated with doxorubicin and images were taken from the cell at the 1st, 6th, or 24th hours of incubation with doxorubicin (Figure 3-24).

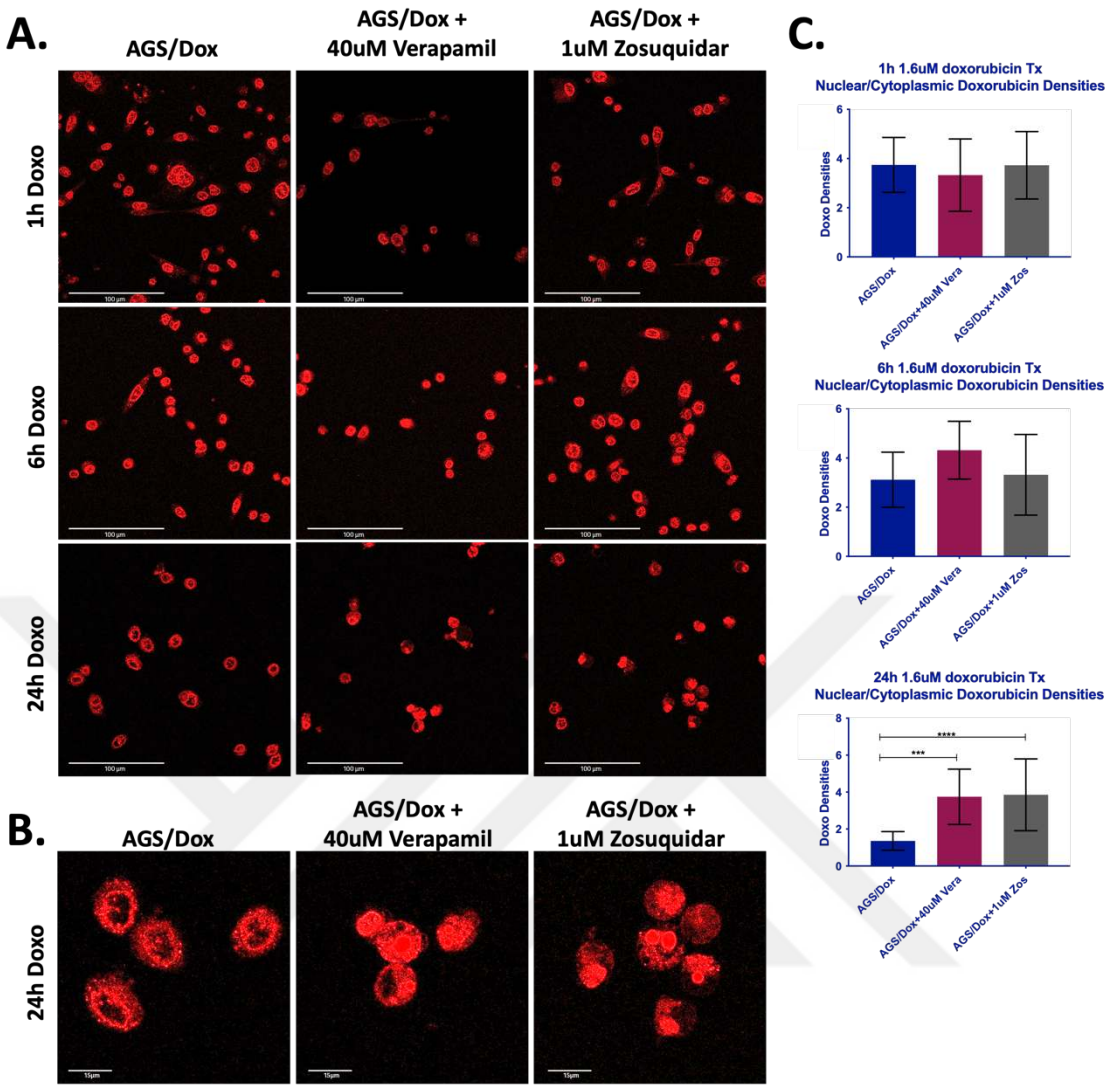

Figure 3-24 A. The effect of verapamil and zosuquidar on intracellular doxorubicin accumulation in AGS/Dox cells, (Scale bar, 100 µm.) and **B.** Nuclear doxorubicin zoomed in images of cells at 24th hour of doxorubicin treatment (Scale bar, 15 µm.)**C.** Densitometric analysis of the confocal images in A. (20 cells/experiment, ordinary one-way ANOVA, * $p<0.05$, ** $p<0.01$, *** $p<0.001$, **** $p<0.0001$)

We observed that while only doxorubicin-treated AGS/Dox cells had the lowest nuclear doxorubicin accumulation at 24 hours of doxorubicin treatment, AGS/Dox cells preincubated either with P-gp inhibitors verapamil or zosuquidar, have significantly

higher doxorubicin nuclear/cytoplasmic doxorubicin ratio at 24th hour. Also, at 24 hours of treatment, most cells in inhibitor groups were dead.

These suggested that nuclear P-gp can be involved in the nuclear sparing of doxorubicin in AGS/Dox cells.

3.21 The Effect of P-gp Inhibitors on the Doxorubicin Resistance

To understand whether inhibition of P-gp by P-gp inhibitors can overcome resistance to doxorubicin we assessed the concentration-response curves for doxorubicin in the presence or absence of P-gp inhibitors verapamil and zosuquidar. To examine the change in the concentration-response curves of doxorubicin, doxorubicin-resistant AGS/Dox cells were exposed to 20 µM verapamil or 1 µM zosuquidar for two hours. Then, AGS/Dox cells were exposed to 9 different concentrations of doxorubicin (200 µM - 0.781 µM) for 120 hours and the MTT cell survival test was performed. The concentration-response curves are given in figure 3-25.

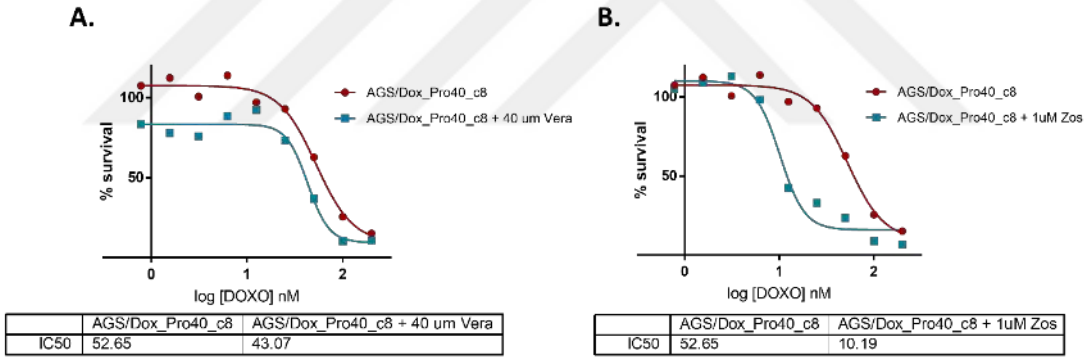

	AGS/Dox_Pro40_c8	AGS/Dox_Pro40_c8 + 40 um Vera
IC50	52.65	43.07

	AGS/Dox_Pro40_c8	AGS/Dox_Pro40_c8 + 1uM Zos
IC50	52.65	10.19

Figure 3-25 Effect of P-gp inhibitors verapamil or zosuquidar on doxorubicin concentration-response curves in AGS/Dox cells. AGS/Dox cells were exposed to nine different doses of doxorubicin after two hours of exposure to **A.** 20 µM verapamil or **B.** 1 µM zosuquidar. Concentration-response curves were generated following MTT cell survival testing.

As in nuclear accumulation studies, 40 uM verapamil which is competitive inhibitor of P-gp caused a slight increase in sensitivity to doxorubicin of AGS/Dox cells. On the other hand, zosuquidar, which is a direct inhibitor of P-gp significantly increased the sensitivity to doxorubicin, it caused around 5-fold more sensitivity to doxorubicin-resistant AGS/Dox cells.

3.22 Assessment of Other Efflux Pumps

P-gp is not the only efflux pump that may lead to the nuclear efflux of doxorubicin. There are other important efflux pumps which are BCRP, LRP, and MRP-1. Recent studies suggest that these efflux pumps can also be localized on the nuclear membrane. Doxorubicin is also the substrate for all these pumps. Therefore, MRP1, LRP, and BCRP, may also be operating nuclear sparing and resistance in our cells, in addition to P-gp.

To test this hypothesis, we have investigated the expression of these pumps in subcellular fractions, whole-cell lysate, cytoplasmic fraction, and nuclear fraction in resistant and control cells by the western blot method. Lamin was used as a nuclear marker and GAPDH as a cytoplasmic marker in western blot studies. Western blot images and densitometric analysis are given in figure 3-26.

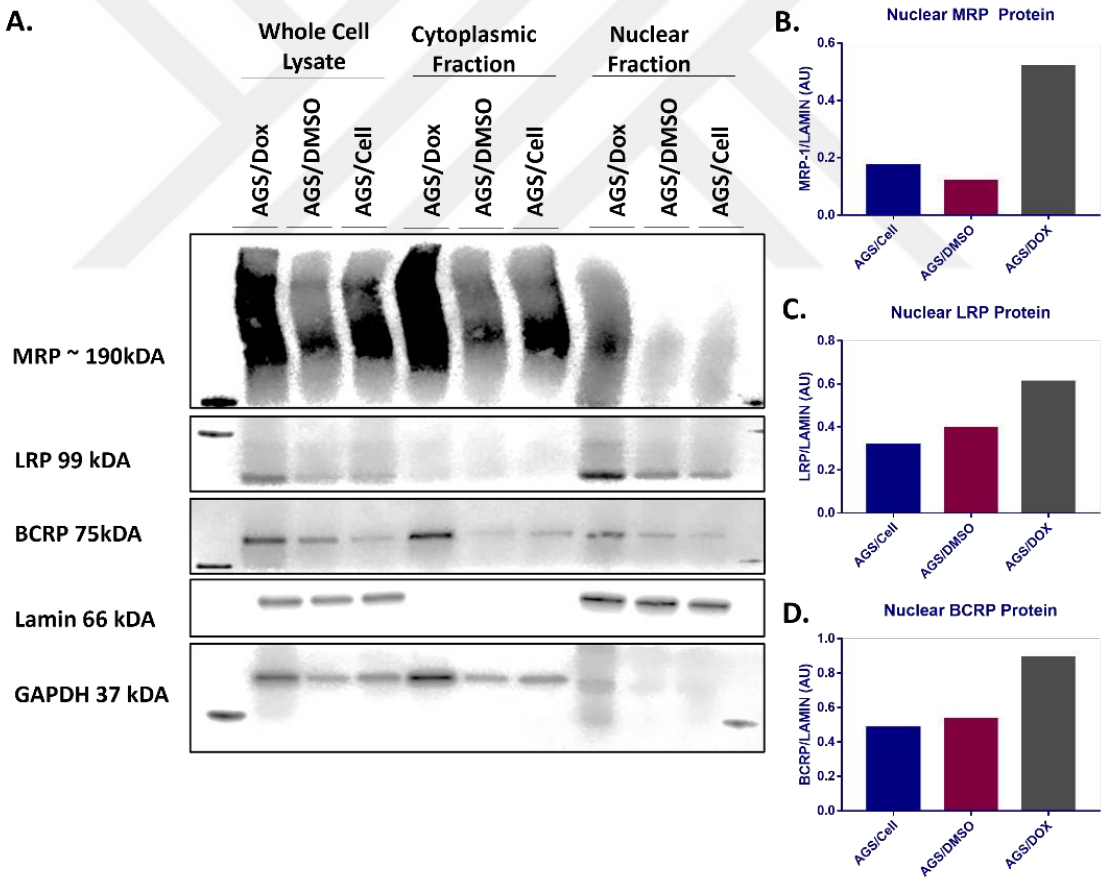

Figure 3-26 Investigation of three other efflux pumps expression in subcellular fractions by western blot in AGS/Dox, AGS/DMSO and AGS/Cell control cells and, the densitometric analysis of **B.** Nuclear MRP protein, **C.** Nuclear LRP Protein, **D.** Nuclear BCRP protein

We observed that all these three other pumps also increased in resistant cells compared to control cells in the nuclear fractions. While BCRP increased predominantly in the nuclear fractions, MRP and LRP show a significant increase in the cytoplasmic fraction of doxorubicin resistant AGS/Dox cells compared to AGS control cells. It is worth noting that, P-gp inhibitors also have a potential to inhibit other efflux pumps. Even though there was no evidence that LRP could be inhibited by verapamil and zosuquidar, MRP-1 and BCRP could be successfully inhibited by them (Römermann et al., 2013). Therefore, by using these P-gp inhibitors, we could also inhibit other pumps in resistant cells.

3.23 Establishment of P-gp Knock-Out AGS Cells

Since the nuclear expression of the other efflux pumps also increased in AGS/Dox cells and P-gp inhibitors can also have an inhibitory action on these pumps, the causal relationship of nuclear P-gp with nuclear sparing and chemoresistance needed further validation. To validate that the nuclear sparing and chemoresistance are mainly induced by nuclear P-gp in AGS cells, we investigated the effect of suppressing P-gp expression in AGS cell models. For this purpose, first, we used CRISPR/Cas9 genome editing techniques for stable knock out of P-gp. We designed three guide RNAs using the CHOP CHOP program and lentiviral vectors. We transfected our AGS/Dox and AGS cell models with pLentr1a_guideRNA [1-2-3] and investigated the expression of P-gp in those cells (figure 3-27).

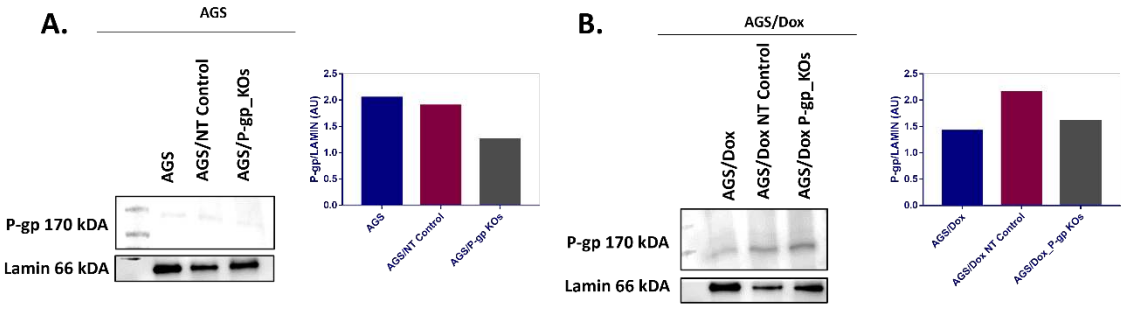

Figure 3-27 Investigation of P-gp expression in pLentr1a_guideRNA [1-2-3] transfected cells, vehicle control cells, and parental cells. Western blot images and densitometric analysis results for P-gp expression **(A.)** in AGS cells and **(B.)** AGS/Dox resistant cells.

We observed that, while there was a decrease in the expression of P-gp in AGS parental control cell lines, we could not observe a decrease in resistant cell lines. Polyploidy may be the reason for the failure of CRISPR/Cas9 knock out in AGS/Dox cells, since AGS cells tend to transform into a polyploid state upon exposure to doxorubicin and AGS/Dox cells predominantly show polyploid phenotype. Previous studies showed that the polyploid status of many cell lines decreases the efficiency of CRISPR/Cas9 genome editing techniques (Wassef et al., 2017). This could be the reason why P-gp expression in AGS/Dox cells could not be decreased by CRISPR/Cas9 strategy.

After that, we tested siRNAs specific to the hMDR1 (Sigma Aldrich MISSION® esiRNA EHU131661) to knock down P-gp. We transfected AGS/Dox-Pro40_c8 cells, our latest resistant cell model, with siRNA specific to P-gp or siRNA control that does not target a gene as a control group. We collected cells after the second and third days of transfection and investigated the P-gp expression with western blot (figure 3-28).

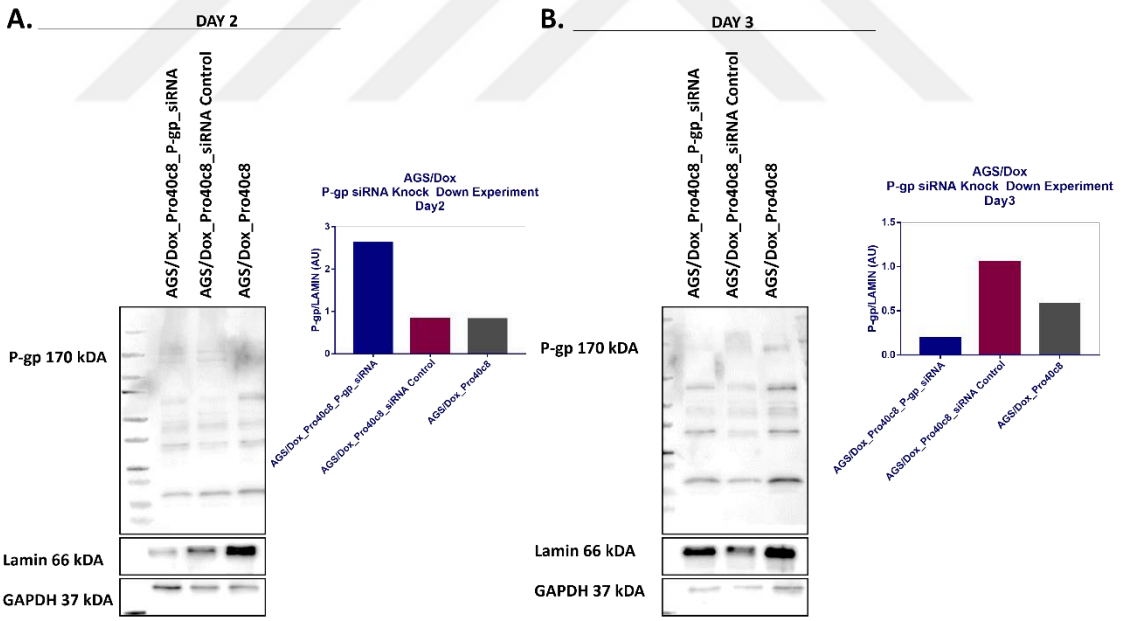

Figure 3-28 Evaluation of P-gp expression by western blot in AGS/Dox cells transfected with P-gp siRNA, or control siRNA at the second **(A.)** and third day **(B.)** of siRNA transfection.

We observed that there is a significant decrease in the expression of P-gp in P-gp siRNA-transfected AGS/Dox_Pro40c8 cells at the 3th day of transfection. Therefore, we decided to continue with hMDR siRNA for P-gp knockdown experiments.

With further experiments, we investigated the knock down efficiency of P-gp specific siRNA in AGS/Dox_Pro40c8 cells in comparison to the P-gp expression in AGS/DMSO, and AGS control cells. Western blot results for these experiments and their densitometric analysis are shown in Figure 3-29.

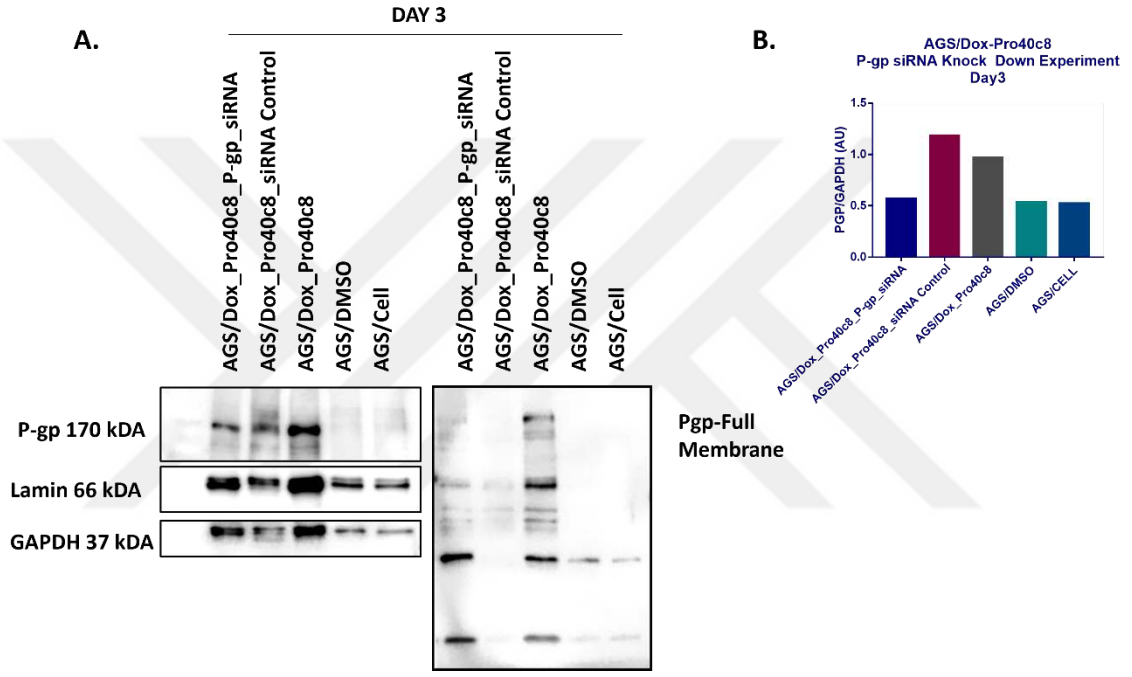

Figure 3-29 Evaluation of P-gp expression by western blot in AGS/Dox cells transfected with P-gp siRNA, or control siRNA compared to control cells; AGS/Dox, AGS/DMSO and AGS/Cell by western blot **(A.)** and densitometric analysis **(B.)** Samples are collected at the 3th day of transfection.

We observed that transfection with P-gp siRNA could decrease the P-gp expression in AGS/Dox_Pro40c8 cells to the P-gp expression level in parental AGS cells (Figure 3-30).

3.24 Intracellular Distribution of P-gp in AGS/Dox_Pro40c8_P-gp_siRNA and AGS/Dox_Pro40c8 cells

To validate the P-gp knockdown in AGS/Dox cells with siRNA and observe the intracellular distribution of P-gp, immunofluorescence images were obtained from AGS/Dox_Pro40c8 cells, P-gp knock-down AGS/Dox_8_P-gp_siRNA cells, and control cell groups (Figure 3-30).

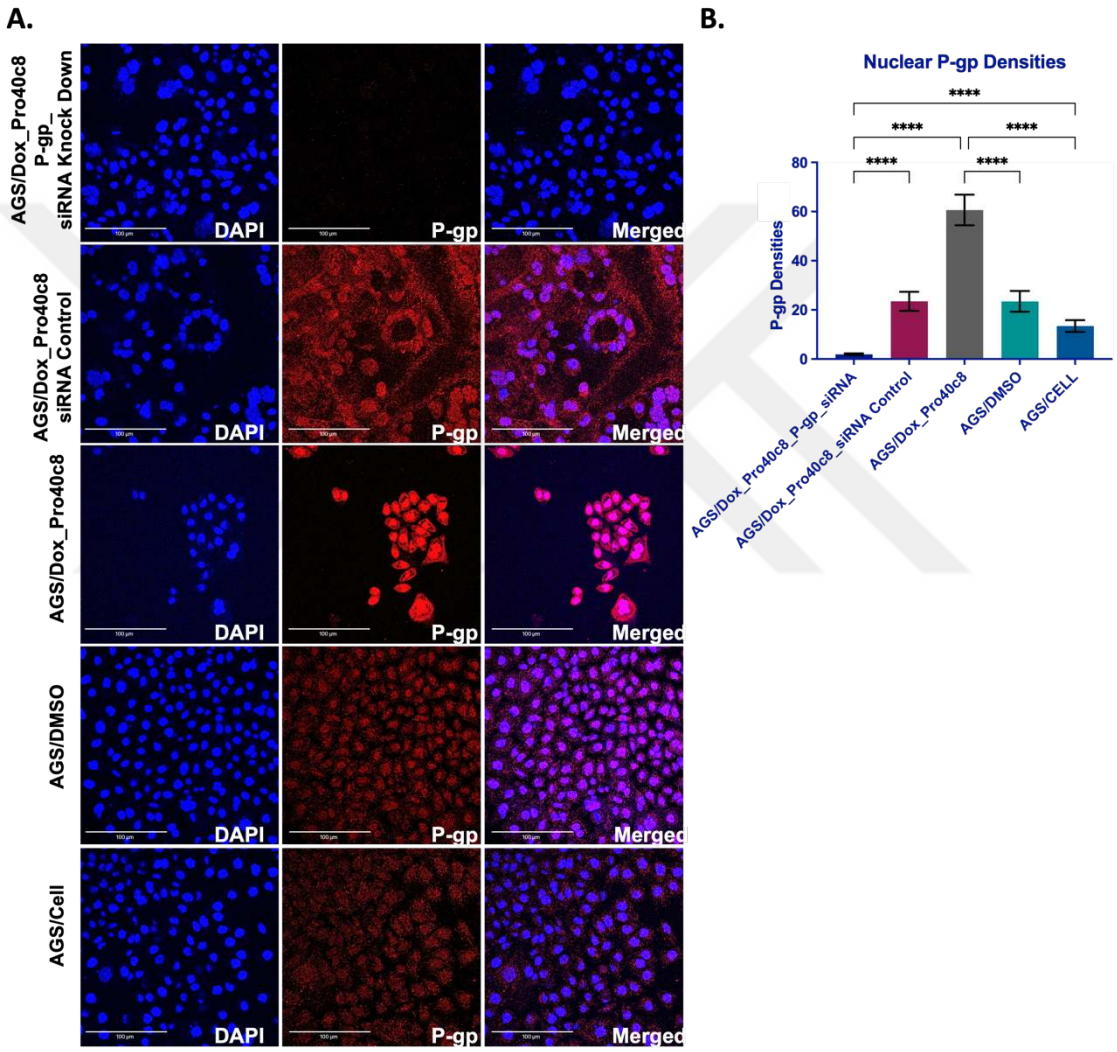

Figure 3-30 A. Intracellular distribution of P-gp in P-gp knock down (AGS/Dox_Pro40c8_P-gp_siRNA) and control cell groups: AGS/Dox_Pro40c8_siRNA Control, AGS/Dox_Pro40c8, AGS/DMSO, AGS/Cell and **B.** Densitometric analysis of the nuclear P-gp expression in the images at A. The nucleus was stained with DAPI (blue), and P-glycoprotein was immunolabelled with AlexaFluor 594 tagged antibody (red).

Scale bar, 100 µm. (20 cells/experiment, ordinary one-way ANOVA, * $p<0.05$, ** $p<0.01$, *** $p<0.001$, **** $p<0.0001$)

In AGS/Dox cells P-gp siRNA could successfully knock down the p-gp expression. The P-gp expression in siRNA transfected AGS/Dox cells was even lower than parental AGS/Cell Control.

3.25 Intracellular Distribution of Doxorubicin in P-gp Knockdown AGS/Dox cells

To validate the role of P-gp in nuclear sparing, we investigated the intracellular distribution of doxorubicin in P-gp knockdown AGS/Dox_Pro40c8_P-gp_siRNA and control cell groups under the confocal microscope. We exposed all cell groups to 1.6 µM doxorubicin for 1, 6, and 24 hours to visualize doxorubicin distribution kinetics (Figure 3-31).

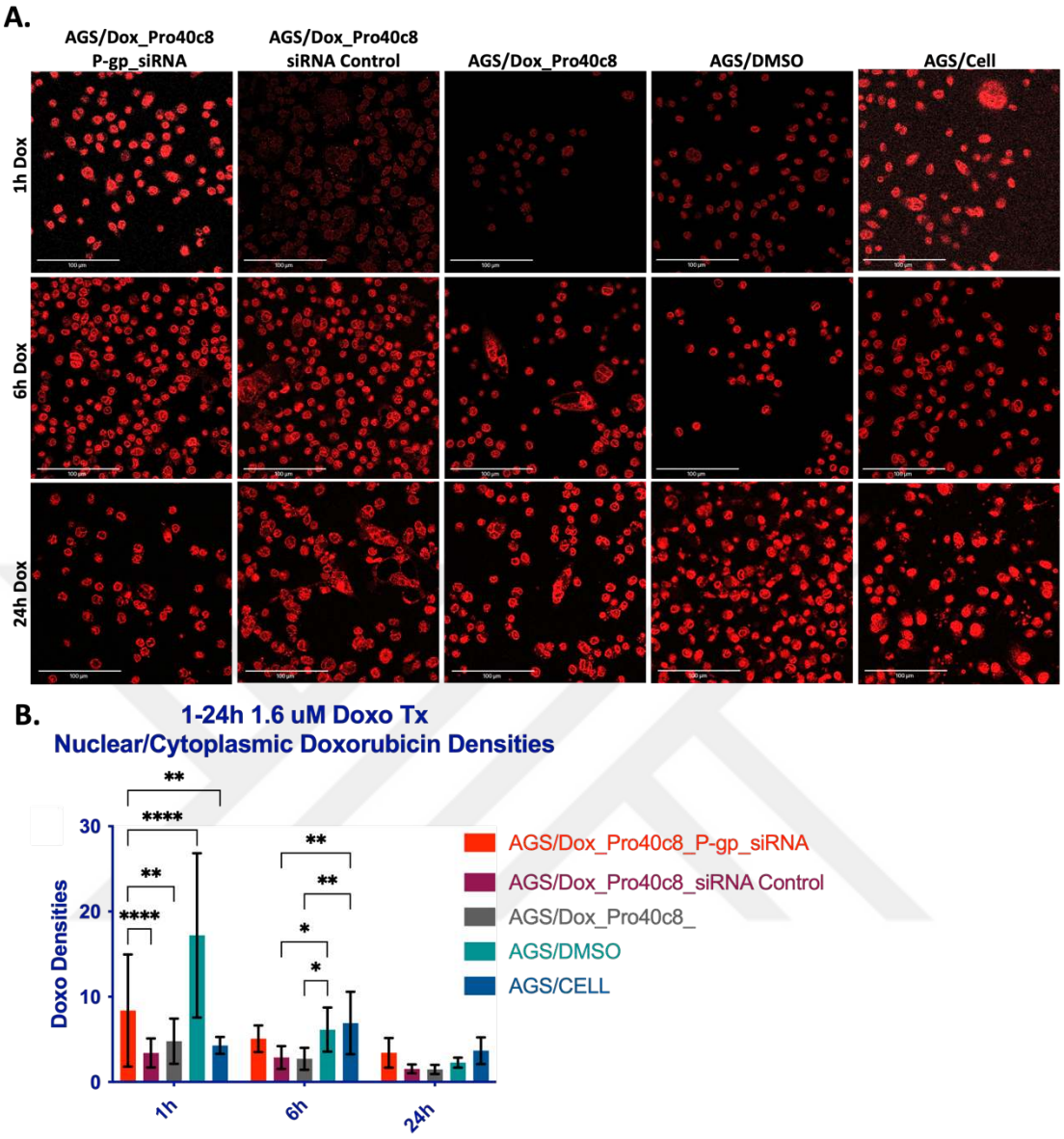

Figure 3-31 A. Intracellular distribution of doxorubicin in P-gp knock down AGS/Dox_Pro40c8_P-gp_siRNA and control cell groups; AGS/Dox_Pro40c8_siRNA Control, AGS/Dox_Pro40c8, AGS/DMSO, AGS/Cell and **B.** their time scheduled densitometric analysis. Scale bar, 100 µm. (20 cells/experiment, ordinary one-way ANOVA, * $p<0.05$, ** $p<0.01$, *** $p<0.001$, **** $p<0.0001$)

In AGS/Dox cells, the nuclear accumulation and N/C ratio of doxorubicin were the lowest as expected. This ratio continuously decreased through the doxorubicin treatment period in resistant cells (figure 3-31B). Similar to previous experiments nuclear sparing was much more prominent 24 hours after doxorubicin application. Control siRNA transfected AGS/Dox cells (AGS/Dox_Pro40c8_siRNA_Control), showed a similar pattern with

AGS/Dox cells. As we always observed, in DMSO Control cells doxorubicin influx and efflux were faster compared to other cells probably due to the effect of DMSO on membrane permeability. Our previous studies suggested that there was a passive diffusion of doxorubicin involved in the changes we observed in DMSO control cells, which is a process independent of the active displacement of doxorubicin that we observed in AGS/Dox cells. When we knock down the P-gp expression in AGS/Dox cells, we observed that nuclear accumulation of doxorubicin increased. At 24 hours of doxorubicin treatment, the N/C doxorubicin ratio of AGS/Dox_Pro40c8_P-gp_siRNA cells became the same level as parental AGS/Cells. So, by eliminating the function of P-gp, we could reverse the nuclear sparing in resistant cells.

3.26 Assessment of Doxorubicin-Induced Increase in Nuclear P-gp in P-gp Knockdown Cells

In our previous studies, we observed that exposure to doxorubicin increases nuclear expression of P-gp and leads to translocation of P-gp from cytoplasm to nucleus. Despite that P-gp specific siRNA was able to suppress P-gp expression very efficiently in AGS/Dox cells, we wondered whether doxorubicin could induce increased nuclear expression of P-gp, or nuclear translocation of existing P-gp in knockdown cells. Figure 3-32 shows the intracellular distribution of P-gp after exposure to 1.6 μM doxorubicin for 1, 6, 24 hours in AGS/Dox_Pro40c8, parental control cells and AGS/Dox_Pro40c8_P-gp_siRNA cells, with immunofluorescence imaging.

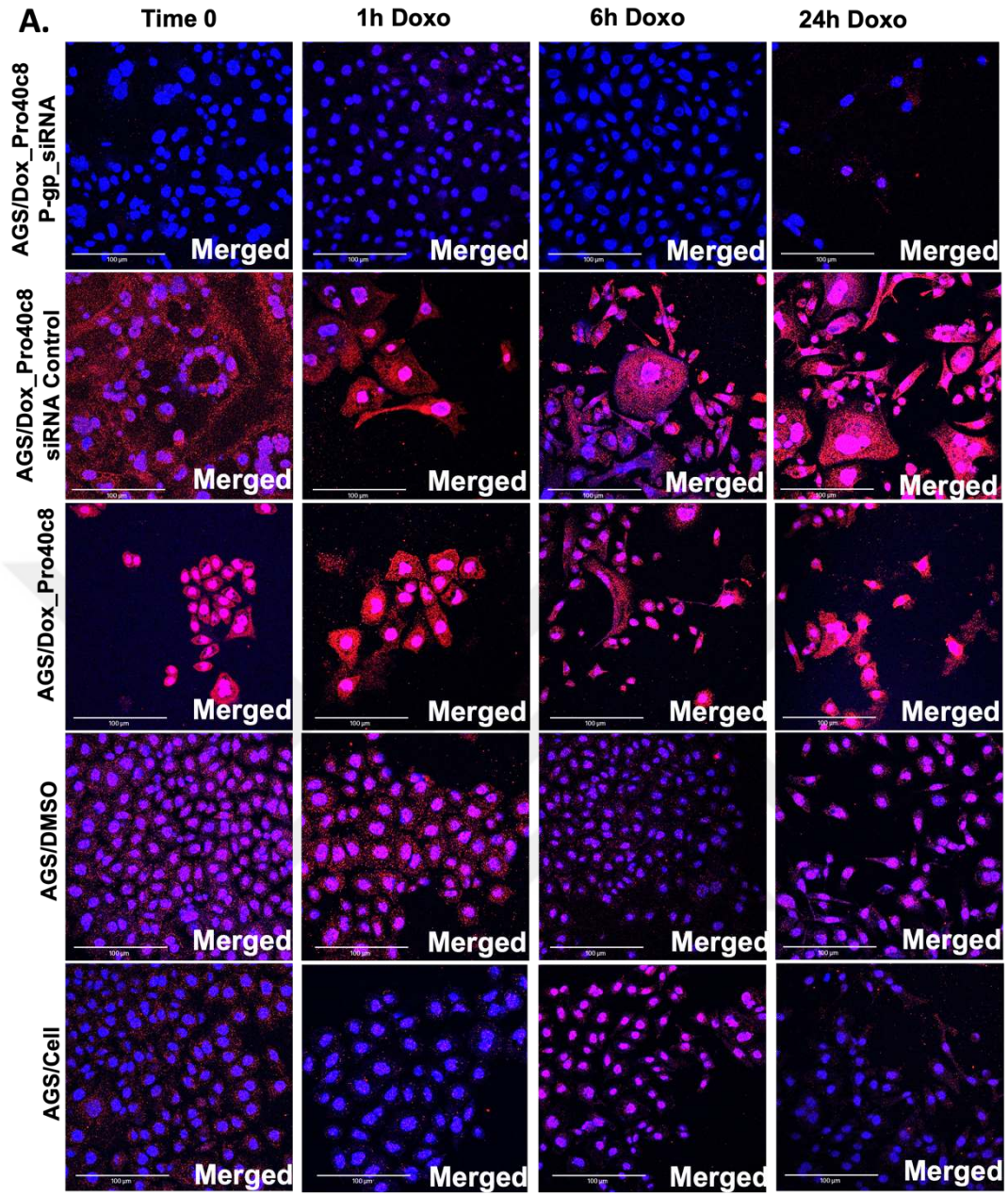
A.
Time 0
1h Doxo
6h Doxo
24h Doxo
AGS/Dox_Pro40c8 P-gp_siRNA
AGS/Dox_Pro40c8 siRNA Control
AGS/Dox_Pro40c8
AGS/DMSO
AGS/Cell
Merged

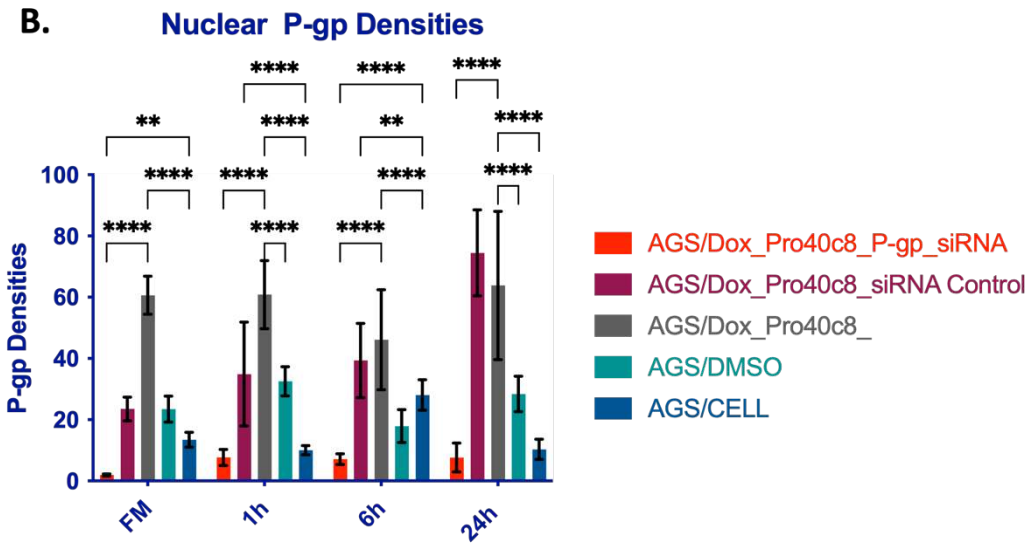
B.
Nuclear P-gp Densities
P-gp Densities
100
80
60
40
20
0
FM
1h
6h
24h
****
**
AGS/Dox_Pro40c8_P-gp_siRNA
AGS/Dox_Pro40c8_siRNA Control
AGS/Dox_Pro40c8_
AGS/DMSO
AGS/CELL

Figure 3-32 A. Intracellular distribution of P-gp after exposure to doxorubicin for 1-, 6-, or 24-hours in AGS/Dox_Pro40c8_P-gp_siRNA and control cell groups; AGS/Dox_Pro40c8_siRNA Control, AGS/Dox_Pro40c8, AGS/DMSO, AGS/Cell and **B.** their time scheduled densitometric analysis. Scale bar, 100 μm. (20 cells/experiment, ordinary one-way ANOVA, * $p<0.05$, ** $p<0.01$, *** $p<0.001$, **** $p<0.0001$)

While at time zero there was a very low-level P-gp expression (around 0) in AGS/Dox_Pro40c8_P-gp_siRNA cells, exposure to doxorubicin caused a very minimal increase in P-gp expression. However, this expression level was lower than parental AGS/Cell control cells at all time points. In AGS/Dox_Pro40c8_siRNA_control cells which are still resistant to doxorubicin, we observed that when the doxorubicin exposure time increased, P-gp in the nucleus increased like in the AGS control cells.

Moreover, exposure to doxorubicin caused a significant decrease in the cell number of AGS/Dox_Pro40c8_P-gp_siRNA cells. Especially at the 24th hour of doxorubicin treatment, their cell numbers were even lower than parental AGS cells. A decrease in cell numbers in P-gp knock down cells may suggest that a decrease in P-gp expression lowers the survival against doxorubicin exposure and reverses the resistance in AGS/Dox cells.

3.27 The Effect of P-gp knock-down on doxorubicin resistance in AGS/Dox cells

To validate the decrease in cell number in AGS/Dox Pro40c8-p-gp sirna knock down cells after exposure to doxorubicin, in one group we treat P-gp Knock down cells and control cells with 50 nM doxorubicin for 24 hours and in parallel with it in the control group they incubated in fresh medium. We chose doxorubicin concentration as a 50 nM since it was the new IC50 value of AGS/Dox_Pro40c8 cells for doxorubicin. Then we observed the confluency under phase contrast microcopy (Figure3-33). We took pictures from at least three different sites of each well.

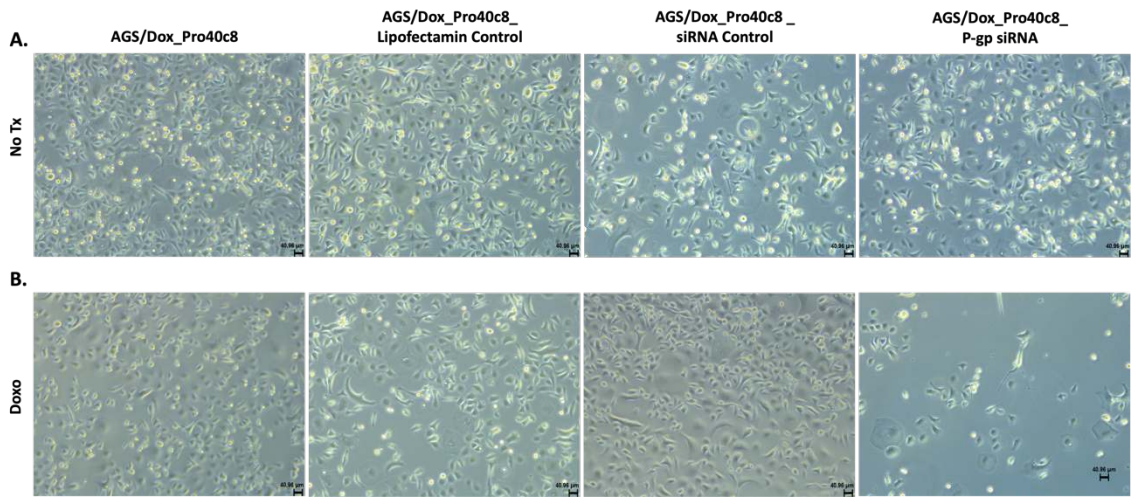

Figure 3-33 Phase contrast images of AGS/Dox_Pro40c8, AGS/Dox_Pro40c8_P-gp_siRNA and control cells **A.** Cells were incubated at fresh medium **B.** Cells were treated with 50 nM doxorubicin for 24 hours. Scale bar, 40 µm.

We observed that, in resistant AGS/Dox cells, treatment with doxorubicin did not decrease the confluency below 50%. However, in P-gp knockdown, AGS/Dox cells' confluency decreased below 50%. By this, we validated our previous studies that suggested when we knocked down P-gp in AGS/Dox cells, their survival against doxorubicin treatment significantly decreased compared to control groups.

In our studies, we observed that P-gp siRNA successfully reversed the increased P-gp expression to parental AGS/Cell level, restored nuclear accumulation of doxorubicin, and significantly decreased the cell number after doxorubicin exposure. Therefore, we wonder whether P-gp knock-down with siRNA could reverse the resistance in AGS/Dox_Pro40c8 cells. For this purpose, we have investigated the concentration-response curves for doxorubicin and calculated IC50 values with colony formation assay (Figure 3-34).

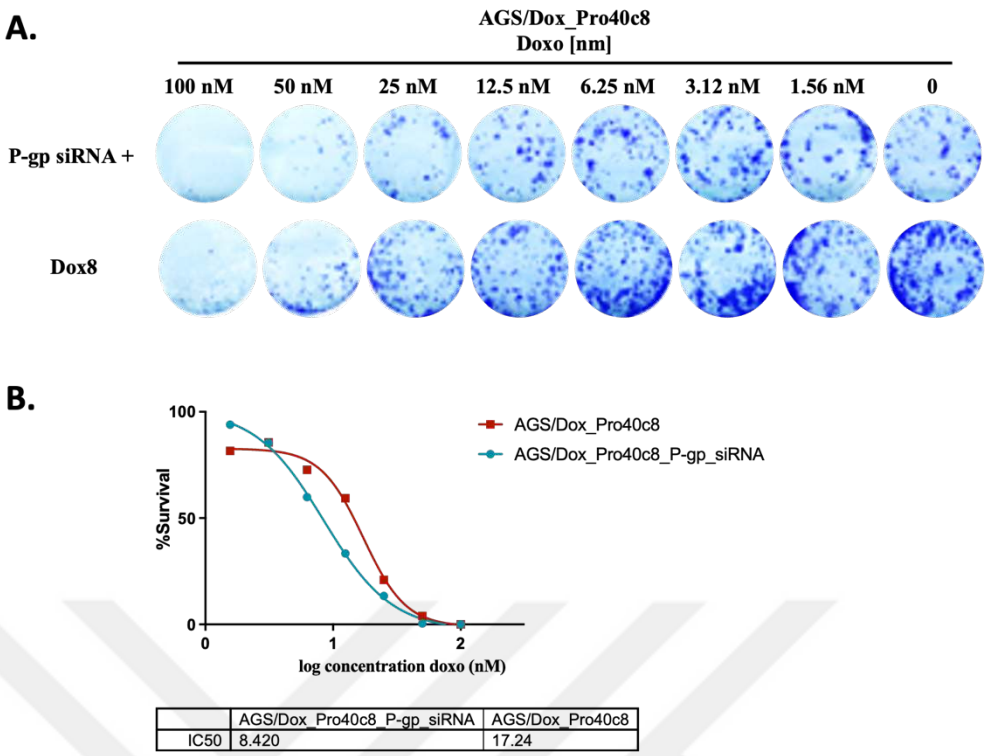

	AGS/Dox_Pro40c8_P-gp_siRNA	AGS/Dox_Pro40c8
IC50	8.420	17.24

Figure 3-34 Effect of P-gp siRNA on doxorubicin concentration-response curves in AGS/Dox_Pro40c8 cells **A.** Representative colony formation plates for AGS/Dox_Pro40c8 and P-gp siRNA transfected AGS/Dox_Pro40c8_P-gp_siRNA cells **B.** Doxorubicin concentration-response curves of corresponding cells

As supporting our previous results, transfection of P-gp siRNA caused a significant decrease in the colony numbers and caused a left shift in the concentration-response curves of AGS/Dox_Pro40c8 cells. Knockdown of P-gp expression in doxorubicin-resistant cells causes increased sensitivity to doxorubicin.

4. DISCUSSION

The main aim of today's cancer chemotherapy protocols is to kill rapidly proliferating cancer cells. Although chemotherapy shrinks the initial tumor mass in the short term, surviving resistant cancer cells continue to grow and develop a new tumor mass with increased population heterogeneity and resistance (Janku, 2014; Wang et al., 2019). Therefore, intrinsic resistance and acquired resistance is a major problem in cancer treatment.

Doxorubicin is one of the most potent and widely used chemotherapeutics in cancer treatment. Its' primary mechanism of action is through binding to DNA and inhibition of topoisomerase II. Thereby, doxorubicin inhibits DNA synthesis and leads to DNA damage. Due to this mechanism of action, the intra-nuclear concentration of doxorubicin is an important determinant for its anti-cancer efficacy. In sensitive cancer cells, doxorubicin predominantly accumulates at the nucleus leading to cell death. On the other hand, nuclear accumulation could not be achieved in resistant cells despite the presence of the drug in the cytoplasm. This phenomenon is known as "nuclear sparing" in the literature (Lewin et al., 2007). However, the underlying mechanism for nuclear sparing and its causal relationship with chemoresistance is unknown yet.

Gastric cancer is one of the most common and lethal cancer. The 5th-year survival rate is significantly low in patients due to the disease generally being diagnosed at advanced stages. In the advanced stage, today's treatment protocols are based on platinum derivatives, anthracyclines, and taxane combinations (Ajani et al., 2022). Genome profiling studies conducted that, in primary tumors, topoisomerase II expression, was significantly higher compared to normal gastric tissue (Figure 4-1) (Chandrashekar et al., 2022). This finding strengthened the anthracyclines' roles in combination therapy. However, it was reported that doxorubicin-resistant gastric cancer cells significantly reduced the expression of topoisomerase II (Marin et al., 2020). Therefore, the adaptive reduction of topoisomerase II expression by gastric cancer cells may be an important mechanism of chemotherapy resistance to anthracyclines. On the other hand, the adaptive increase in P-gp expression, which plays a very important role in resistance to anthracyclines, may also be an important resistance mechanism in gastric cancer cells. Consistent with this, it was conducted that, 87% of gastric cancer patients had P-gp positivity in Turkey (Gürel et al., 1999). P-gp positivity increases in correlation with

anthracycline resistance and recurrence of the disease. Although this rate is known, it is not known whether the intracellular location of P-gp in cancer cells, changes in nuclear P-gp expression pattern, and its association with resistance to anthracyclines in gastric cancer. All those knowledges suggest that gastric cancer cells developed adaptive changes to cytotoxic drugs. Especially the development of multidrug resistance both to the conventional chemotherapeutics and molecular targeted agents is the main challenge in gastric cancer therapy. For this reason, gastric cancer was considered as a model in your study.

In this study, we aim to investigate the role of nuclear P-glycoprotein in nuclear sparing and resistance to doxorubicin in gastric cancer. P-glycoprotein is the first discovered ABC-type drug efflux pump localized on the cell membrane which decreases the intracytoplasmic concentration of various chemotherapeutics including doxorubicin (Jiunn H. Lin & Masayo Yamazaki, 2003). While P-gp was thought to be only localize in the cellular membrane since its first discovery, now it is known that P-gp can move from the cell membrane to the intracellular compartments and localize in the endoplasmic reticulum, Golgi, mitochondria, endosome, lysosome, and nucleus membrane (Calcabrini et al., 2000). These observations suggested that nuclear P-gp's may be crucial mediators of nuclear sparing in cancer cells.

To understand the relation between acquired resistance, nuclear P-gp expression, and nuclear sparing, we established gastric adenocarcinoma cell lines that show different resistance to doxorubicin. Contrary to our expectations, these AGS/Dox cells did not show a gradually increasing resistance to doxorubicin but rather exhibited a fluctuation in resistance indexes. We thought that AGS/Dox cells could develop adaptive changes during prolonged exposure to doxorubicin, and these adaptive changes may cause variable resistance index. When we analyzed the correlation between nuclear P-gp expressions and the resistance index of all these resistant cell lines, we observed that nuclear P-gp expression increased in correlation with increasing resistance index. While P-gp expression significantly increased throughout the cell in AGS/Dox compared to AGS control cells, this increase was more prominent in the nucleus. Interestingly we observed that there is a slight increase in the expression of P-gp in AGS/DMSO cells that are exposed to the equimolar concentration of doxorubicin through the resistance development periods.

To observe the difference between doxorubicin influx and efflux kinetics in cells that show different levels of resistance to doxorubicin and express different levels of nuclear P-gp, we observe them under confocal microscope by using the autofluorescence property of doxorubicin. As we hypothesized, increased nuclear P-gp expression in AGS/Dox resistant cells was highly associated with a decreased nuclear accumulation of doxorubicin compared to parental AGS cells. These findings suggest that increased expression of nuclear p-glycoproteins' may be an important mechanism for nuclear sparing and acquired resistance to doxorubicin in gastric cancer.

Doxorubicin is an auto fluorescent molecule. It is emitted between 560nm-590 nm when excited at 490 nm which enables us to track doxorubicin under confocal microscopy. Therefore, we used this auto fluorescent property of doxorubicin while investigating its intracellular distribution. However, doxorubicin is not so bright fluorescent molecule. With low doses, its intensity is not enough to track it. To track it efficiently under a microscope; we had two chances; first, using doxorubicin at high doses, and second, increasing the laser power to very high levels. When we tried to use a low dose of doxorubicin but high laser power; we realized that increasing laser power caused a significant increase in heat and much more rapid detachment of our cells. Therefore, the only chance was using high-dose doxorubicin. The 1.6 μM doxorubicin is the lowest concentration that we could track it. This doxorubicin concentration was around 250-fold more than the naïve AGS cells' IC50 value. In future studies, we will tag doxorubicin and one other anthracycline agent with a more powerful fluorophore molecule, and we will repeat the same investigations with low-dose doxorubicin. In this way, we will have a chance to eliminate the effect of high-dose doxorubicin.

Then we decided to investigate, whether overexpressing the P-gp in naive AGS cells also causes a decrease in nuclear doxorubicin accumulation, an increase in doxorubicin efflux from the nucleus, and a right shift in concentration-response curves. We observed that just by ectopically expressing P-gp in naïve AGS cells, we established 416-fold more resistant cells. Therefore, increased P-gp expression is an important factor for acquired resistance.

In P-gp overexpressing AGS/P-gp_Oexp cells in which we ectopically expressed the P-gp protein using the lentiviral system, the P-gp was predominantly localized in the cytoplasm, unlike our resistant AGS/Dox cells. We thought that the difference between

these two cell populations was due to doxorubicin. We exposed AGS/P-gp_Oexp cells to high-dose doxorubicin. We observed that the expression of P-gp located in the nuclear membrane increased as the exposure time to doxorubicin increased. This suggested to us that exposure to doxorubicin may displace the cytoplasmic pool to the nuclear pool in cells overexpressing P-gp. The underlying mechanism of P-gp translocation induced by doxorubicin is not yet known. We have two hypotheses; first, doxorubicin can cause the translocation of P-gp to the nucleus through regulation of the nuclear localization signal. Second, doxorubicin can change the glycosylation profile of P-gp and cause its translocation to the nucleus.

P-gp is a glycoprotein that undergoes intense glycosylation. Based on the amino acid number, the expected molecular weight of non-glycosylated P-gp is 140 kDa. By glycosylation, the molecular weight of P-gp increases to 170 kDa . The glycosylation of P-gp takes place in the ER and Golgi (Wojtowicz et al., 2015). P-gp is known to have more than 50 isoforms with different glycosylation patterns (Greer & Ivey, 2007). However, the contribution of these oligosaccharides to the structure and function of P-gp remains unclear. In previous studies, 70-80 kDa P-gp has been observed in immune cells NK cells and in vinca alkaloid-resistant human leukemic lymphoblasts, and they named them mini P-gp (Trambas et al., 2001). Although the mechanisms of this mini P-gp formation cannot be known, recent studies suggest that glycosylation may be responsible. Tunicamycin is the inhibitor of glycosylation. In a study conducted with doxorubicin-resistant LoVo colon cancer and W1PR ovarian cancer cells, it was shown that by using tunicamycin, 70 kDa unglycosylated P-gp was expressed. These mini P-gps were located in the cytoplasm instead of the cell membrane (Wojtowicz et al., 2015). Considering all these studies, we thought that the glycosylation pattern of P-gp may be responsible for intracellular P-gp traffics. We will investigate these mechanisms in our future studies. In this study we mainly focused on our first hypothesis. Based on the literature search, even if there is no initial NLS in P-gp, alternative splicing may lead to the addition of NLS to the P-gp sequence in doxorubicin-treated cells.

To test the importance of NLS in P-gp translocation to the nucleus, we established AGS/P-gp_NLS cells which are the naive AGS cells that were transducted with P-gp with NLS sequence plasmid. We observed that P-gp was predominantly located in the nucleus of AGS/P-gp_NLS cells, compared to the cytoplasmic dominance of P-gp in AGS/P-

gp_Oexp cells, which were transduced with plasmids which include P-gp sequence without NLS. These findings point out the importance of NLS in the nuclear localization of P-gp.

When we compare, AGS/Dox, AGS/P-gp_Oexp, and AGS/P-gp_NLS cell's P-gp expression pattern, we observed that they have significantly increased P-gp expression compared to control groups and increased nuclear-sparing ability with decreasing nucleus/cytoplasmic doxorubicin ratio. This similarity points out the possible importance of P-gp expression in the nuclear sparing of doxorubicin and the development of resistance.

Also, we observed in all those three groups of cells showed increased nuclear sparing by time, after exposure to doxorubicin. They had the highest nuclear-sparing pattern at the 24th hour of doxorubicin treatment. To understand why nuclear sparing started around 6 hours and reached its highest at 24 hours we compared the nuclear sparing and P-gp localization profiles. We found that nuclear P-gp also increased by increasing by time after doxorubicin treatment, reaching to a maximum around the 24^{th} hour of treatment.

An increase in the nuclear P-gp by time after doxorubicin treatment makes us think, are those P-gp's newly synthesized P-gp or already existing cytoplasmic P-gp's could translocate to the nucleus? To better observe the processes behind the increase in nuclear P-gp expression after doxorubicin exposure we decided to track the translocation of P-gp by live-cell imaging of GFP-tagged P-gp expressing cells in future experiments. Also, we plan to study the kinetics of nuclear P-gp expression after doxorubicin exposure in conditions where gene transcription or protein synthesis is inhibited.

The localization of P-gp, especially in the nuclear membrane, has the potential to bring about very important results in terms of chemotherapy resistance. To eliminate the obstacle to the success of P-gp in chemotherapy, studies have been continuing for years on drugs that inhibit drug efflux by P-gp and their translation to the clinic. After observing that P-gp expression increased in correlation with resistance induced by continuous exposure to doxorubicin, we wondered if we could reverse the resistance by inhibiting or silencing the P-gp. For this, we primarily used verapamil, a first-generation P-gp inhibitor, and zosuquidar, a third-generation P-gp inhibitor (Palmeira et al., 2012a). These inhibitors only at high concentrations, 40 μM and 1 μM, respectively, could decrease the

nuclear sparing effect of P-gp at the 24th hour of doxorubicin treatment. Then, we investigated the P-gp inhibitor's effect on doxorubicin resistance in AGS/Dox cells. We assessed the concentration-response curves for doxorubicin in the presence or absence of P-gp inhibitors verapamil and zosuquidar. We observed that first-generation P-gp inhibitor verapamil caused a slight left shift in the concentration response curve. This may be because, verapamil is a competitive inhibitor of P-gp, and nuclear P-gp expression in resistant cells reached a significantly high level in AGS/Dox cells. Therefore, even if we used a high dose of verapamil, it could not be enough for inhibiting all P-gp's in cells. Since the first- and second-generation P-gp inhibitors are themselves P-gp substrates, they can be effluxed by the P-gp in the cell membrane before reaching the nuclear P-gp. Therefore, even if they can competitively inhibit drug efflux from the cytoplasm; they may not be as effective in preventing drug efflux from the nucleus. On the other hand, by using, zosuquidar, we observed a significant increase in sensitivity to the doxorubicin in AGS/Dox cells. Third-generation P-gp inhibitor, zosuquidar is a direct inhibitor that binds directly to P-gp and inhibits non-competitively and, also, has a higher potency than first-generation inhibitors. However, because third-generation P-gp inhibitors bind irreversibly to P-gp in the cell membrane, their access to nuclear P-gp may be much more difficult than their access to cell membrane P-gp. Therefore, their potency to inhibit nuclear P-gp may be lower than their potency to inhibit cell membrane P-gp. If our hypothesis is correct, this would require the use of higher doses of P-gp inhibitors to increase drug concentration in the nucleus, which is the main target of cytotoxicity, although they may increase drug concentration in the cytoplasm. This may also explain why P-gp inhibitors require use in doses reaching toxic doses to overcome chemotherapy resistance in the clinic.

Despite the importance of P-gp in multi-drug resistance, the inability of P-gp inhibitors to provide the expected effect in overcoming chemotherapy resistance has been tried to be explained by other drug carriers such as MRP1 (MDR-associated proteins), BCRP (breast cancer resistance protein), which may be responsible for multi-drug resistance. However, many P-gp inhibitors are also inhibitors of these pumps. To ensure that, a decrease in the nuclear sparing capability of resistant cells and a left shift in concentration-response curves by P-gp inhibitors is through the inhibition of P-gp but not through other pumps, we knocked down P-gp by P-gp specific siRNAs. We observed that, knocking down P-gp in AGS/Dox cells could reverse the nuclear sparing in these

cells. Their nucleus/ cytoplasmic doxorubicin ratio increased to the level in parental AGS cells. P-gp specific siRNAs also decreased the survival in AGS/Dox cells. These results highly point out the importance of specifically P-gp no other efflux pumps in nuclear sparing in gastric adenocarcinoma cells.

5. CONCLUSION

Our findings suggest that the increased expression of nuclear P-gps and translocation of P-gps from cytoplasmic pool to the nucleus may be important mechanisms for nuclear sparing and acquired resistance to doxorubicin in gastric cancer. Further delineation of the mechanisms by which doxorubicin induces increased expression of nuclear P-gps and nuclear translocation of P-gps, may put forth new molecules targeting which may overcome nuclear sparing of doxorubicin and acquired chemoresistance in cancer cells.

BIBLIOGRAPHY

Aitini, E., Rabbi, C., Mambrini, A., Cavazzini, G., Pari, F., Zamagni, D., Cantore, M., Pagani, M., Sorio, M., Lusenti, A., Adami, F., & Smerieri, F. (2001). Epirubicin, cisplatin and continuous infusion 5-fluorouracil (ECF) in locally advanced or metastatic gastric cancer: a single institution experience. *Tumori*, *87*(1), 20-24. https://doi.org/10.1177/030089160108700105

Ajani, J. A., D'Amico, T. A., Bentrem, D. J., Chao, J., Cooke, D., Corvera, C., Das, P., Enzinger, P. C., Enzler, T., Fanta, P., Farjah, F., Gerdes, H., Gibson, M. K., Hochwald, S., Hofstetter, W. L., Ilson, D. H., Keswani, R. N., Kim, S., Kleinberg, L. R., . . . Pluchino, L. A. (2022). Gastric Cancer, Version 2.2022, NCCN Clinical Practice Guidelines in Oncology. *Journal of the National Comprehensive Cancer Network*, *20*(2), 167-192. https://doi.org/10.6004/jnccn.2022.0008

Alfarouk, K. O., Stock, C.-M., Taylor, S., Walsh, M., Muddathir, A. K., Verduzco, D., Bashir, A. H. H., Mohammed, O. Y., Elhassan, G. O., Harguindey, S., Reshkin, S. J., Ibrahim, M. E., & Rauch, C. (2015). Resistance to cancer chemotherapy: failure in drug response from ADME to P-gp. *Cancer Cell International*, *15*(1), 71. https://doi.org/10.1186/s12935-015-0221-1

Amin, M. L. (2013). P-glycoprotein Inhibition for Optimal Drug Delivery. *Drug Target Insights*, *7*, 27-34. https://doi.org/10.4137/dti.S12519

Arbabi Bidgoli, S. (2006). Comparative studies of Bcl-2 expression and its relation to P53, P-glycoprotein, Topo IIa, thymidylate synthase, thymidine phosphorylase and GST pi as anticancer therapy targets in GI cancers. *Annals of Oncology*, 45-46.

Ashida, H., Enan, E., & Matsumura, F. (1996). Protective action of dehydroascorbic acid on the Ah receptor-dependent and receptor-independent induction of lipid peroxidation in adipose tissue of male guinea pig caused by TCDD administration. *Journal of Biochemical Toxicology*, *11*(6), 269-278. https://doi.org/https://doi.org/10.1002/(SICI)1522-7146(1996)11:6<269::AID-JBT2>3.0.CO;2-I

Bachur, N. R. (2002). Anthracyclines. In J. R. Bertino (Ed.), *Encyclopedia of Cancer (Second Edition)* (pp. 57-61). Academic Press. https://doi.org/https://doi.org/10.1016/B0-12-227555-1/00006-X

Baghirova, S., Hughes, B. G., Hendzel, M. J., & Schulz, R. (2015). Sequential fractionation and isolation of subcellular proteins from tissue or cultured cells. *MethodsX*, *2*, 440-445. https://doi.org/10.1016/j.mex.2015.11.001

Baguley, B. C. (2010). Multiple Drug Resistance Mechanisms in Cancer. *Mol Biotechnol*, 308–316.

Baldini, N., Scotlandi, K., Serra, M., Shikita, T., Zini, N., Ognibene, A., Santi, S., Ferracini, R., & Maraldi, N. M. (1995). Nuclear immunolocalization of P-glycoprotein in multidrug-resistant cell lines showing similar mechanisms of doxorubicin distriubiton. *Eur. J. Cell. biol.*, 226-239.

Beck, W. T., Morgan, S. E., Mo, Y.-Y., & Bhat, U. G. (1999). Tumor cell resistance to DNA topoisomerase II inhibitors: new developments. *Drug Resistance Updates*, *2*(6), 382-389. https://doi.org/https://doi.org/10.1054/drup.1999.0110

Bhatia, P., Bernier, M., Sanghvi, M., Moaddel, R., Schwarting, R., Ramamoorthy, A., & Wainer, I. W. (2012). Breast cancer resistance protein (BCRP/ABCG2) localises to the nucleus in glioblastoma multiforme cells. *Xenobiotica*, 748–755.

Braakman, I., & Hebert, D. N. (2013). Protein folding in the endoplasmic reticulum. *Cold Spring Harb Perspect Biol*, *5*(5), a013201. https://doi.org/10.1101/cshperspect.a013201

Burrow, S. M., Phoenix, D. A., Wainwright, M., & Tobin, M. J. (2003). Intracellular localisation studies of doxorubicin and Victoria Blue BO in EMT6-S and EMT6-R cells using confocal microscopy. *Cytotechnology*, 15-25.

Cai, B., Miao, Y., Liu, Y., Xu, X., Guan, S., Wu, J., & Liu, Y. (2013). Nuclear Multidrug-Resistance Related Protein 1 Contributes to Multidrug-Resistance of Mucoepidermoid Carcinoma Mainly via Regulating Multidrug-Resistance Protein 1: A Human Mucoepidermoid Carcinoma Cells Model and Spearman's Rank Correlation Analysis. *PLos*.

Cai, B. L., Xu, X. F., Fu, S. M., Shen, L. L., Zhang, J., & Guan, S. M. (2011). Nuclear translocation of MRP1 contributes to multidrug resistance of mucoepidermoid carcinoma. *Oral Oncology*, 1134-1141.

Calcabrini, A., Meschini, S., Stringaro, A., Cianfriglia, M., Arancia, G., & Molinari, A. (2000). Detection of P-glycoprotein in the nuclear envelope of multidrug resistant cells. *Histochem. J.*, 599-605.

Carvalho, C., Santos, R. X., Cardoso, S., Correia, S., Oliveira, P. J., Santos, M. S., & Moreira, P. I. (2009). Doxorubicin: the good, the bad and the ugly effect. *Curr Med Chem*, *16*(25), 3267-3285. https://doi.org/10.2174/092986709788803312

Chandrashekar, D. S., Karthikeyan, S. K., Korla, P. K., Patel, H., Shovon, A. R., Athar, M., Netto, G. J., Qin, Z. S., Kumar, S., Manne, U., Creighton, C. J., & Varambally, S. (2022). UALCAN: An update to the integrated cancer data analysis platform. *Neoplasia*, *25*, 18-27. https://doi.org/10.1016/j.neo.2022.01.001

Chen, Y. L., Yang, T. J., Wu, C. L., & Chen, K. C. (2016). Mechanisms Underlying Lung Resistance-Related Protein (LRP)-Mediated Doxorubicin Resistance of Non-Small Cell Lung Cancer Cells. *Chinese Journal of Physiology*, 331-347.

Chern, Y.-J., & Tai, I. T. (2020). Adaptive response of resistant cancer cells to chemotherapy. *Cancer Biol. Med.*, 842-863.

Chu, E., & DeVita Jr., V. T. (2018). *Physicians' Cancer Chemotherapy Drug Manual 2018*. Jones & Bartlett Learning.

Cole, S. P., Bhardwaj, G., Gerlach, J. H., Mackie, J. E., & Grant, C. E. (1992). Overexpression of transporter gene in a multidrug resistant human lung cancer cell line. *Science*, 1650-1654.

Cullinan, S. A., Moertel, C. G., Fleming, T. R., Rubin, J. R., Krook, J. E., Everson, L. K., Windschitl, H. E., Twito, D. I., Marschke, R. F., Foley, J. F., Pfeifle, D. M., & Barlow, J. F. (1985). A Comparison of Three Chemotherapeutic Regimens in the Treatment of Advanced Pancreatic and Gastric Carcinoma: Fluorouracil vs Fluorouracil and Doxorubicin vs Fluorouracil, Doxorubicin, and Mitomycin. *JAMA*, *253*(14), 2061-2067. https://doi.org/10.1001/jama.1985.03350380077025

Czabotar, P. E., Lessene, G., Strasser, A., & Adams, J. M. (2014). Control of apoptosis by the BCL-2 protein family: implications for physiology and therapy. *Nature Reviews Molecular Cell Biology*, *15*(1), 49-63. https://doi.org/10.1038/nrm3722

Davidson, A. L., & Chen, J. (2004). ATP-binding cassette transporters in bacteria. *Annu Rev Biochem*, *73*, 241-268. https://doi.org/10.1146/annurev.biochem.73.011303.073626

de Ménorval, M. A., Mir, L. M., Fernández, M. L., & Reigada, R. (2012). Effects of dimethyl sulfoxide in cholesterol-containing lipid membranes: a comparative study of experiments in silico and with cells. *PLoS One*, *7*(7), e41733. https://doi.org/10.1371/journal.pone.0041733

Dean, M., Moitra, K., & Allikmets, R. (2022). The human ATP-binding cassette (ABC) transporter superfamily. *Hum Mutat*, *43*(9), 1162-1182. https://doi.org/10.1002/humu.24418

Deepthi, A., Raju, S., Kalyani, A., Udaya Kiran, M., & Vanaja, A. (2013). Targeted Drug Delivery to the Nucleus and its Potential Role in Cancer Chemotherapy. *J. Pharm. Sci.* , 48-56.

Doyle, L. A., & Ross, D. D. (2003). Multidrug resistance mediated by the breast cancer resistance protein BCRP (ABCG2). *oncogene*, 7340–7358.

Emran, T. B., Shahriar, A., Mahmud, A. R., Rahman, T., Abir, M. H., Siddiquee, M. F.-R., Ahmed, H., Rahman, N., Nainu, F., Wahyudin, E., Mitra, S., Dhama, K., Habiballah, M. M., Haque, S., Islam, A., & Hassan, M. M. (2022). Multidrug Resistance in Cancer: Understanding Molecular Mechanisms, Immunoprevention and Therapeutic Approaches [Review]. *Frontiers in Oncology*, *12*. https://doi.org/10.3389/fonc.2022.891652

Featherstone, J. M., Speers, A. G., Lwaleed, B. A., Hayes, M. C., Cooper, A. J., & Birch, B. R. (2005). The nuclear membrane in multidrug resistance: microinjection of epirubicin into bladder cancer cell lines. *BJU Int.*, 1091-1098.

Fu, D. (2013). Where is it and How Does it Get There – Intracellular Localization and Traffic of P-glycoprotein [Mini Review]. *Frontiers in Oncology*, *3*. https://doi.org/10.3389/fonc.2013.00321

Fu, D., & Roufogalis, B. D. (2007). Actin disruption inhibits endosomal traffic of P-glycoprotein-EGFP and resistance to daunorubicin accumulation. *Am J Physiol Cell Physiol*, *292*(4), C1543-1552. https://doi.org/10.1152/ajpcell.00068.2006

Gervasoni, J. E., Fields, S. Z., Krishna, S., Baker, M. A., Rosado, M., Thuraisamy, K., Hindenburg, A. A., & Taub, R. N. (1991). Subcellular Distribution of Daunorubicin in P-Glycoprotein-positive and -negative Drug-resistant Cell Lines Using Laser-assisted Confocal Microscopy. *Cancer Reseacrh*, 4955-4963.

Gottesman, M. M., Fojo, T ., Bates, S.E. (2002). Multidrug resistance in cancer: role of ATP-dependent transporters. *Nat Rev Cancer*, 48-58.

Gottesman, M. M., & Ling, V. (2006). The molecular basis of multidrug resistance in cancer: the early years of P-glycoprotein research. *FEBS Lett*, *580*(4), 998-1009. https://doi.org/10.1016/j.febslet.2005.12.060

Greer, D. A., & Ivey, S. (2007). Distinct N-glycan glycosylation of P-glycoprotein isolated from the human uterine sarcoma cell line MES-SA/Dx5. *Biochim Biophys Acta*, *1770*(9), 1275-1282. https://doi.org/10.1016/j.bbagen.2007.07.005

Gryko, M., Pryczynicz, A., Zareba, K., Kędra, B., Kemona, A., & Guzińska-Ustymowicz, K. (2014). The expression of Bcl-2 and BID in gastric cancer cells. *J Immunol Res*, *2014*, 953203. https://doi.org/10.1155/2014/953203

Gürel, S., Yerci, Ö., Filiz, G., Dolar, E., Yilmazlar, T., Nak, S. G., Gülten, M., Zorluoglu, A., & Memik, F. (1999). High Expression of Multidrug Resistance-1 (MDR-1) and its Relationship with Multiple Prognostic Factors in Gastric Carcinomas in Patients in Turkey. *Journal of International Medical Research*, *27*(2), 79-84. https://doi.org/10.1177/030006059902700204

Harris, L., Batist, G., Belt, R., Rovira, D., Navari, R., Azarnia, N., Welles, L., Winer, E., & Group, T. D.-S. (2002). Liposome-encapsulated doxorubicin compared with conventional doxorubicin in a randomized multicenter trial as first-line therapy of metastatic breast carcinoma. *Cancer*, *94*(1), 25-36. https://doi.org/https://doi.org/10.1002/cncr.10201

Hollenstein, K., Dawson, R. J. P., & Locher, K. P. (2007). Structure and mechanism of ABC transporter proteins. *Current Opinion in Structural Biology*, *17*(4), 412-418. https://doi.org/https://doi.org/10.1016/j.sbi.2007.07.003

Holohan, C., Van Schaeybroeck, S., Longley, D., & Johnstan, P. (2013). Cancer Drug Resistance: an evolving paradigm. *Nat. Rev. Cancer*, 714-726.

Housman, G., Byler, S., Heerboth, S., Lapinska, K., Longacre, M., Snyder, N., & Sarkar, S. (2014). Drug Resistance in Cancer: An Overview. *Cancers (Basel);*, 1769–1792.

Hu, T., To, K. K., Wang, L., Zhang, L., Lu, L., Shen, J., Chan, R. L., Li, M., Yeung, J. H., & Cho, C. H. (2014). Reversal of P-glycoprotein (P-gp) mediated multidrug resistance in colon cancer cells by cryptotanshinone and dihydrotanshinone of Salvia miltiorrhiza. *Phytomedicine*, *21*(11), 1264-1272. https://doi.org/10.1016/j.phymed.2014.06.013

Ilic, M., & Ilic, I. (2022). Epidemiology of stomach cancer. *World J Gastroenterol*, *28*(12), 1187-1203. https://doi.org/10.3748/wjg.v28.i12.1187

Janku, F. (2014). Tumor heterogeneity in the clinic: is it a real problem? *Ther Adv Med Oncol*, *6*(2), 43-51. https://doi.org/10.1177/1758834013517414

Jaramillo, A. C., Al Saig, F., Cloos, J., Jansen, G., & Peters, G. J. (2018). How to overcome ATP-binding cassette drug efflux transporter-mediated drug resistance? *Cancer Drug Resistance*, *1*(1), 6-29. https://doi.org/10.20517/cdr.2018.02

Jones, P. M., & George, A. M. (2004). The ABC transporter structure and mechanism: perspectives on recent research. *Cell Mol Life Sci*, *61*(6), 682-699. https://doi.org/10.1007/s00018-003-3336-9

Joost, H. G., & Schürmann, A. (2001). Subcellular fractionation of adipocytes and 3T3-L1 cells. *Methods Mol Biol*, *155*, 77-82. https://doi.org/10.1385/1-59259-231-7:077

Kasi, P. V. A. (2022). Anthracyclines. *StatPearls*. https://www.ncbi.nlm.nih.gov/books/NBK538187/

Katzenstein, H. M., Malogolowkin, M. H., Krailo, M. D., Piao, J., Towbin, A. J., McCarville, M. B., Tiao, G. M., Dunn, S. P., Langham, M. R., McGahren, E. D., Finegold, M. J., Ranganathan, S., Weldon, C. B., Thompson, P. A., Trobaugh-Lotrario, A. D., O'Neill, A. F., Furman, W. L., Chung, N., Randazzo, J., . . .

Meyers, R. L. (2022). Doxorubicin in combination with cisplatin, 5-flourouracil, and vincristine is feasible and effective in unresectable hepatoblastoma: A Children's Oncology Group study. *Cancer*, *128*(5), 1057-1065. https://doi.org/10.1002/cncr.34014

Ke, W., Yu, P., Wang, J., Wang, R., Guo, C., Zhou, L., Li, C., & Li, K. (2010). MCF-7/ADR cells (re-designated NCI/ADR-RES) are not derived from MCF-7 breast cancer cells: a loss for breast cancer multidrug-resistant research. *Med. Oncol.*, 135-141.

Keizer, H. G., Pinedo, H. M., Schuurhuis, G. J., & Joenje, H. (1990). Doxorubicin (adriamycin): a critical review of free radical-dependent mechanisms of cytotoxicity. *Pharmacol Ther*, *47*(2), 219-231. https://doi.org/10.1016/0163-7258(90)90088-j

Khasraw, M., Bell, R., & Dang, C. (2012). Epirubicin: is it like doxorubicin in breast cancer? A clinical review. *Breast*, *21*(2), 142-149. https://doi.org/10.1016/j.breast.2011.12.012

Kiyokawa, H., Igawa, Y., Muraishi, O., Katsuyama, Y., Iizuka, K., & Nishizawa, O. (1999). DISTRIBUTION OF DOXORUBICIN IN THE BLADDER WALL AND REGIONAL LYMPH NODES AFTER BLADDER SUBMUCOSAL INJECTION OF LIPOSOMAL DOXORUBICIN IN THE DOG. *The Journal of Urology*, *161*(2), 665-667. https://doi.org/https://doi.org/10.1016/S0022-5347(01)61991-8

Kiyomiya, K., Satoh, J., Horie, H., Kurebe, M., Nakagawa, H., & Matsuo, S. (2002). Correlation between nuclear action of anthracycline anticancer agents and their binding affinity to the proteasome. *Int J Oncol.* , 1081-1085.

Kluck, G. E. G., Durham, K. K., Yoo, J. A., & Trigatti, B. L. (2020). High Density Lipoprotein and Its Precursor Protein Apolipoprotein A1 as Potential Therapeutics to Prevent Anthracycline Associated Cardiotoxicity. *Front Cardiovasc Med*, *7*, 65. https://doi.org/10.3389/fcvm.2020.00065

Krishna, R., & Mayer, L. D. (2000). Multidrug resistance (MDR) in cancer mechanisms, reversal using modulators of MDR and the role of MDR modulators in influencing the pharmacokinetics of anticancer drugs. *Eur. J. Pharm. Sci.*, 265-283.

Kufer, T. A., Kremmer, E., Adam, A. C., Philpott, D. J., & Sansonetti, P. J. (2008). The pattern-recognition molecule Nod1 is localized at the plasma membrane at sites of bacterial interaction. *Cellular Microbiology*, *10*(2), 477-486. https://doi.org/https://doi.org/10.1111/j.1462-5822.2007.01062.x

Lanford, R. E., Kanda, P., & Kennedy, R. C. (1986). Induction of nuclear transport with a synthetic peptide homologous to the SV40 T antigen transport signal. *Cell*, *46*(4), 575-582. https://doi.org/https://doi.org/10.1016/0092-8674(86)90883-4

Lange, A., Mills, R. E., Lange, C. J., Stewart, M., Devine, S. E., & Corbett, A. H. (2007). Classical nuclear localization signals: definition, function, and interaction with importin α. *Journal of Biological Chemistry*, *282*(8), 5101-5105.

Lee, S. J., Matsuura, Y., Liu, S. M., & Stewart, M. (2005). Structural basis for nuclear import complex dissociation by RanGTP. *Nature*, *435*(7042), 693-696.

Legha, S. S., Benjamin, R. S., Mackay, B., Ewer, M., Wallace, S., Valdivieso, M., Rasmussen, S. L., Blumenschein, G. R., & Freireich, E. J. (1982). Reduction of

doxorubicin cardiotoxicity by prolonged continuous intravenous infusion. *Ann Intern Med*, *96*(2), 133-139. https://doi.org/10.7326/0003-4819-96-2-133

Lehne, G., & Rugstad, H. E. (1998). Cytotoxic effect of the cyclosporin PSC 833 in multidrug-resistant leukaemia cells with increased expression of P-glycoprotein. *British Journal of Cancer*, *78*(5), 593-600. https://doi.org/10.1038/bjc.1998.546

Lei, Z.-N., Teng, Q.-X., Tian, Q., Chen, W., Xie, Y., Wu, K., Zeng, Q., Zeng, L., Pan, Y., Chen, Z.-S., & He, Y. (2022). Signaling pathways and therapeutic interventions in gastric cancer. *Signal Transduction and Targeted Therapy*, *7*(1), 358. https://doi.org/10.1038/s41392-022-01190-w

Lewin, J. M., Lwaleed, B. A., Cooper, A. J., & Birch, B. R. (2007). The Direct Effect of Nuclear Pores on Nuclear Chemotherapeutic Concentration in Multidrug Resistant Bladder Cancer: The Nuclear Sparing Phenomenon. *Journal of Urology*, *177*(4), 1526-1530. https://doi.org/doi:10.1016/j.juro.2006.11.048

Lim, Z. F., & Ma, P. C. (2019). Emerging insights of tumor heterogeneity and drug resistance mechanisms in lung cancer targeted therapy. *J Hematol Oncol*, *12*(1), 134. https://doi.org/10.1186/s13045-019-0818-2

Lin, J. H., & Yamazaki, M. (2003). Role of P-glycoprotein in pharmacokinetics: clinical implications. *Clin Pharmacokinet.*, 59-98.

Longley, D., & Johnston, P. (2005). Molecular mechanisms of drug resistance. *The Journal of Pathology*, *205*(2), 275-292. https://doi.org/https://doi.org/10.1002/path.1706

Lordick, F., Carneiro, F., Cascinu, S., Fleitas, T., Haustermans, K., Piessen, G., Vogel, A., & Smyth, E. C. (2022). Gastric cancer: ESMO Clinical Practice Guideline for diagnosis, treatment and follow-up. *Ann Oncol*, *33*(10), 1005-1020. https://doi.org/10.1016/j.annonc.2022.07.004

Ma, J., Shen, H., Kapesa, L., & Zeng, S. (2016). Lauren classification and individualized chemotherapy in gastric cancer. *Oncol Lett*, *11*(5), 2959-2964. https://doi.org/10.3892/ol.2016.4337

MacDonald, J. S., Schein, P. S., Woolley, P. V., Smythe, T., Ueno, W., Hoth, D., Smith, F., Boiron, M., Gisselbrecht, C., Brunet, R., & Lagarde, C. (1980). 5-Fluorouracil, doxorubicin, and mitomycin (FAM) combination chemotherapy for advanced gastric cancer. *Ann Intern Med*, *93*(4), 533-536. https://doi.org/10.7326/0003-4819-93-4-533

MacGowan, G. A., O'Callaghan, D., Webb, H., & Horgan, J. H. (1992). The effects of verapamil on training in patients with ischemic heart disease. *Chest*, *101*(2), 411-415. https://doi.org/10.1378/chest.101.2.411

Mansoori, B., Mohammadi, A., Davudian, S., Shirjang, S., & Baradaran, B. (2017). The Different Mechanisms of Cancer Drug Resistance: A Brief Review. *Adv Pharm Bull*, *7*(3), 339-348. https://doi.org/10.15171/apb.2017.041

Marin, J. J., Al-Abdulla, R., Lozano, E., Briz, O., Bujanda, L., Banales, J. M., & Macias, R. I. (2016). Mechanisms of Resistance to Chemotherapy in Gastric Cancer. *Anticancer Agents Med Chem*, *16*(3), 318-334. https://doi.org/10.2174/1871520615666150803125121

Marin, J. J. G., Perez-Silva, L., Macias, R. I. R., Asensio, M., Peleteiro-Vigil, A., Sanchez-Martin, A., Cives-Losada, C., Sanchon-Sanchez, P., Sanchez De Blas,

B., Herraez, E., Briz, O., & Lozano, E. (2020). Molecular Bases of Mechanisms Accounting for Drug Resistance in Gastric Adenocarcinoma. *Cancers (Basel)*, *12*(8). https://doi.org/10.3390/cancers12082116

McGowan, J., Chung, R., Maulik, A., & Piotrowska, I. (2017). Anthracycline Chemotherapy and Cardiotoxicity. *Cardiovasc Drugs Ther.*, 63-75.

Miettinen, M., Rikala, M. S., Rys, J., Lasota, J., & Wang, Z. F. (2012). Vascular endothelial growth factor receptor 2 as a marker for malignant vascular tumors and mesothelioma: an immunohistochemical study of 262 vascular endothelial and 1640 nonvascular tumors. *Am J Surg Pathol*, *36*(4), 629-639. https://doi.org/10.1097/PAS.0b013e318243555b

Minotti, G., P., M., Salvatorelli, E., Cairo, G., & Gianni, L. (2004). Anthracyclines: Molecular Advances and Pharmacologic Developments in Antitumor Activity and Cardiotoxicity. *PHARMACOLOGICAL REVIEWS*, 185–229.

Miura, K., Kinouchi, M., Ishida, K., Fujibuchi, W., Naitoh, T., Ogawa, H., Ando, T., Yazaki, N., Watanabe, K., Haneda, S., Shibata, C., & Sasaki, I. (2010). 5-fu metabolism in cancer and orally-administrable 5-fu drugs. *Cancers (Basel)*, *2*(3), 1717-1730. https://doi.org/10.3390/cancers2031717

Molinari, A., Calcabrini, A., Meschini, S., Stringaro, A., Crateri, P., Toccacieli, L., Marra, M., Colone, M ., Cianfriglia, M., & Arancia, G. (2002). Subcellular detection and localization of the drug transporter P glycoprotein in cultured tumour cells. *Curr Protein Pept Sci*, 653-670.

Molinari, A., Cianfriglia, M., Meschini, S., Calcabrini, A., & Arancia, G. (1994). P-glycoprotein expression in the Golgi apparatus of multidrug-resistant cells. *International Journal of Cancer*, *59*(6), 789-795. https://doi.org/https://doi.org/10.1002/ijc.2910590614

Mossink, M. H., van Zon, A., Scheper, R. J., Sonneveld, P., & Wiemer, E. A. (2003). Vaults: a ribonucleoprotein particle involved in drug resistance? *Oncogene*, 7458-7467.

Muley, H., Fadó, R., Rodríguez-Rodríguez, R., & Casals, N. (2020). Drug uptake-based chemoresistance in breast cancer treatment. *Biochemical Pharmacology*, *177*, 113959. https://doi.org/https://doi.org/10.1016/j.bcp.2020.113959

Munteanu, E., Verdier, M., Grandjean-Forestier, F., Stenger, C., Jayat-Vignoles, C., Huet, S., Robert, J., & Ratinaud, M. H. (2006). Mitochondrial localization and activity of P-glycoprotein in doxorubicin-resistant K562 cells. *Biochem Pharmacol.*, 1162-1174.

Murray, S., Briasoulis, E., Linardou, H., Bafaloukos, D., & Papadimitriou, C. (2012). Taxane resistance in breast cancer: mechanisms, predictive biomarkers and circumvention strategies. *Cancer Treat Rev*, *38*(7), 890-903. https://doi.org/10.1016/j.ctrv.2012.02.011

Nedeljković, M., & Damjanović, A. (2019). Mechanisms of Chemotherapy Resistance in Triple-Negative Breast Cancer-How We Can Rise to the Challenge. *Cells*, *8*(9). https://doi.org/10.3390/cells8090957

Nitiss, J. L., Soans, E., Rogojina, A., Seth, A., & Mishina, M. (2012). Topoisomerase assays. *Curr Protoc Pharmacol*, *Chapter 3*, Unit 3.3. https://doi.org/10.1002/0471141755.ph0303s57

Nobili, S., Landini, I., Mazzei, T., & Mini, E. (2012). Overcoming tumor multidrug resistance using drugs able to evade P-glycoprotein or to exploit its expression. *Med Res Rev.*, 1220-1262.

Nooter, K., Bosman, F. T., Burger, H., van Wingerden, K. E., & Flens, M. J. (1996). Expression of the multidrug resistance-associated protein MRP gene in primary non small cell lung cancer. *Ann. Oncol.*, 75-81.

Orditura, M., Galizia, G., Sforza, V., Gambardella, V., Fabozzi, A., Laterza, M. M., Andreozzi, F., Ventriglia, J., Savastano, B., Mabilia, A., Lieto, E., Ciardiello, F., & De Vita, F. (2014). Treatment of gastric cancer. *World J Gastroenterol*, *20*(7), 1635-1649. https://doi.org/10.3748/wjg.v20.i7.1635

Palmeira, A., Sousa, E., Vasconcelos, M. H., & Pinto, M. M. (2012a). Three decades of P-gp inhibitors; skimming through several generations and scaffolds. *Curr Med Chem.* , 1946-2025.

Palmeira, A., Sousa, E., Vasconcelos, M. H., & Pinto, M. M. (2012b). Three decades of P-gp inhibitors: skimming through several generations and scaffolds. *Curr Med Chem*, *19*(13), 1946-2025. https://doi.org/10.2174/092986712800167392

Peters, G. J. (2019). From 'Targeted Therapy' to Targeted Therapy. *Anticancer Research*, *39*(7), 3341. https://doi.org/10.21873/anticanres.13476

Piazuelo, M. B., & Correa, P. (2013). Gastric cancer: Overview. *Colombia Médica*, *44*, 192-201. http://www.scielo.org.co/scielo.php?script=sci_arttext&pid=S1657-95342013000300011&nrm=iso

Pils, D., Pinter, A., Reibenwein, J., Alfanz, A., Horak, P., Schmid, B. C., Hefler, L., Horvat, R., Reinthaller, A., Zeillinger, R., & Krainer, M. (2007). In ovarian cancer the prognostic influence of HER2/neu is not dependent on the CXCR4/SDF-1 signalling pathway. *British Journal of Cancer*, *96*(3), 485-491. https://doi.org/10.1038/sj.bjc.6603581

Pisano, C., Cecere, S. C., Di Napoli, M., Cavaliere, C., Tambaro, R., Facchini, G., Scaffa, C., Losito, S., Pizzolorusso, A., & Pignata, S. (2013). Clinical Trials with Pegylated Liposomal Doxorubicin in the Treatment of Ovarian Cancer. *Journal of Drug Delivery*, *2013*, 1-12. https://doi.org/10.1155/2013/898146

Qu, J., Chen, W., Hu, R., & Feng, H. (2016). The Injury and Therapy of Reactive Oxygen Species in Intracerebral Hemorrhage Looking at Mitochondria. *Oxid Med Cell Longev*, *2016*, 2592935. https://doi.org/10.1155/2016/2592935

Rivankar, S. (2014). An overview of doxorubicin formulations in cancer therapy. *J Cancer Res Ther*, *10*(4), 853-858. https://doi.org/10.4103/0973-1482.139267

Römermann, K., Wanek, T., Bankstahl, M., Bankstahl, J. P., Fedrowitz, M., Müller, M., Löscher, W., Kuntner, C., & Langer, O. (2013). (R)-[(11)C]verapamil is selectively transported by murine and human P-glycoprotein at the blood-brain barrier, and not by MRP1 and BCRP. *Nucl Med Biol*, *40*(7), 873-878. https://doi.org/10.1016/j.nucmedbio.2013.05.012

Rosenberg, A. J., Rademaker, A., Hochster, H. S., Ryan, T., Hensing, T., Shankaran, V., Baddi, L., Mahalingam, D., Mulcahy, M. F., & Benson, A. B., 3rd. (2019). Docetaxel, Oxaliplatin, and 5-Fluorouracil (DOF) in Metastatic and Unresectable Gastric/Gastroesophageal Junction Adenocarcinoma: A Phase II Study with

Long-Term Follow-Up. *Oncologist*, *24*(8), 1039-e1642. https://doi.org/10.1634/theoncologist.2019-0330

Roychoudhury, S., Kumar, A., Bhatkar, D., & Sharma, N. K. (2020). Molecular avenues in targeted doxorubicin cancer therapy. *Future Oncology*, *16*(11), 687-700. https://doi.org/10.2217/fon-2019-0458

Sartiano, G. P., Lynch, W. E., & Bullington, W. D. (1979). Mechanism of action of the anthracycline anti-tumor antibiotics, doxorubicin, daunomycin and rubidazone: preferential inhibition of DNA polymerase alpha. *J Antibiot (Tokyo)*, *32*(10), 1038-1045. https://doi.org/10.7164/antibiotics.32.1038

Sikic, B. I., Fisher, G. A., Lum, B. L., Halsey, J., Beketic-Oreskovic, L., & Chen, G. (1997). Modulation and prevention of multidrug resistance by inhibitors of P-glycoprotein. *Cancer Chemotherapy and Pharmacology*, *40*(1), S13-S19. https://doi.org/10.1007/s002800051055

Sikora, T., Morawska, K., Lisowski, W., Rytel, P., & Dylong, A. (2022). Application of Optical Methods for Determination of Concentration of Doxorubicin in Blood and Plasma. *Pharmaceuticals (Basel)*, *15*(2). https://doi.org/10.3390/ph15020112

Solazzo, M., Fantappiè, O., Lasagna, N., Sassoli, C., Nosi, D., & Mazzanti, R. (2006). P-gp localization in mitochondria and its functional characterization in multiple drug-resistant cell lines. *Experimental Cell Research*, *312*(20), 4070-4078. https://doi.org/https://doi.org/10.1016/j.yexcr.2006.09.005

Stahl, M., Kasimir-Bauer, S., & Harstrick, A. (1997). Down-regulation of topoisomerase II by camptothecin does not prevent additive activity of the topoisomerase II inhibitor etoposide in vitro. *Anticancer Drugs*, *8*(7), 671-676. https://doi.org/10.1097/00001813-199708000-00005

Sun, J., Zhao, J., Yang, Z., Zhou, Z., & Lu, P. (2021). Identification of gene signatures and potential therapeutic targets for acquired chemotherapy resistance in gastric cancer patients. *Journal of Gastrointestinal Oncology*, *12*(2), 407-422. https://jgo.amegroups.com/article/view/51324

Suzuki, K., Bose, P., Leong-Quong, R. Y. Y., Fujita, D. J., & Riabowol, K. (2010). REAP: A two minute cell fractionation method. *BMC Research Notes*, *3*(1), 294. https://doi.org/10.1186/1756-0500-3-294

Szaflarski, W., Sujka-Kordowska, P., Januchowski, R., Wojtowicz, K., Andrzejewska, M., Nowicki, M., & Zabel, M. (2013). Nuclear localization of P-glycoprotein is responsible for protection of the nucleus from doxorubicin in the resistant LoVo cell line. *Biomed Pharmacother.*, 497-502.

Thorn, C. F., Oshiro, C., Marsh, S., Hernandez-Boussard, T., McLeod, H., Klein, T. E., & Altman, R. B. (2011). Doxorubicin pathways: pharmacodynamics and adverse effects. *Pharmacogenet Genomics*, *21*(7), 440-446. https://doi.org/10.1097/FPC.0b013e32833ffb56

Thorn, C. F., Oshiro, C ., Marsh, S ., Hernandez-Boussard, T ., McLeod, H ., Klein, T.E ., Altman, R.B. (2011). Doxorubicin pathways: pharmacodynamics and adverse effects. *Pharmacogenet. Genomics*, 440-446.

Trambas, C., Wang, Z., Cianfriglia, M., & Woods, G. (2001). Evidence that natural killer cells express mini P-glycoproteins but not classic 170 kDa P-glycoprotein. *Br J Haematol*, *114*(1), 177-184. https://doi.org/10.1046/j.1365-2141.2001.02885.x

Tsuruo, T., Iida, H., Tsukagoshi, S., & Sakurai, Y. (1981). Overcoming of vincristine resistance in P388 leukemia in vivo and in vitro through enhanced cytotoxicity of vincristine and vinblastine by verapamil. *Cancer Res*, *41*(5), 1967-1972.

Volkova, M., & Russell, R. (2012). Anthracycline Cardiotoxicity: Prevalence, Pathogenesis and Treatment. *Current Cardiology Reviews*, *7*(4), 214-220. https://doi.org/10.2174/157340311799960645

Wadler, S., Green, M., & Muggia, F. (1985). The role of anthracyclines in the treatment of gastric cancer. *Cancer Treat Rev*, *12*(2), 105-132. https://doi.org/10.1016/0305-7372(85)90003-9

Wang, J. Q., Wu, Z. X., Yang, Y., Teng, Q. X., Li, Y. D., Lei, Z. N., Jani, K. A., Kaushal, N., & Chen, Z. S. (2021). ATP-binding cassette (ABC) transporters in cancer: A review of recent updates. *J Evid Based Med*, *14*(3), 232-256. https://doi.org/10.1111/jebm.12434

Wang, X., Zhang, H., & Chen, X. (2019). Drug resistance and combating drug resistance in cancer. *Cancer Drug Resist*, *2*(2), 141-160. https://doi.org/10.20517/cdr.2019.10

Wassef, M., Luscan, A., Battistella, A., Le Corre, S., Li, H., Wallace, M. R., Vidaud, M., & Margueron, R. (2017). Versatile and precise gene-targeting strategies for functional studies in mammalian cell lines. *Methods*, *121-122*, 45-54. https://doi.org/https://doi.org/10.1016/j.ymeth.2017.05.003

Wohrer, S. S., Raderer, M., & Hejna, M. (2004). Palliative chemotherapy for advanced gastric cancer. *Ann Oncol*, *15*(11), 1585-1595. https://doi.org/10.1093/annonc/mdh422

Wojtowicz, K., Januchowski, R., Nowicki, M., & Zabel, M. (2015). Inhibition of protein glycosylation reverses the MDR phenotype of cancer cell lines. *Biomedicine & Pharmacotherapy*, *74*, 49-56. https://doi.org/https://doi.org/10.1016/j.biopha.2015.07.001

Wu, G., Peng, H., Tang, M., Yang, M., Wang, J., Hu, Y., Li, Z., Li, J., Li, Z., & Song, L. (2021). ZNF711 down-regulation promotes CISPLATIN resistance in epithelial ovarian cancer via interacting with JHDM2A and suppressing SLC31A1 expression. *EBioMedicine*, *71*, 103558. https://doi.org/10.1016/j.ebiom.2021.103558

Wu, Q., Yang, Z, Nie, Y., Shi, Y., Fan, D.,. (2014). Multi - drug resistance in cancer chemotherapeutics: mechanisms and lab approaches. *Cancer Lett.*, 159-166.

Xu, H. Q., Ma, M., Ma, Y. P., Zhang, S. Y., Li, W. J., Wei, D., & Wang, J. J. (2021). Identification and Expression Characterization of ATP-Binding Cassette (ABC) Transporter Genes in Melon Fly. *Insects*, *12*(3). https://doi.org/10.3390/insects12030270

Xu, H. W., Xu, L., Hao, J. H., Qin, C. Y., & Liu, H. (2010). Expression of P-glycoprotein and multidrug resistance-associated protein is associated with multidrug resistance in gastric cancer. *J Int Med Res*, *38*(1), 34-42. https://doi.org/10.1177/147323001003800104

Xu, J., Liu, D., Niu, H., Zhu, G., Xu, Y., Ye, D., Li, J., & Zhang, Q. (2017). Resveratrol reverses Doxorubicin resistance by inhibiting epithelial-mesenchymal transition (EMT) through modulating PTEN/Akt signaling pathway in gastric cancer.

Journal of Experimental & Clinical Cancer Research, *36*(1), 19. https://doi.org/10.1186/s13046-016-0487-8

Yao, Q., Qi, X., & Xie, S. H. (2020). Sex difference in the incidence of cardia and non-cardia gastric cancer in the United States, 1992-2014. *BMC Gastroenterol*, *20*(1), 418. https://doi.org/10.1186/s12876-020-01551-1